USING SEQUENTIAL HYDROCHEMICAL ANALYSES TO CHARACTERIZE WATER QUALITY VARIABILITY AT MAMM CREEK GAS FIELD AREA, SOUTHEAST PICEANCE BASIN, COLORADO

by

Tamee R. Albrecht

A thesis submitted to the Faculty and Board of Trustees of the Colorado School of Mines in partial fulfillment of the requirements for the degree of Master of Science (Hydrology).

Golden, Colorado

Date _____

Signed: _____
Tamee R. Albrecht

Signed: _____
Dr. Geoffrey Thyne
Thesis advisor

Signed: _____
Dr. John McCray
Thesis advisor

Golden, Colorado

Date _____

Signed: _____
Dr. John McCray
Director
Hydrologic Science and Engineering

2017-002976-0000704

ABSTRACT

Water resources in semi-arid western Colorado are scarce and especially vulnerable to impact by petroleum production activities, however, this area is also experiencing steady growth in the exploration and production of natural gas. Hydrochemical data from the southeast Piceance Basin was characterized using sequential multivariate statistics, spatial analysis, and geochemical modeling in order to determine if anthropogenic impact has occurred, and try to distinguish potential indicators of impact by natural gas production.

Hierarchical clustering of normalized and standardized chemical data from 620 water samples revealed statistically distinct water facies. Low TDS waters are Ca-Mg-HCO_3, and high TDS waters are either Na-SO_4-HCO_3 or Na-Cl type. Samples with a significant Na-Cl component are typically accompanied by elevated dissolved methane concentrations. Principal component analysis shows the influence of Na-Cl-F-TDS and redox indicators (Fe, Mn, CH_4, and SO_4) on the variability of the total dataset. Samples with elevated iron, manganese, and benzene, occur mainly at the known location of a large methane gas seep caused by well completion problems. However, this distinctive water chemistry is also found elsewhere. Spatial correlation with major faults and fractures shows that the occurrence of high TDS, Na-SO_4-HCO_3 water appears to be structurally controlled. The hypothesis that clusters showing strong influence of a Na-Cl component or redox indicators indicate anthropogenic impact by natural gas production was then tested.

Regional statistical analysis of background water quality suggests that both low and high TDS waters of Ca-Na-HCO_3 to Na-SO_4-HCO_3 type are regionally consistent with areas not impacted by natural gas production, however, samples with significant iron and manganese, dissolved methane or Na-Cl are not.

Methane, a primary constituent of natural gas, shows increasing mean values and occurrence of high values over a period of time when drilling of gas wells was increasing. Methane associated with benzene, iron and manganese is typically of thermogenic origin, and shows similar isotopic values to that of production gas. Methane associated with a Na-Cl component may be derived from reduction of CO_2, and isotopic values of CO_2

2017-002976-0000705

from the production interval suggest that the Williams Forks Formation may be the source of this compound.

The production interval is also the most likely source of chloride to water samples from wells in the study area. Geochemical modeling suggests that mixing with produced water is a necessary component (10%) of one statistical cluster of water samples, and a possible minor component (1-2%) of three other clusters. However, since one of the latter three clusters is structurally controlled, this suggests that mixing with up to 2% formation water composition may occur naturally. Na/Cl molar ratios help to distinguish clusters with Na/Cl molar ratios approaching that of produced water from those with more natural signatures.

Therefore, indicators of impact by methane gas and drilling fluids include elevated benzene concentrations, thermogenic methane, and elevated iron and manganese. Furthermore, samples with sodium-chloride molar ratios approaching that of produced water, elevated methane sourced from CO_2-reduction, and evidence of sulfate reduction processes may also be consistent with anthropogenic impact by produced waters in the study area.

2017-002976-0000706

TABLE OF CONTENTS

ABSTRACT iii

LIST OF FIGURES viii

LIST OF TABLES xii

ACKNOWLEDGEMENTS xiv

CHAPTER 1: INTRODUCTION 1

1.1 Purpose and Objectives 4

1.2 Previous Work 4

CHAPTER 2: STUDY AREA 10

2.1 Geology 11

2.1.1 Lithology 12

2.1.2 Geologic Structures 15

2.2 Hydrology 16

2.2.1 Precipitation 17

2.2.2 Surface Water 17

2.2.3 Groundwater 19

2.2.3.1 Aquifers and Connectivity 19

2.2.3.2 Recharge 20

2.2.4 Water Quality 21

2.3 Occurrence of Natural Gas 22

2.3.1 Exploration and Production 22

2.3.2 Produced Water 23

CHAPTER 3: METHODS 25

3.1 Database 25

3.1.1 Database Contents 26

3.1.2 Uncertainties 26

3.1.3 Database Reduction 27

2017-002976-0000707

3.1.4 Data Quality 28
3.2 Multivariate Statistical Analysis 29
3.2.0 Hierarchical Cluster Analysis 29
3.3 Evaluation of Spatial Coherence 30
3.4 Principal Component Analysis 30
3.5 Inverse Modeling 30
3.6 Methods Model 31
CHAPTER 4 : CHARACTERIZATION OF HYDROCHEMICAL VARIABILITY 33
4.1 Characterizing Hydrochemical Variability at the Study Area 33
4.1.1 Group 1 34
4.1.2 Group 2 34
4.1.3 Group 3 35
4.1.4 Group 4 36
4.1.5 Piper Diagram 36
4.2 Sample Source 36
4.3 Spatial Analysis 38
4.3.0 Spatial Analysis of Chemical Parameters 39
4.4 Controls of Dataset Variability 44
4.4.0 Interaction Between Hydrochemical Clusters 49
CHAPTER 5: HYDROCHEMICAL CONCEPTUAL MODEL 51
5.1 Background Water Chemistry 51
5.2 Impacted Water Chemistry 52
CHAPTER 6: TESTING THE HYDROCHEMICAL CONCEPTUAL MODEL 57
6.1 Establishing a Regional Context for the Observed Hydrochemistry 57
6.1.1 SSPA Dataset 57
6.1.2 Battlement Mesa Dataset 59
6.1.3 Comparison with the Study Area 60
6.2 Temporal Analysis 62
6.2.1 Cluster Membership Over Time 62

2017-002976-0000708

6.2.2 Occurrence of Methane Over Time 68
6.2.2.0 Source of Methane 72
6.2.3 Spatial Buffering 74
6.2.4 Benzene Analysis 77
6.2.4.0 Reactive Transport 79
6.3 Inverse Geochemical Modeling 83
6.3.1 Model Input 84
6.3.2 Modeling Results 85
6.4 Indicators of Anthropogenic Impact 85
CHAPTER 7: CONCLUSIONS 89
7.1 Future Work 91
7.2 Recommendations 92
REFERENCES CITED 93
APPENDIX A 100
APPENDIX B ..... CD
APPENDIX C ..... CD
APPENDIX D ..... CD
APPENDIX E ..... CD

2017-002976-0000709

LIST OF FIGURES

Figure 1.1: Nationwide predicted annual natural gas production through 2030 in trillion cubic feet. Data from Energy Information Administration (2007)..... 1

Figure 1.2: General location of Piceance Basin in Colorado is shown in the upper figure. In the lower figure, the approximate area of the Piceance Basin is shown in the olive stipple, and the location of the study area is highlighted in red..... 3

Figure 2.1: The upper figure shows the location of the study area in the Piceance Basin of Colorado. The lower figure is a base map of the study area, outlined in black. 11

Figure 2.2: Geologic section of the late Cretaceous and early Eocene units near the study area. Adapted from Shroba and Scott (2003)1997). Units are labeled as: Km=Mancos shale, Kmv=Mesaverde Group, Tw=Wasatch Formation (general), Twa=Atwell Gulch member of Wasatch, Twm=Molina member of Wasatch, Tws=Shire member of Wasatch..... 13

Figure 2.3: Bedrock geology in the study area. Modified from URS (2006)..... 14

Figure 2.4: Major structural features transcribed over the study area. Modified from Tremain and Tyler (1995). 16

Figure 2.5: Average total precipitation by month over a record from 1910 – 2006 for Rifle, Colorado. From Western Regional Climate Center (2007)..... 17

Figure 2.6: Monthly average streamflow (cfs) for gage 09090700 on the East Divide Creek near Silt from 1959 – 1964. From Colorado Department of Water Resources (2007). 18

Figure 2.7: Monthly average streamflow (cfs) for gage 09089500 on the West Divide Creek near Raven from 1997 – 2005. From USGS (2007)..... 19

Figure 3.1: Histogram of percent charge-balance error for selected samples..... 28

Figure 3.2: Flowchart of methodology steps. From Thyne et al. (2004)..... 32

Figure 4.1: Dendogram of hierarchical clustering of 620 water samples. The dashed black line, the phenom line, shows the distance (a measure of degree of similarity) that defines the number of clusters was chosen for analysis..... 33

2017-002976-0000710

Figure 4.2: Mean concentrations of each of 13 parameters for each cluster. Note the vertical log-scale on left, and secondary axis on right. “Alk” stands for alkalinity.. 35

Figure 4.3: Piper diagram showing relative concentrations of major ions by cluster..... 37

Figure 4.4: Percentage of surface and groundwater samples by cluster..... 38

Figure 4.5: Spatial distribution of clusters in group 1 over the study area, with bedrock geology and major structural features. Lithology from URS (2006); structural features modified from Tremain and Tyler (1997) and URS (2006)..... 40

Figure 4.6: Spatial distribution of group 2 over the study area, with bedrock geology and major structural features. Lithology from URS (2006); structural features modified from Tremain and Tyler (1997) and URS (2006). 41

Figure 4.7: Spatial distribution of clusters in group 3 over the study area, with bedrock geology and major structural features. Lithology from URS (2006); structural features modified from Tremain and Tyler (1997) and URS (2006)..... 42

Figure 4.8: Spatial distribution of clusters in group 4 over the study area, with bedrock geology and major structural features. Lithology from URS (2006); structural features modified from Tremain and Tyler (1997) and URS (2006)..... 43

Figure 4.9: TDS concentrations contoured by inverse distance over the study area with water samples plotted by cluster. Note the lack of data points in the southwest, central and northern portions of the study area. Usability of interpolated contours in these areas is limited. Groundwater flow is generally to the north..... 45

Figure 4.10: Chloride concentrations contoured over the study area with water samples by cluster. Note the lack of data points in the southwest, central and northern portions of the study area. Usability of interpolated contours in these areas is limited. 46

Figure 4.11: Dissolved methane concentrations contoured over the study area with water samples by cluster. Note the lack of data points in the southwest, central and northern portions of the study area. Usability of interpolated contours in these areas is limited..... 47

Figure 4.12: Scatterplot of clusters in PC2 vs. PC1 space. The primary parameters controlling each principal component are shown on their respective axes..... 50

Figure 4.13: Scatterplot of clusters in PC3 vs. PC1 space. The primary parameters controlling each principal component are shown on their respective axes..... 50

2017-002976-0000711

Figure 5.1: Log-log plot of sodium versus total dissolved solids (TDS) concentration. Points symbolized by cluster..... 52

Figure 5.2: Log-log plot of sulfate versus TDS concentration. Points symbolized by cluster. 54

Figure 5.3: Plot of mean sodium versus TDS concentrations, with conservative mixing curve. PW-A and PW-B are produced water compositions from the study area..... 55

Figure 5.4: Log-log plot of mean molar sulfate-chloride ratio versus chloride concentration for each cluster. PW-A and PW-B are produced water compositions. The dashed line indicates hypothetical mixing. 56

Figure 6.1: Dendogram showing hierarchical clustering of 70 groundwater samples. Group SSPA 1 is to the left, and SSPA 2 is to the right..... 58

Figure 6.2: Dendogram of 9 clusters from the study area (1a-1, 1a-2, 1b, 2, 3a, 3b-1, 3b-2, 4a, and 4b), 2 clusters from the SSPA study (SSPA 1 and SSPA 2), and means of 3 datasets from Battlement Mesa area (BM 1969, 1997-99, and 2004-6). 61

Figure 6.3: Water samples taken in 1997, 2001, and 2002 plotted by cluster..... 63

Figure 6.4: Water samples taken in 2003 plotted by cluster..... 64

Figure 6.5: Water samples taken in 2004 plotted by cluster..... 65

Figure 6.6: Water samples taken in 2005 plotted by cluster..... 66

Figure 6.7: Log of mean dissolved methane concentrations (mg/L) by year. R^2=0.80.... 69

Figure 6.8: Number of new gas wells drilled by year..... 69

Figure 6.9: Mean methane concentration by year versus cumulative gas wells present in the study area that year. R^2=0.76..... 70

Figure 6.10: Mean methane concentration by year versus new natural gas wells drilled in the study area that year. R^2=0.55..... 70

Figure 6.11: Percent of water samples by year with methane concentrations greater than 1 mg/L. R^2=0.98..... 71

2017-002976-0000712

Figure 6.12: Percentage of water samples by year with chloride concentrations greater than 250 mg/L. R^2=0.90 72

Figure 6.13: Isotopic ratios in methane from different sources in the study area, including water samples from clusters 2, 3b-1, 3b-2, and water samples of unknown cluster. Vertical orange line shows the δC^{13} values predicted for CH_4 derived from CO_2-reduction of CO_2 sourced from the Williams Fork 73

Figure 6.14: Locations of gas wells, not including proposed locations. Gas wells data from COGCC (12/2006) 75

Figure 6.15: Location of problem gas wells 76

Figure 6.16: Worst-case model of reactive transport of benzene concentration with distance from a continuous source after 2 years. Source is 12,000 ppb benzene 81

Figure 6.17: Median-case model of reactive transport of benzene concentration with distance from a continuous source after 2 years. Source is 12,000 ppb benzene 82

Figure 6.18: Best-case model of reactive transport of benzene concentration with distance from a continuous source after 2 years. Source is 12,000 ppb benzene 82

Figure 6.19: Log-log plot of Na/Cl molar ratio versus molar sulfate concentration. "BM" = Battlement Mesa water, average. "SSPA1" and "SSPA2" are cluster means for S.S. Papadopulos and Associates (2007) data. "PW-A" and "PW-B" are produced waters outlined in Table 6.8 87

Figure A1: Correlation of field and lab pH measurements. R^2=0.44 100

2017-002976-0000713

LIST OF TABLES

Table 2.1: Water use statistics for Garfield County, Colorado for 2000 (USGS, 2000).. 10

Table 2.2: Well depth and static depth to water ranges and means for alluvial and bedrock wells in the study area. Modified from URS (2006)..... 20

Table 4.1: Mean water chemistry for water clusters. Concentrations in mg/L, except pH in standard units. "Alk" represents alkalinity, as $CaCO_3$. The number of samples in each cluster is indicated by *n*..... 34

Table 4.2: Percentage of surface and groundwater samples by cluster..... 37

Table 4.3: Loading of each parameter on the first five principal components (PC), and the percent of variance explained..... 48

Table 4.4: Summary of preliminary interpretations for the first three principal components..... 49

Table 5.1: Mean nitrate concentrations by cluster..... 53

Table 6.1: Mean water chemistry for water clusters. Concentrations in mg/L, except pH in standard units. The number of samples in each cluster is indicated by *n*..... 59

Table 6.2: Mean water chemistry for water sampling events. Concentrations in mg/L, except pH in standard units. The number of samples in each cluster is indicated by *n*. ND indicates no data. 60

Table 6.3: Number of water samples in selected database by year. 62

Table 6.4: Cluster and group membership over time..... 67

Table 6.5: Number of dissolved methane measurements (n) taken by year, with mean of the log-value and standard deviation..... 68

Table 6.6: Percentage of samples by cluster that occur within a certain distance of gas wells, problem wells, and major structural features..... 78

Table 6.7: Mean concentrations of benzene by cluster..... 79

2017-002976-0000714

Table 6.8: Input parameters for reactive transport modeling of benzene under site conditions. Henry's law constants written as inverse..... 80

Table 6.9: Input solutions for inverse modeling in PHREEQC..... 84

Table 6.10: Summary of modeling results for mixing background with produced water plus mineral interaction and cation exchange. Mixing amounts shown in percentages. Model uncertainty is 2%. "PW" = produced water, PW-A is normal text, PW-B is italic. Background water is 1a-1. Mineral phases with + = dissolved, - = precipitated. Mass transfer amounts in mol/kg H_2O..... 86

2017-002976-0000715

ACKNOWLEDGEMENTS

I would like to thank my advisor, Dr. Geoffrey Thyne, for his continued guidance, enthusiasm, and support throughout my graduate studies. I would also like to thank my co-advisor, Dr. John McCray, for his assistance and direction, and to recognize and thank my committee members, Dr. David Benson and Dr. John Curtis, for their interest and involvement.

Thanks to my colleagues in HSE, who provided critical discussion and support throughout my studies.

I would like to acknowledge the Colorado School of Mines for provided financial assistance for two years of graduate work through a teaching assistantship in the Department of Geology and Geological Engineering.

Finally, I would like to thank my family and close friends for their invaluable encouragement, support, and patience.

2017-002976-0000716

In memory of my grandmother.

2017-002976-0000717

CHAPTER 1: INTRODUCTION

With less than 1% of the world's water comprised of freshwater resources, protecting the quality of freshwater resources is imperative. In arid and semi-arid regions where water supplies are stressed due to low recharge by precipitation and high evapotranspiration rates, the need to protect water resources from contamination or degradation is even greater. The Piceance Basin in western Colorado receives only 8-20 inches of precipitation each year, and with high evapotranspiration rates most recharge is removed before it can infiltrate to the water table (URS, 2006).

Nationwide, natural gas production is predicted to increase steadily through the year 2030 (Figure 1.1) (Energy Information Administration, 2007), and the Piceance Basin of western Colorado is currently experiencing some of the fastest growth in natural gas production in the country (Miller, 2007).

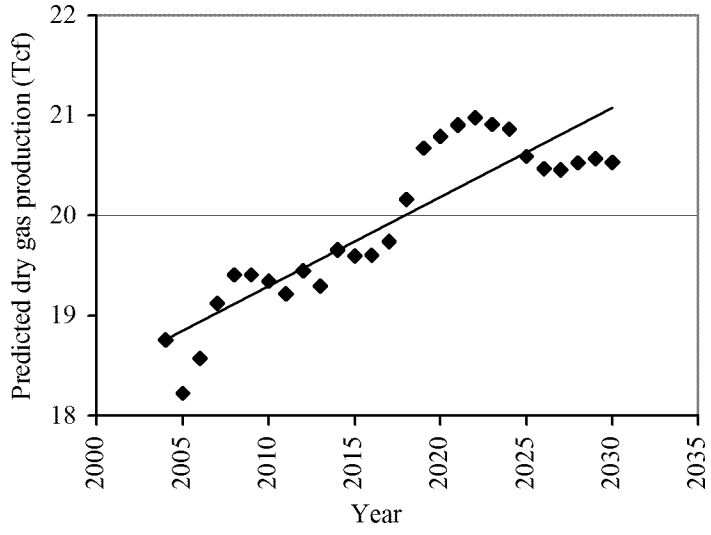

Figure 1.1: Nationwide predicted annual natural gas production through 2030 in trillion cubic feet. Data from Energy Information Administration (2007).

2017-002976-0000718

In the last few years, natural gas production in this region has grown by approximately 20% (Raabe, 2007). Major petroleum companies, such as EnCana, Williams, and Exxon-Mobil, are all planning or currently constructing new natural gas processing plants in the basin, which will be able to process almost 5 times as much natural gas than the current infrastructure capacity (Lonkevich, 2007; Raabe, 2007). In addition to the increasing natural gas production, the Piceance Basin is also being considered for development of its oil shale reserves (26th Annual Oil Shale Symposium, 2006).

Exploration and production activities associated with oil and natural gas resources have the potential to negatively impact local water resources. Impact can occur by land alterations, surface spills, equipment failure, improper treatment of water co-produced with oil or gas, and leaking active or abandoned wells, all of which can release saline water and toxic organic compounds into ground and surface water resources (Kharaka et al., 2005). High levels of salts or fuel components can degrade fish habitat in streams and exceed EPA drinking water standards in domestic water resources. Understanding the character of these impacts and developing better techniques for distinguishing anthropogenic impacts are crucial to protecting our vulnerable water resources.

This study focuses on a natural gas field in the southeastern portion of the Piceance Basin (Figure 1.2), where surface and groundwater resources recently incurred direct impact due to gas production activities. In April 2004, a methane gas seep was identified discharging directly into West Divide Creek in the eastern portion of the study area south of the town of Silt, Colorado. Approximately 115 MMcf (million cubic feet) of gas was released into the streambed. The gas was identified by chemical analyses as nearly identical to produced gas from the Williams Fork Formation (COGCC, 2006). After investigation, the seep was attributed to an improper cementation of production casing from a gas well over 3800 feet away (COGCC, 2006). This event provides an example of potential anthropogenic impacts to water resources by natural gas production, and in the context of the growing natural gas industry in Colorado's Piceance Basin, motivates a thorough characterization of the vulnerability of water resources to such impacts.

2017-002976-0000719

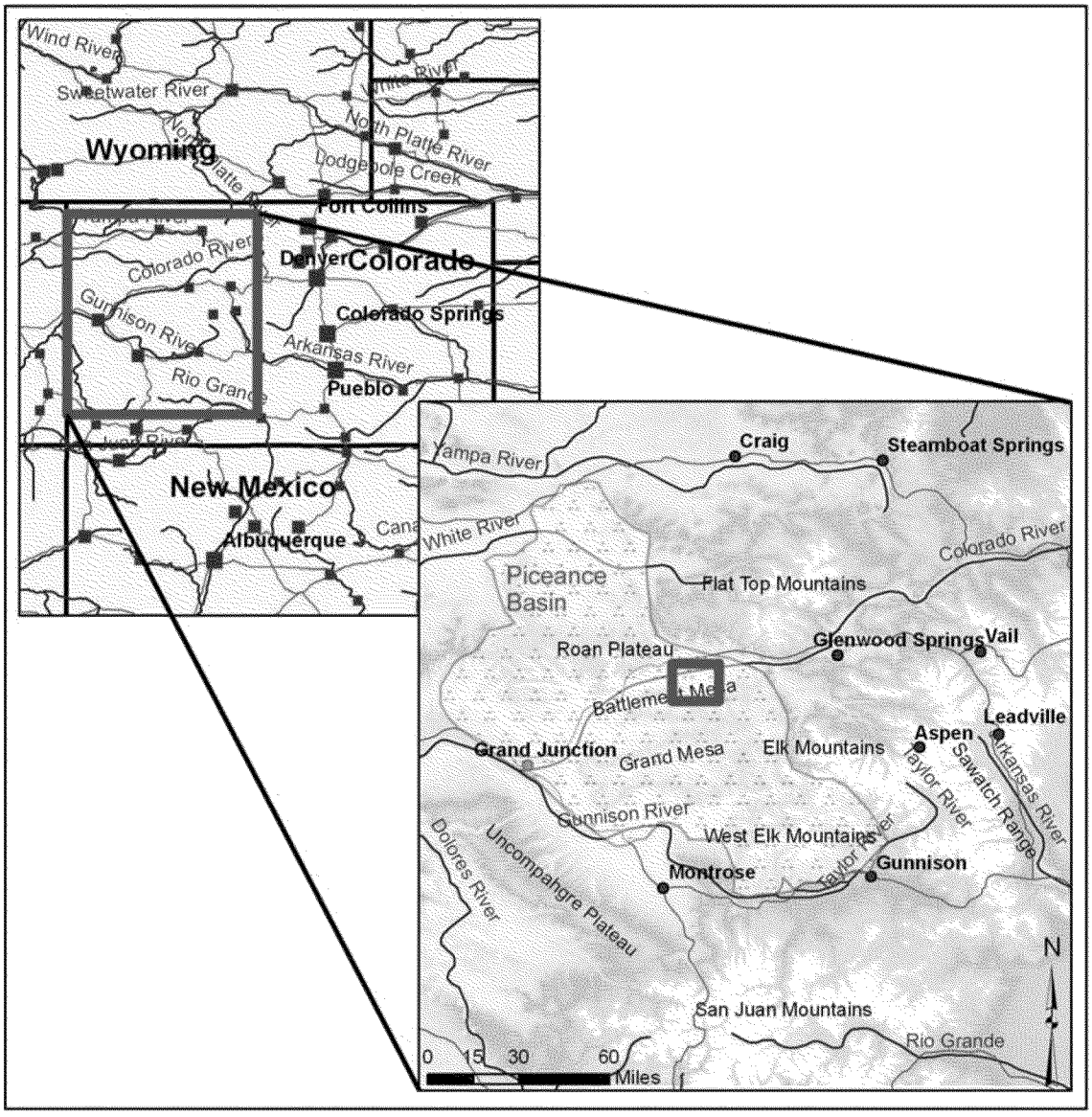

Figure 1.2: General location of Piceance Basin in Colorado is shown in the upper figure. In the lower figure, the approximate area of the Piceance Basin is shown in the olive stipple, and the location of the study area is highlighted in red.

2017-002976-0000720

1.1 Purpose and Objectives

The purpose of this study is to characterize natural water quality variability in the study area, determine if other anthropogenic impact has occurred, and try to distinguish what characteristics may denote impact from natural gas production. The study area in the southeastern portion of the Piceance Basin (Figure 1.2) was chosen due to the availability of a substantial database containing over 70,000 individual measurements of water quality parameters from an area that includes one major natural gas field. In addition, one portion of this area recently experienced direct anthropogenic impact caused by the failure of casing cement in a natural gas production well. By using robust and objective data analysis techniques, this study affords increased sensitivity for distinguishing potential anthropogenic impacts that may not be identified by traditional water quality analysis. The results will be helpful in distinguishing impact at other natural gas and oil fields, and for establishing more effective water quality monitoring programs for water resources protection.

1.2 Previous Work

Gries et al. (1992) reviewed the geologic history and deformation events that led to the formation of the Rocky Mountain region, including the Piceance Basin. Johnson and Flores (2003) reviewed the depositional history of the Piceance Basin from the late Cretaceous through early Eocene stratigraphic units. Their study describes the depositional environment, lithology, and stratigraphic correlation of the Mesaverde Group and Wasatch Formation throughout the Piceance Basin. Lorenz and Nadon (2002) investigated the formation of the Molina member of the Wasatch Formation, noting it's high sand content and tabular sand bodies, which contrasts sharply with the typical mud-dominated lithology of the Wasatch Formation. Geologic maps of the study area include USGS maps of the North Mamm Peak, Rifle, and Silt quadrangles, and the Colorado Geological Survey's Hunter Mesa quadrangle map (Donnell et al., 1989; Madole, 1999; Shroba and Scott, 2001; Shroba and Scott, 1997).

Gries et al. (1992) also reviewed the formation, size, location, and type of hydrocarbon reservoirs in the Rocky Mountains. Johnson and Rice (1990) described the

2017-002976-0000721

occurrence and composition of natural gas reservoirs in the Piceance Basin, including the Williams Fork Formation of the Mesaverde Group. The authors mention the occurrence of CO_2-rich natural gas in some parts of the Wasatch Formation, which may occur due to vertical migration from the underlying Williams Fork Formation. The occurrence of natural gas in the Mesaverde Group is discussed in more detail by Johnson (1989).

Lorenz (2003) described the fracture system in the Piceance Basin in comparison to the San Juan and Green River Basins. Lorenz (2003) discussed how the regional fracture system includes vertical extension fractures that trend between WNW-ESE and WSW-ENE, and are sometimes mineralized by quarts and calcite. Grout and Verbeek (1991) documented five post-Laramide, regional fracture sets, and two sets of inclined joints parallel to the trend of the Divide Creek anticline. Grout et al. (1991) looked at late-Laramide anticlines in the southern Piceance Basin, including the Divide Creek anticline, which is present in the southeastern portion of the study area. These authors also noted local fold-related joint sets running parallel to the trend of the Divide Creek anticline, and overthickening of the Mancos shale under the anticline hinge.

The Colorado Ground Water Association compiled reviews of the major hydrologic provinces in Colorado (Czyzewski, 1999; Hatton, 1999; Lewis-Russ, 1999). These reports provide general information about aquifers, recharge areas, general water quality, and water uses in the Piceance Basin, but only cover the Uinta and Green River Formations, which are not present in the study area. They also discuss the alluvial aquifers around the Colorado River, which provide some water for beneficial use. The authors suggest that the general flow regime of the Piceance Basin includes recharge at outcrops near basin edges, flow toward the center of the basin, and eventual discharge along flowpaths moving toward the Colorado River.

The USGS Ground Water Atlas (1995) also focuses on the Uinta and Green River Formations (Uinta-Animas aquifer), as well as the Mesaverde aquifer. This report suggests that pressure and compaction due to deep burial of the Mesaverde Group in the Piceance Basin provide for very small hydraulic conductivities. Produced water from oil and gas reservoirs in the Piceance Basin was sampled by the USGS during the 1960's. This database shows three produced-water samples from the Mesaverde Group in the Mamm Creek field that are Na-Cl and Na-Cl-HCO_3-type, brackish waters (Breit, 2002).

2017-002976-0000722

The Colorado Geological Survey's Ground Water Atlas of Colorado (Topper et al., 2003) reviews the hydrologic system, aquifer units, water use, and water quality of the Piceance Basin. The authors interpret the Uinta, Green River, Fort Union, and Mesaverde units as aquifers, but not the Wasatch Formation. The authors suggest that fracturing and mineral dissolution has enhanced the naturally low hydraulic conductivity of Tertiary units in the southern Piceance Basin. The authors also point out that groundwater hydraulic head is typically at or near the ground surface near drainages, suggesting discharge of groundwater into streams.

Recent water quality studies conducted near the study area include a Phase IV report by S.S. Papadopulos & Associates (SSPA)(2007), and an annual monitoring report for the Battlement Mesa area by Cordilleran Compliance Services (2007). SSPA (2007) sampled 70 groundwater wells between 1996 – 2005 in an area north of the Colorado River between the towns of New Castle and Rifle, which lies directly north of this project's study area. SSPA found the predominance of a Na-SO_4-HCO_3 signature with TDS ranging from 400-5,500 mg/L. No measurable dissolved methane, BTEX, or MTBE were found in any samples (S.S. Papadopulos & Associates, 2007). Cordilleran Compliance Services, Inc. (2007) has performed annual water quality sampling in the Battlement Mesa area of Garfield County since 2004, which lies directly to the southwest of the study area. Water types from surface water and groundwater from the Green River Formation are consistently low TDS, Na-Ca-HCO_3-SO_4 type in this area. No considerable levels of BTEX, MTBE, or methane were detected during sampling events between 1997 – 1999 and 2004 – 2006 (Cordilleran Compliance Services, 2007). Some natural gas drilling began in the Battlement Mesa area in the fall of 2005, and only data collected through 2006 has been reviewed.

URS Corporation completed a Phase I Hydrogeologic Characterization of the Mamm Creek field area in 2006. URS investigated the geology, history of natural gas drilling, hydrogeology, and water quality in the area. Assessment of water quality was conducted using various graphical techniques such as Schoeller plots and Stiff diagrams, cluster analysis of chemical parameters, spatial depiction of individual chemical parameters, and principal component analysis of major ions (URS, 2006). URS determined that lower TDS groundwaters (<1,000 mg/L) were typically metal-

2017-002976-0000723

bicarbonate type, and could be found primarily on Grass Mesa and Hunter Mesa, but also at other locations in the study area. Two high TDS waters were distinguished: a Na-Cl water and a Na-SO_4 water. URS (2006) suggested that the Na-Cl waters were probably caused by mixing with water from a deeper formation, and that vertical migration of deeper waters may be enhanced by faults and fractures associated with the Divide Creek anticline and the thinned Wasatch Formation in the eastern portion of the study area. The origin of Na-SO_4 waters is unknown, although URS (2006) suggested that TDS, Na, SO_4, and Cl appear to increase with depth below ground surface. Surface waters were determined by URS (2006) to be primarily metal-bicarbonate type. URS (2006) also investigated organic parameters associated with natural gas deposits, such as benzene and methane. Benzene was found in surface waters and monitoring wells at the West Divide Creek seep (URS, 2006). Methane has been found in domestic wells at concentrations up to 37 mg/L in other sections of the study area; URS (2006) determined that most of these wells contain methane produced by CO_2-reduction or bacterial fermentation mechanisms, except three wells which have methane of unknown origin. Thermogenic methane was found in water wells around the Divide Creek anticline. Both thermogenic and biogenic methane can be associated with natural gas deposits (Johnson and Rice, 1990). URS (2006) suggested that methane contamination around the anticline may be associated with leaking old or abandoned wells. Due to the lack of strong baseline data, the observed water chemistries could not be definitively attributed to natural or anthropogenic causes (URS, 2006). Although a large number of water quality samples were considered in the URS study, multiple chemical variables were not considered in concert, nor were hypotheses about processes and sources of water quality variability tested.

The use of graphical techniques for characterization of large water quality datasets has presented limitations when compared to multivariate techniques. Multivariate statistical techniques better elucidate dominant water chemistries and controlling parameters in large datasets (Guler et al., 2002). Multivariate statistical techniques have been effectively applied to distinguishing the occurrence and level of anthropogenic impact (Helena et al., 2000; Pereira et al., 2003; Shrestha and Kazama, 2007; Simeonov et al., 2003; Yacob, 2004). Lee et al. (2001) also used multivariate statistical techniques with inorganic, organic and physical parameters to characterize

2017-002976-0000724

hydrocarbon impact from leaking USTs. The current study employs multivariate statistical methods to characterize the main controls on water quality variability, and to identify potential anthropogenic impact in the study area.

Many studies have tried to distinguish the occurrence of petroleum-related impact to ground and surface waters. Geochemical indicators that distinguish oil-field brine from water derived from halite dissolution were reviewed by Richter and Kreitler (1993). These include (1) sharp increases in chloride content to a concentration greater than 50 mg/L, (2) trends noticed on Piper plots showing mixing between Ca-Mg-HCO_3 type water and Na-Cl type water, (3) low HCO_3/Cl and SO_4/Cl ratios, (4) distinction of Na/Cl weight ratios of oil field brines from that of halite dissolution (saturation with respect to halite produces a weight ratio of Na to Cl of 0.648), (5) elevated Ca/Cl and Mg/Cl and lower SO_4/Cl ratios than halite solutions, (6) comparison of Br/Cl or I/Cl ratios (both higher for oil field brines), (7) mixing diagrams, and (8) combinations of these techniques. Davis et al. (1998) review multiple uses of the Cl/Br ratio in determining the origin and evolution of waters, including distinguishing oil-field brine sources from halite dissolution fluids. Similar bivariate and comparative techniques were utilized by Andrew et al. (2005) to characterize the chemical composition and evolution of produced water associated with Palm Valley gas field in Australia. Bivariate techniques were also applied by Izbicki et al. (2005), along with isotopic studies, to identify processes affecting water compositions and to identify water chemistry as derived from seawater, seawater evaporation, or oil-field brine. Bivariate techniques can be useful for identifying impact, however work best if chloride concentrations are very high (Richter and Kreitler, 1993) and may not adequately identify impacted samples that have been subsequently diluted by fresh water. In addition, bivariate techniques do not completely illuminate the processes controlling water chemistry variability. Cl/Br and Na/Cl ratios were combined with mass-balance calculations of mixing scenarios by Fontes and Matray (1993). These authors described groundwater compositions in terms of potential mixing models showing that the waters were derived from various fractions of produced and fresh water, with the addition of water-rock interactions. Uliana (2005) combined bivariate and graphical techniques, comparative statistics and mass-balance mixing and thermodynamic equilibrium models on 15 water samples to identify the source of

2017-002976-0000725

salinization of a shallow aquifer in Texas. Three scenarios were tested: (1) evaporation, (2) mixing, then equilibrium with mineral phases, (3) equilibrium with mineral phases, followed by mixing and secondary equilibrium with mineral phases.

The effectiveness of combining multivariate statistical methods, spatial analysis, and geochemical modeling to interpret natural water quality controls was demonstrated by Guler and Thyne (2004) and Thyne et al. (2004) who adequately identified the effects of natural weathering processes and anthropogenic inputs on water chemistry. Yacob (2004) used this method to examine the impact of septic tank effluent on water quality. This methodology is applied in this study to distinguish potential impacts of natural gas drilling, and to identify geochemical processes and anthropogenic sources that may be influencing water quality in the study area.

2017-002976-0000726

CHAPTER 2: STUDY AREA

The study area covers approximately 110 square miles in and around the Mamm Creek natural gas field in the southeast Piceance Basin of western Colorado (Figure 2.1). The area extends south of the Colorado River, between the towns of Rifle and Silt, in Garfield County, Colorado. The study area has moderate relief with land elevations ranging from 5,280 ft above mean sea level (amsl) along the Colorado River, to 9,400 ft amsl in the southwest section of the area (URS, 2006). The Piceance Basin is part of the Colorado Plateau physiographic province, and the southern portion displays the characteristic landforms of this area, such as deep valleys and broad plateaus, while the northern portion of the basin shows a more classic basin physiography, with beds dipping inward from all sides (USGS, 1995).

In 2000, Garfield County had a population of 43,790, 34% of which relied on self-supplied domestic groundwater wells as their primary water supply (USGS, 2000). The other 66% were served by municipal water supply. Major industries in the area include natural gas development, tourism, ranching and farming. The agricultural industry irrigates primarily by surface flooding over approximately 43,540 acres (Garfield County, 2007). This industry extracts over 400 million gallons per day of water from surface water sources for irrigation (Table 2.1) (USGS, 2000).

Table 2.1: Water use statistics for Garfield County, Colorado for 2000 (USGS, 2000).

Withdrawals by use and water type	Surface water (Mgal/d)	Groundwater (Mgal/d)
Municipal water supply	8.37	0.71
Domestic, self-supplied	0	1.79
Industrial, self-supplied	0	0
Irrigation	407.7	2.23
Total	**416.07**	**4.73**

2017-002976-0000727

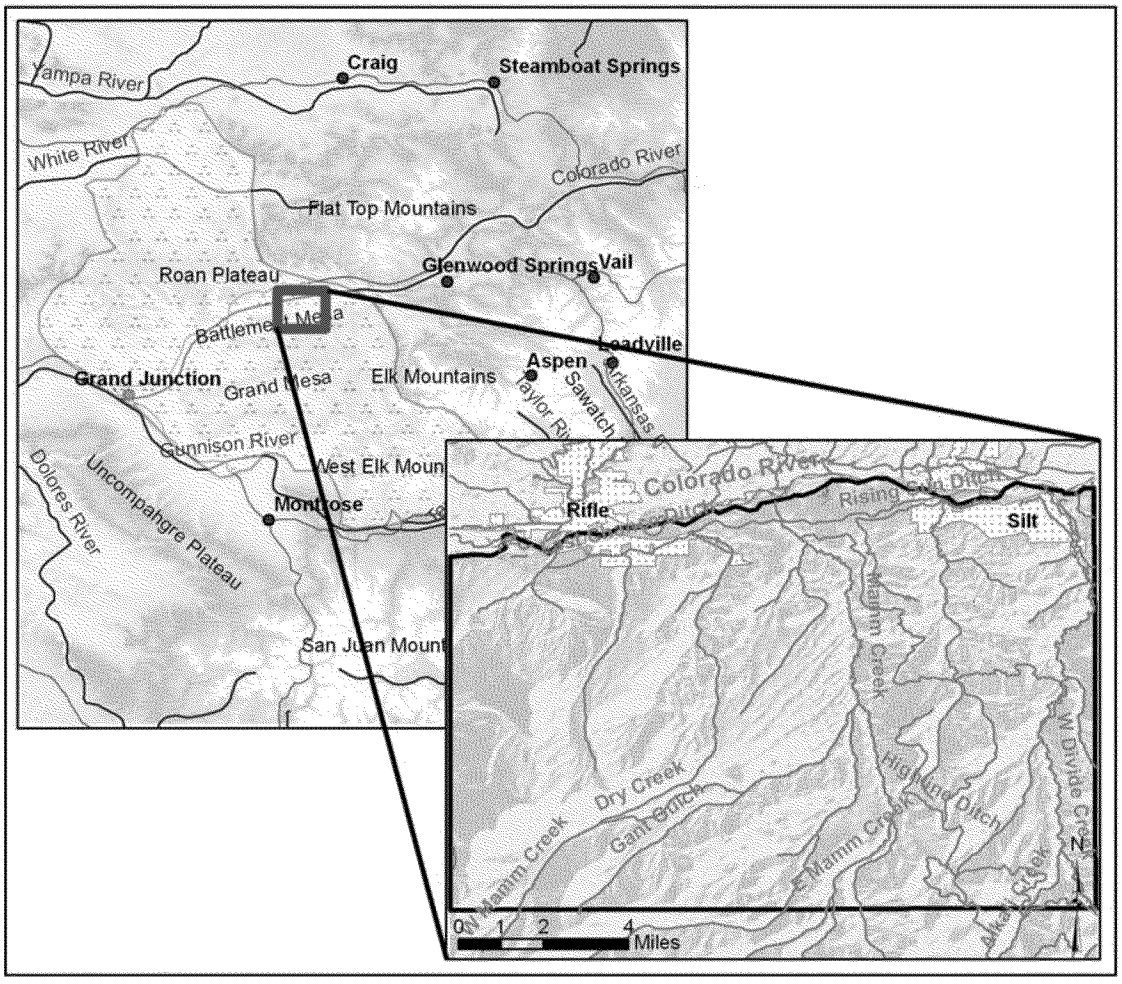

Figure 2.1: The upper figure shows the location of the study area in the Piceance Basin of Colorado. The lower figure is a base map of the study area, outlined in black.

2.1 Geology

The Piceance Basin is a structural and stratigraphic basin, formed during the Laramide orogeny (70 – 40 Ma). The Laramide orogeny created folds, faulted folds, and thrust wedges under compression directions which rotated from east-west, northeast-southwest to north-south through the late Cretaceous to early Eocene (Gries et al., 1992). Laramide-related compression and thrusting caused subsidence of the Piceance Basin, and uplifting of the Douglas Creek Arch, the Park and Sawatch Ranges, the White River and Uncompahgre uplifts, which bound the basin (Figure 2.1) (Johnson and Flores, 2003; Lorenz and Nadon, 2002). The Grand Hogback monocline runs along the eastern edge of the Piceance Basin, and is approximately 135 km in length (Grout and Verbeek, 1991).

2017-002976-0000728

Over 7,000 m of sediment accumulated during the Cambrian through Upper Cretaceous and overlies the Precambrian basement. An additional 2,500-3,300 m of sediment accumulated in the basin during the late Paleocene and Eocene, which is composed of weathering detritus and fluvial sequences (Grout et al., 1991; Grout and Verbeek, 1991).

2.1.1 Lithology

The geologic section for major late Cretaceous through Eocene units in the southern Piceance Basin consists of the following, from oldest to youngest: the Mancos Shale (Km), the Mesaverde Group (Kmv), and the Wasatch Formation (Tw and Tws) (Figure 2.2). The Wasatch Formation consists of three members, the Atwell Gulch member (Twa), the Molina member (Twm), and the Shire member (Tws). The geologic section also shows the general thickness of each unit in the western portion of the study area. The Shire member of the Wasatch Formation is eroded away over the Divide Creek anticline (Figure 2.3).

The Mancos Shale is an upper Cretaceous marine to marginal marine shale deposit. Overlying the Mancos Shale is the upper Cretaceous Mesaverde Group, which consists of lenticular sandstone bodies interbedded with shale and mudstone (Grout and Verbeek, 1991). The lowermost unit of the Mesaverde Group is the Iles Formation, consisting of interbedded sandstone, shale and coal beds (Grout et al., 1991), and the uppermost unit is the Williams Fork Formation, which consists of fluvial sandstones and interfingered marginal-marine shale sequences (Grout and Verbeek, 1991). In between the Iles and Williams Fork Formations is a coalbed methane zone named the Cameo-Fairfield zone (URS, 2006). The Williams Fork Formation is the primary reservoir for natural gas in the study area.

An unconformity lies above the Mesaverde Group, separating the upper Cretaceous strata from the Tertiary Wasatch Formation. A thin conglomeratic sandstone unit (15-122m thick) precedes the unconformity. This unit was identified by Grout and Verbeek (1991) and named the upper Cretaceous Ohio Creek Member. Grout and Verbeek (1991) describe it as coarse-grained, weathered and kaolinitic, possibly representing a paleo-weathering surface.

2017-002976-0000729

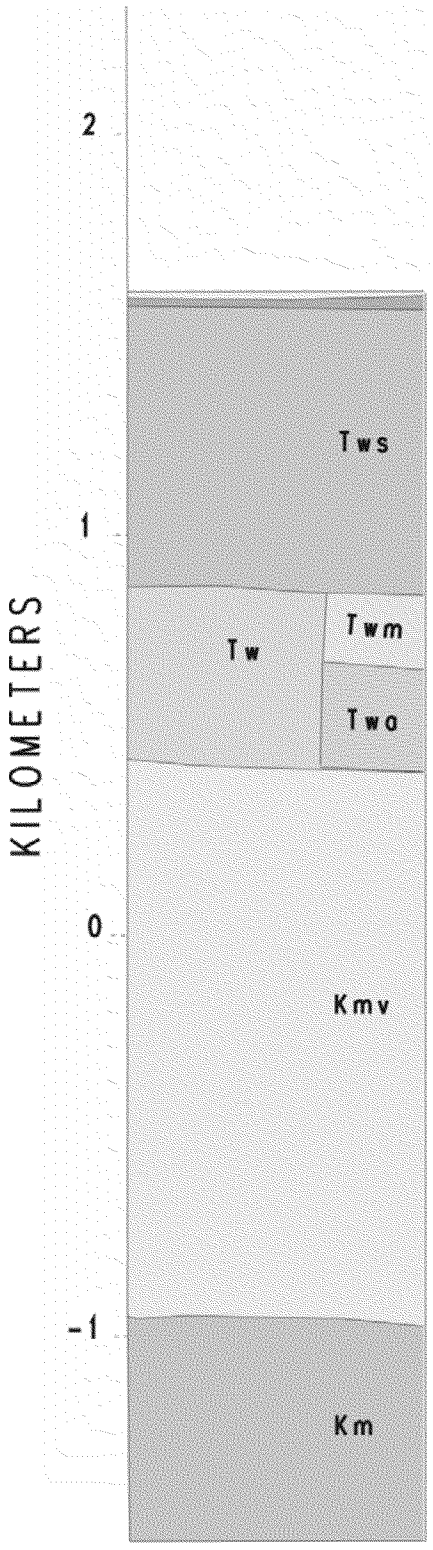

Figure 2.2: Geologic section of the late Cretaceous and early Eocene units near the study area. Adapted from Shroba and Scott (2003)1997). Units are labeled as: Km=Mancos shale, Kmv=Mesaverde Group, Tw=Wasatch Formation (general), Twa=Atwell Gulch member of Wasatch, Twm=Molina member of Wasatch, Tws=Shire member of Wasatch.

2017-002976-0000730

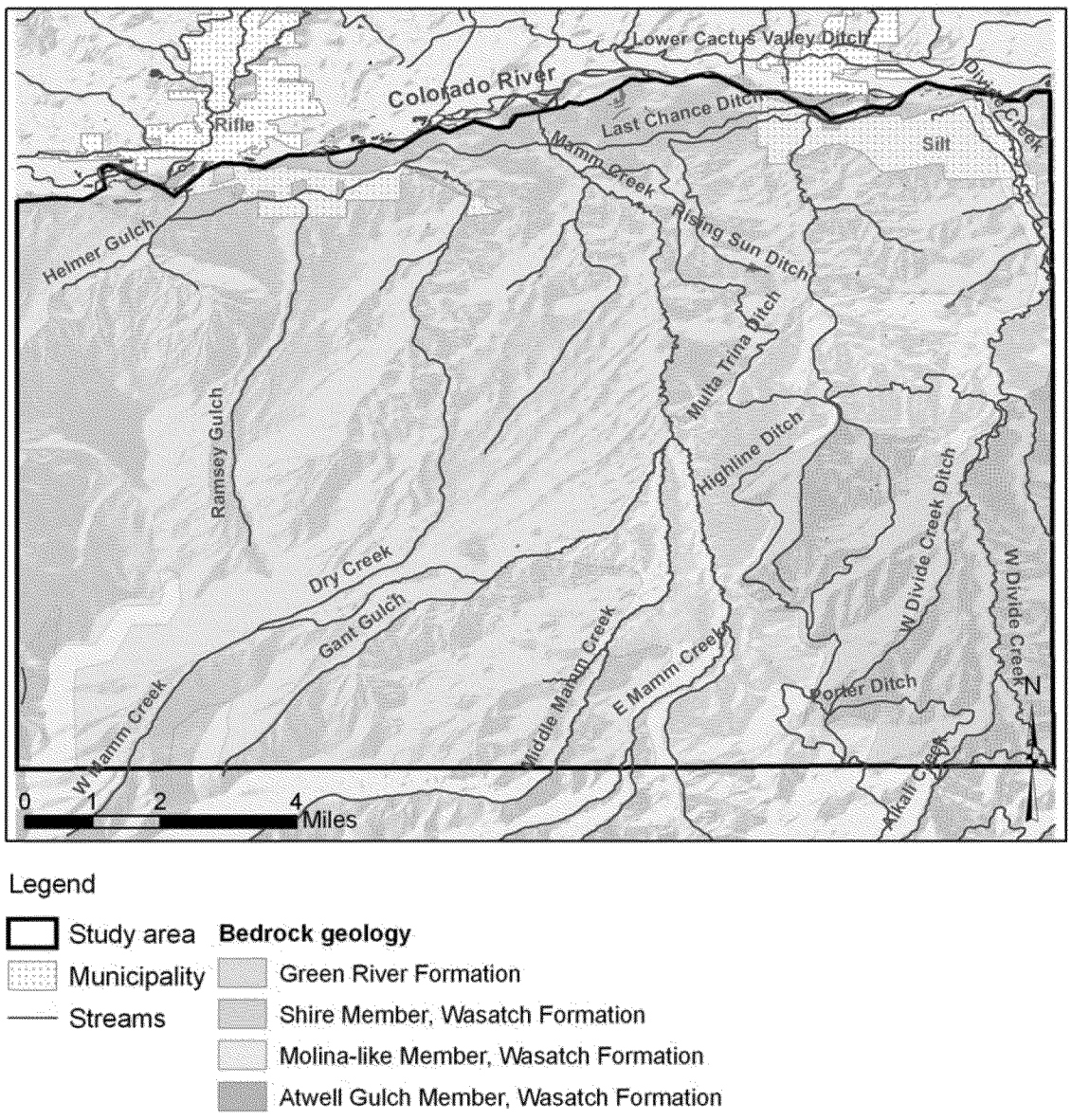

Legend

Study area
Municipality
Streams

Bedrock geology

Green River Formation
Shire Member, Wasatch Formation
Molina-like Member, Wasatch Formation
Atwell Gulch Member, Wasatch Formation

Figure 2.3: Bedrock geology in the study area. Modified from URS (2006).

The Wasatch Formation is an upper coastal plain, fluvial and alluvial deposit, which varies from 1,200 to 5,400 ft thick in the study area (URS, 2006). The Wasatch Formation is primarily composed of variegated mudstone and secondary lenticular and amalgamated sandstones (Grout and Verbeek, 1991), however it is subdivided into three primary units based on lithologic differences. The oldest member, the Atwell Gulch Member, is a nonmarine deposit consisting of mudstone, quartzose sandstones, and volcanic-rich sandstones and conglomerates (Johnson and Flores, 2003). The overlying Molina Member is generally a nonmarine, mudstone, sandstone, and conglomerate

2017-002976-0000731

deposit (Lorenz and Nadon, 2002; URS, 2006). A unique interval within the Molina Member contains up to 65% yellowish sandstones which are tabular and more laterally extensive that the channel sandstone structures typical of the rest of the Wasatch Formation (Lorenz and Nadon, 2002). These sandstone bodies are more resistant than other members of the Wasatch Formation due to calcium carbonate cementation in the sandstone pores (URS, 2006). Johnson and Flores (2003) note that gas has been produced from this interval in Parachute and Piceance Creek fields. Other than this interval, the entire Wasatch Formation consists of only 3-20% sandstone in discontinuous intervals (URS, 2006). The Shire Member (above the sandstone-rich interval) is a nonmarine multi-colored mudstone with less than 3% sandstone in channel structures (URS, 2006).

2.1.2 Geologic Structures

The major structural deformations in the study area were formed during the Laramide orogeny. The Grand Hogback is a large monocline caused by a basement-involved blind thrust fault (Grout and Verbeek, 1991). It appears as a sinuous ridge running 135 km along the eastern border of the Piceance Basin, to the northeast of the study area. The Divide Creek anticline, also formed by Laramide thrusting, is about 35 km long and 15 km wide, with its long axis running adjacent and parallel to the Grand Hogback (Grout et al., 1991). The nose of the anticline plunges into the southeastern corner of the study area. Gravity data shows high-density material under the Divide Creek anticline, which likely represents overthickening of the underlying Mancos Shale (Grout et al., 1991).

Upper Cretaceous through Eocene strata in the study area are affected by eight sets of extension joints (Grout and Verbeek, 1991; Lorenz, 2003). Three joint sets, including two sets running parallel to the Divide Creek anticline limbs, are syn-Laramide in age. The other five sets are post-Laramide fractures ranging in orientation from west-northwest – east-southeast clockwise to east-northeast – west-southwest (Grout and Verbeek, 1991). Fractures studied by Lorenz (2003) were commonly mineralized by quartz and calcite with less frequent occurrences of kaolinite. Apertures ranged from zero to several centimeters, with an average range of 0.24-0.50 mm. Extensive folding and

2017-002976-0000732

faulting in the vicinity of the Divide Creek anticline may enhance permeability to both gas and water (URS, 2006). Major fracture traces are shown in Figure 2.4.

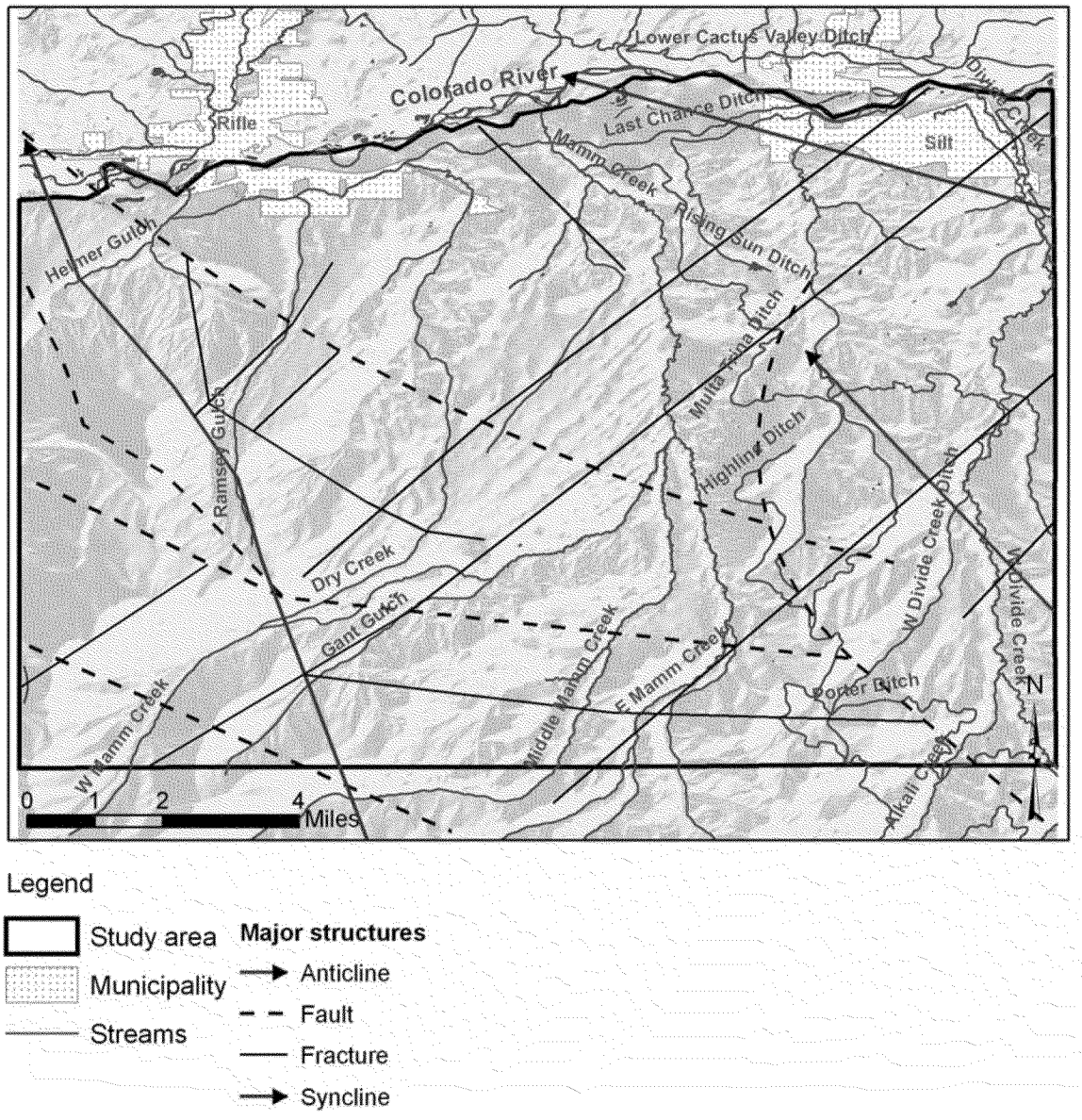

Figure 2.4: Major structural features transcribed over the study area. Modified from Tremain and Tyler (1995).

2.2 Hydrology

The Piceance Basin experiences a semi-arid climate. Due to topographic and structural characteristics, recharge and runoff is obtained from uplifted areas around basin

2017-002976-0000733

edges, and regional flow is directed toward the center of the basin, which is drained primarily by the Colorado River.

2.2.1 Precipitation

In the southeastern Piceance Basin, average annual precipitation ranges from eight to twenty inches, which falls as snow and summer thunderstorms (URS, 2006). However, much of the summer rainfall is lost by direct runoff or evapotranspiration; and much of the snowfall is lost by sublimation (Weeks et al., 1974). Average monthly precipitation in the town of Rifle for a record of approximately 96 years is shown in Figure 2.5 (WRCC, 2007).

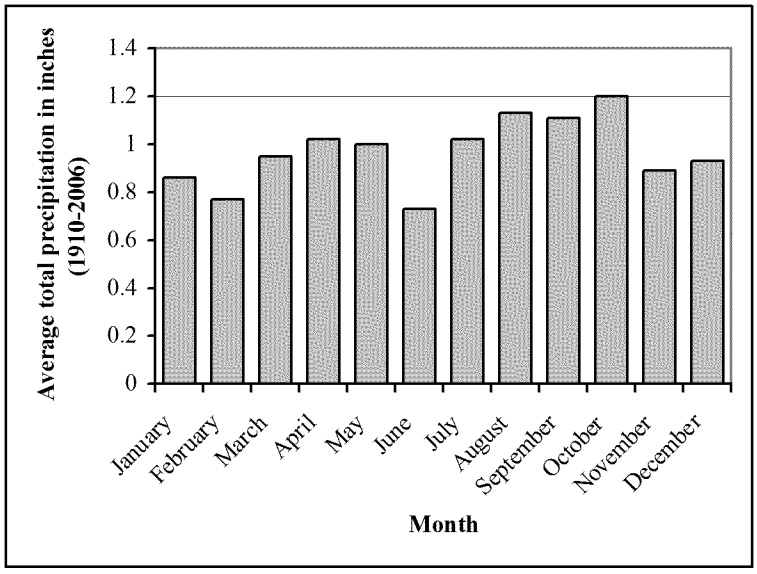

Figure 2.5: Average total precipitation by month over a record from 1910 – 2006 for Rifle, Colorado. From Western Regional Climate Center (2007).

2.2.2 Surface Water

The Piceance Basin is drained by the Colorado, Gunnison, North Fork Gunnison and White Rivers, however, in the southern portion of the basin, the Colorado River is the primary drainage (USGS, 1995). The Colorado River runs approximately east to west, and tributaries to the Colorado River drain from south to north through the study area, and include Dry Creek, Mamm Creek, Dry Hollow Creek, West Divide Creek, East

2017-002976-0000734

Divide Creek, and Divide Creek. Streamflow data from a gaging station in the study area, located on East Divide Creek near Silt, shows a record of six years in Figure 2.6.

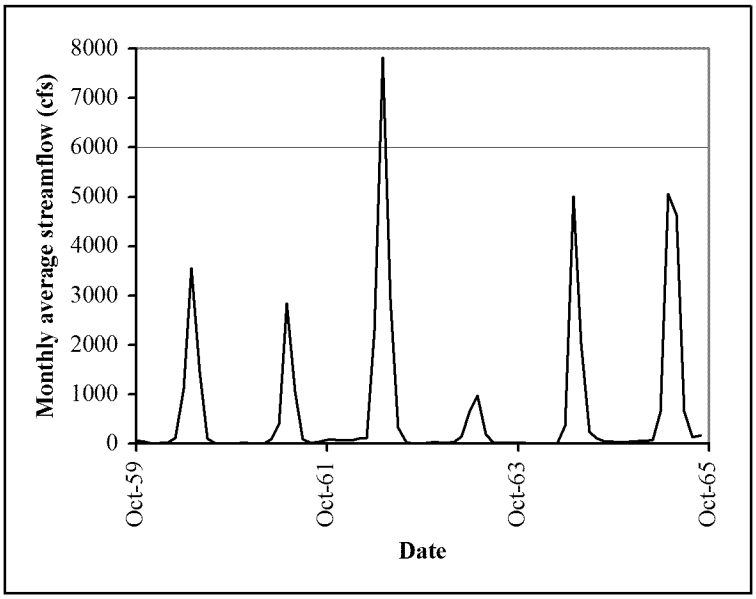

Figure 2.6: Monthly average streamflow (cfs) for gage 09090700 on the East Divide Creek near Silt from 1959 – 1964. From Colorado Department of Water Resources (2007).

A stream gage was operated in more recent years on West Divide Creek, near the town of Raven, approximately five miles south of the study area. Data for this gage is shown in Figure 2.7 for 1997 – 2005, the years during which water quality data for this study was collected.

The high flows that occur in May of each year show the surface discharge dependency on spring snowmelt runoff rather that direct precipitation for high flows. Streams in the study area receive runoff from surrounding highlands including Battlement Mesa to the southwest, Elk Mountain, Hightower Mountain and Haystack Mountain to the south, and Bald Mountain to the east. In late summer, fall and winter, the stream flow in these tributaries can be very low or zero (Colorado Division of Water Resources, 2007).

2017-002976-0000735

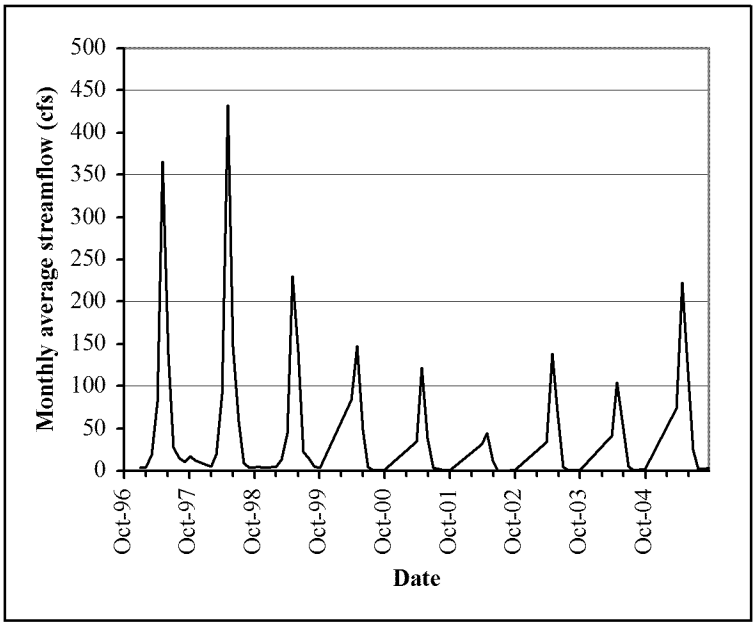

Figure 2.7: Monthly average streamflow (cfs) for gage 09089500 on the West Divide Creek near Raven from 1997 – 2005. From USGS (2007).

2.2.3 Groundwater

In Garfield County, groundwater is the primary source of water for self-supplied domestic wells (see Table 2.1) (USGS, 2000). In the study area, groundwater occurs in alluvial and bedrock aquifers.

2.2.3.1 Aquifers and Connectivity

Alluvial aquifers consist of unconsolidated, Pleistocene alluvial and terrace deposits, bordering the Colorado River and tributaries to the Colorado (Crifasi, 1999). Discontinuous sandstone bodies in the Wasatch Formation form a marginal bedrock aquifer in the study area, however in the northern portion of the basin where additional Tertiary units are still present, the Wasatch Formation is considered a confining unit for the overlying Green River Formation aquifer (Topper et al., 2003). The Green River Formation is an Eocene sandstone and shale unit. The median pumping rate calculated by URS (2006) for alluvial wells is 19.5 gpm, whereas bedrock wells screened in the Wasatch Formation have a median pumping rate of 9.5 gpm. The range and mean of both well depth and static depth to water below ground surface (bgs) is tabulated in Table 2.2.

2017-002976-0000736

Table 2.2: Well depth and static depth to water ranges and means for alluvial and bedrock wells in the study area. Modified from URS (2006).

	Number of wells tested	Total depth: range and mean (ft bgs)	Static depth to water: range and mean (ft bgs)
Alluvial wells	48	12-100 / 59	1-81 / 30
Wasatch wells	388	32-600 / 200	0-342 / 73

Groundwater flow in the Wasatch Formation, as determined by the potentiometric surface, is north and northwest toward the Colorado River, and is generally a subdued replica of topography (URS, 2006; USGS, 1995). Groundwater head is typically at or near the surface in stream valleys, which suggests that groundwater is well connected with alluvial aquifers (Topper et al., 2003). Due to the low porosity and hydraulic conductivity of the Wasatch Formation, flow in this unit is likely fracture-controlled (S.S. Papadopulos & Associates, 2007).

Directly below the Wasatch Formation is the Mesaverde Group, which includes the gas production interval of the Williams Fork Formation. In some areas, the Mesaverde Group is considered an aquifer, however its hydraulic conductivity is greatly reduced due to overburden pressure, compaction and cementation (USGS, 1995). However, Grout and Verbeek (1991) suggest that a high degree of fracturing may introduce some secondary permeability in this unit. A coal-bearing zone called the Cameo zone lies below the Williams Fork Formation and is overpressured in the east-central portion of the Piceance Basin and the northwest side of the study area (URS, 2006). This may cause groundwater in the Williams Fork Formation to flow toward the southeast (URS, 2006).

2.2.3.2 Recharge

Alluvial aquifers are recharged by rainfall, snowmelt, and losses from streams (USGS, 1995). Aquifer recharge is limited by low precipitation, high runoff, and high evaporation rates (Weeks et al., 1974). Bedrock aquifers are primarily recharged by infiltration of precipitation and snowmelt at outcropping areas near the edges of the basin and in highlands, such as the West Elk Mountains and Grand Mesa (see Figure 2.1) (USGS, 1995). In mountainous areas bordering the study area, annual precipitation can be close to 30 inches (USGS, 1995). Recharge from basin edges moves down and toward

2017-002976-0000737

the center of the basin through fractures and permeable pathways in bedrock units and ultimately discharges to the Colorado River (Czyzewski, 1999).

2.2.4 Water Quality

Water quality changes drastically from recharge to discharge areas. In alluvial aquifers, an increase of 100-fold in total dissolved solid (TDS) levels may be observed over the flowpath (Czyzewski, 1999). In bedrock aquifers, an increase of 2 to 10-fold in TDS levels is common (Topper et al., 2003). In the northern portion of the basin, groundwater contains 500 – 10,000 mg/L TDS depending on proximity to recharge areas (Topper et al., 2003).

Limited information about existing water types is available. However, the USGS (1995) determined that the Uinta-Animas aquifer (underlain by the Wasatch Formation, a confining layer) in the Piceance Basin typically contains water of calcium or magnesium-bicarbonate type near recharge areas. The aquifer water is characterized as higher TDS, sodium-bicarbonate or sodium-sulfate type near discharge areas (USGS, 1995). On Battlement Mesa, located directly to the southwest of the study area, water types are typically Na-Ca-HCO_3-SO_4 or Na-HCO_3-SO_4 (Cordilleran Compliance Services, 2007). A study by S.S. Papadopulos and Associates (2007) conducted in the area north of the Colorado River from New Castle to Rifle, found Ca-Mg-HCO_3 and higher TDS, Na-SO_4 or Na-SO_4-HCO_3-Cl in the Wasatch Formation (Cordilleran Compliance Services, 2007).

In general, surface waters in this area typically have lower TDS concentrations and are calcium or magnesium-bicarbonate in type (USGS, 1995). Drainages north of the Colorado River generally carry Ca-Mg-SO_4-HCO_3 type water (S.S. Papadopulos & Associates, 2007). Water-bearing areas of the Mesaverde Group can contain variable amounts of dissolved solids (1,000 – 10,000 mg/L), depending on the distance from the recharge area (USGS, 1995). Water co-produced with natural gas from the Mesaverde Group is Na-Cl or Na-Cl-HCO_3 type, and the unit is underlain by the Mancos Shale (Breit, 2002; URS, 2006).

2017-002976-0000738

2.3 Occurrence of Natural Gas

Natural gas in the study area is produced primarily from the Williams Fork Formation of the Mesaverde Group, where gas began accumulating during the Eocene and is currently trapped by stratigraphic and diagenetic controls (URS, 2006). Regionally, this reservoir is a continuous-type gas accumulation, however, at the study area, gas is reservoired in low permeability sandstone bodies. Spencer (1995) determined that sand bodies in the Williams Fork varied from 10-50 feet in thickness, however, a study by Williams Production RMT Company (2006) determined that sand bodies ranged between 0.5–29 feet thick, and 40.1–2791 feet wide. Classified as a dry "tight-gas sandstone", the Williams Fork Formation has an in situ permeability to gas of less than or equal to 0.1 milliDarcy (mD), and poorly connected and irregularly distributed pores (National Energy Technology Laboratory, 2006). Hydraulic fracturing, or "fracing", is commonly necessary to produce economic quantities of gas in tight-gas sandstones. Fracing stimulates conductivity between the wellbore and the natural fracture pathways by inducing artificial fracturing through the injection of high-pressure water or saltwater mixed with sand (National Energy Technology Laboratory, 2006).

2.3.1 Exploration and Production

Petroleum exploration in the Piceance Basin region began in the late 1800's (Spencer, 1995), however, the first gas well was not drilled in the study area until 1959 (URS, 2006). Between 1959 and the beginning of 2005, 978 gas wells have been drilled in the study area, 777 of which are owned by EnCana Corporation. An additional 234 wells were permitted and 141 wells are on abandoned status as of 2005 (URS, 2006).

EnCana acquired Mamm Creek field in 2001 and has since conducted the majority of drilling in the area. In 2006, EnCana drilled approximate 220 wells and plans to drill an additional 449 wells between 2007-2010 (EnCana, 2007). Between 2004 and 2007, EnCana's production rates in Mamm Creek field have increased by over 30%. Bill Barrett Corporation and Williams Production also operate wells in this area (URS, 2006).

Average natural gas production rates in Mamm Creek field are 875 MMcf/day, and wells are on 20-acre spacing. Directional drilling was employed in the study area so that multiple wells could be drilled from one pad (URS, 2006). Natural gas produced

2017-002976-0000739

from the Williams Fork Formation is primarily thermogenic in origin, and contains a relatively high percentage of CO_2 (up to 22% by volume) (Johnson and Rice, 1990). Average well depths are between 6,000 to 8,000 ft below ground surface (bgs), however can range from 2,000 to 18,422 ft bgs (URS, 2006). Surface casings on gas wells are used to protect groundwater aquifers from contamination by gas or hydrocarbons traveling through the annulus of the well. Surface casings in the study area range in depth from 223 to 5,200 ft bgs (URS, 2006). From the bottom of the surface casing to the top of the cemented production interval, the well annulus is not sealed with cement outside of the production casing.

2.3.2 Produced Water

Produced water is formation water from the production interval, which has been extracted along with oil or natural gas. Potential petroleum reservoir rocks are initially saturated with water prior to migration of hydrocarbons into the new reservoir rocks, therefore they typically contain water and liquid and/or gaseous hydrocarbons (Veil et al., 2004). All producing gas wells co-produce some amount of condensate, oil or water with the gas.

Formation waters are commonly sodium-chloride type (Richter and Kreitler, 1993). This signature is either due to a marine origin of the sedimentary units, influx of other brines, or dissolution of subsurface halite deposits, such as salt domes (Kharaka and Hanor, 2005). In produced waters, total dissolved solids (TDS) concentrations can range from 5,000 – 350,000 mg/L, and concentrations of chloride can range from 250 – 17,500 mg/L; in contrast, median values of TDS and chloride for fresh groundwater are 350 and 20 mg/L respectively (Kharaka and Otton, 2003; Langmuir, 1997). A significant concentration of toxic organic compounds can be found in petroleum-associated formation waters, including benzene, toluene, ethylbenzene, xylenes (BTEX), polycyclic aromatic hydrocarbons (PAHs), and phenols. Dissolved metals may also be present, including iron and manganese, which are mobilized from sediments by redox reactions stimulated by organic petroleum compounds (Kharaka and Otton, 2003).

Produced water compositions vary depending on the type of hydrocarbon being produced and site-specific geologic characteristics (Dorea et al., 2007; Utvik, 1999).

2017-002976-0000740

Produced water from the study area has been found to be Na-Cl-HCO_3 or Na-Cl in type (Breit, 2002). Natural gas production yields waters that are generally more toxic than conventional oil production, however, their volumes are smaller. Production rates of water typically increase over the life of the gas field; by the later stages of production, produced water can constitute up to 98% of the total volume of fluid retrieved (Kharaka and Otton, 2003). Coalbed methane (CBM) produced waters are typically low in sulfate concentration and the volume produced decreases over the life of the reservoir (Veil et al., 2004). In the study area, production rates of water from initial well completion tests for 777 wells (including approximately 10 coalbed methane wells) show a range of less than one to 1,677 barrels/day with an average of 70 barrels/day (URS, 2006).

At each drilling pad, a reserve pit is used to temporarily store drilling mud. The majority of these pits are lined. Pits are sometimes used to store flow-back fluids from the hydraulic fracturing process, which can include some condensate. After drilling, pits are dewatered and the remaining solids are buried (URS, 2006). Produced water in the study area is stored temporarily in above-ground storage tanks (ASTs) at the well pads and then transported for treatment or disposal (URS, 2006).

2017-002976-0000741

CHAPTER 3: METHODS

Initially, the geohydrologic system was characterized by review of reports published by the Colorado Geological Survey (2003), the Colorado Ground-Water Association (1999), and the U.S. Geological Survey (1995) (see Chapter 2: Study Area). Additional site-specific information was obtained from a Phase I Hydrogeologic Characterization report written by URS Corportation (2006). Further characterization of hydrochemical variability and testing of processes and sources throughout this study serve to test this understanding of the geohydrologic system.

Multivariate statistical techniques, as well as inspection of chemical trends, are used to fully characterize the complex variability in the dataset and identify controlling parameters. Spatial visualization of water types elucidates the interaction between water chemistry and geologic features. Conducting geochemical models, which simulate different mixing and reaction scenarios, can then test hypotheses about geochemical processes or sources affecting water quality generated from this analysis. By combining these techniques in sequence, this study offers a comprehensive tool to evaluate the observed hydrochemical variability and possible causes.

3.1 Database

Water well and water quality data used in this study was compiled by URS Corporation from databases provided by the Colorado Oil and Gas Commission (COGCC), the U.S. Geological Survey (USGS), and local consultants. An additional 23 samples were added from a study by COGCC focused on the West Divide Creek seep area (COGCC, 2006). Also, three samples for produced water from Mamm Creek field with major ion chemistry were obtained from the USGS Produced Waters database, and two representative samples (labeled PW-A and PW-B for this study) were used for comparison with samples from the database compiled by URS (Breit, 2002).

2017-002976-0000742

3.1.1 Database Contents

The database prepared by URS contains more than 70,000 individual measurements of water quality parameters taken between 1997 and the spring of 2005, and included approximately 200 different parameters. Parameters include major ions, physical data, and some minor ions, trace elements, and organic compounds. However, due to the numerous different sampling efforts that are represented in this database, the suite of parameters measured varies greatly between samples. Spatial coordinates and well type information was available for some samples.

3.1.2 Uncertainties

Sampling and lab analytical methods were not evaluated for consistency nor accuracy. It was assumed that samples were acquired and analyzed according to USGS and EPA standard methods. Uncertainties within the initial database include:

- A small percentage (<1%) of the available data was estimated. These values were incorporated with more certain data.
- A significant number of censored values existed, indicating a measurement below the detection limit. Parameters with a high percentage of non-detect values (greater than 40%) were excluded, and the remaining non-detect values were estimated based on the methods described in Sanford et al. (1993). These methods are described in section 3.1.3.
- Some non-detect parameters did not have a detection limit recorded. These measurements were unable to be estimated, and therefore were excluded.
- It is uncertain whether measurements were made of dissolved or total recoverable concentrations of many parameters. Samples were compared despite this potential source of error.
- Physical measurements, including pH and temperature, were made in both field and lab settings. Some samples included either one or both types. Corrections were made after the data reduction procedures, and are described in section 3.1.3.

Regular sampling of standard locations was not done, making time-series analysis difficult and unproductive. Water well depth information was only available for less than

2017-002976-0000743

60% of the selected wells. A quality check of the depth information compared with the database available from the Colorado State Engineer's office revealed inconsistencies in the compiled data, and not enough information was available in order to trace the origin of the compiled data. Due to these discrepancies, well type was used for analysis instead of well depth.

3.1.3 Database Reduction

The total number of database parameters was reduced according to frequency of occurrence, value and uniqueness of information, and percentage of censored values, in order to develop the largest and most accurate dataset possible. Parameters with less than 40% censored values were retained and the censored values were estimated according to a maximum likelihood method described by Sanford et al. (1993). Although other estimation methods (i.e. replacement ratios of 0.55 or 0.75 of the detection limit) are reliable for up to 20% censored data, replacement factors decrease with increasing standard deviations and number of censored value. The method described by Sanford et al. (1993) reproduces this variation accurately for 90% of the data for up to 40% censored values. This method is based on the premise that the replacement value for censored data should equal the mean of the qualified values (Sanford et al., 1993). Parameters chosen for the initial analysis include calcium, chloride, alkalinity, potassium, fluoride, magnesium, sodium, sulfate, iron, manganese, dissolved methane, pH and total dissolved solids (TDS).

Values for pH were available for all selected samples, however, some were measured in the field and others in the lab. In order to obtain a consistent dataset, field and lab measurement methods were correlated. Since approximately 90% of the data had field pH measurements, compared to 70% of the data that had lab pH measurements, field measurements were retained. Lab pH measurements for the approximately 10% of the samples that had only lab measurements, were adjusted based on a linear regression of 58% of the data which had both lab and field measurements (see Appendix A).

2017-002976-0000744

3.1.4 Data Quality

It was assumed that sampling and laboratory methods were of adequate quality. However, the data quality was checked by calculating the charge-balance error for each sample with concentrations in milliequivalents per liter, as below (Langmuir, 1997):

$$\% \text{ Charge-balance} = 100 \times \frac{\sum \text{cations} - \left(\sum \text{anions}\right)}{\left(\sum \text{cations} + \sum \text{anions}\right)} \qquad \text{(Equation 3.1)}$$

Samples with less than or equal to 10% charge-balance error were retained. A histogram of the percent of charge-balance error for the retained samples is shown in Figure 3.1. The data reduction process produced 620 samples and 13 parameters for analysis (see Appendix B). Less than 10% of the final dataset consisted of censored values.

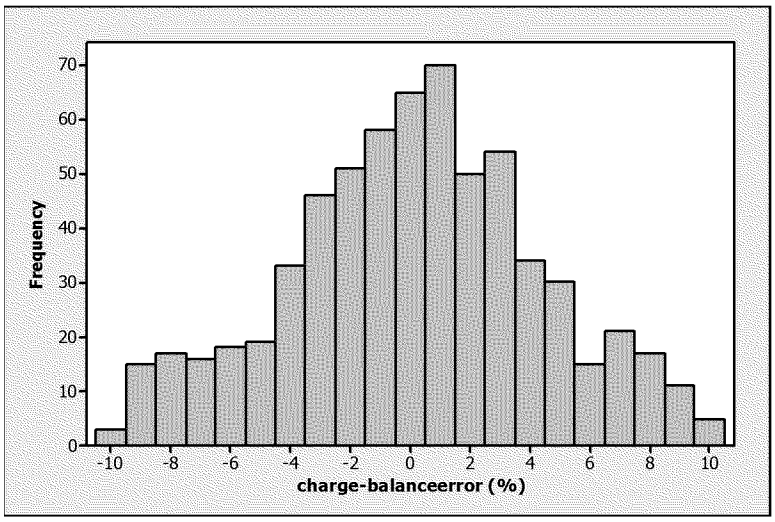

Figure 3.1: Histogram of percent charge-balance error for selected samples.

2017-002976-0000745

3.2 Multivariate Statistical Analysis

Multivariate statistical methods were utilized first to characterize the hydrochemical facies, or water types, that are present in the study area, as well as distinguish samples that may have been impacted by anthropogenic sources. Multivariate statistical techniques are commonly applied to analysis and interpretation of water quality datasets due to the interdependent and irregular nature of the data (McNeil et al., 2005). Similar methods have recently been applied to determine unique water types for large datasets (McNeil et al., 2005), to interpret hydrochemical evolution (Thyne et al., 2004), to distinguish anthropogenic impacts on water quality (Helena et al., 2000; Pereira et al., 2003; Shrestha and Kazama, 2007; Simeonov et al., 2003; Wayland et al., 2003), to identify petroleum contamination by USTs (Lee et al., 2001), and to distinguish initial effects of anthropogenic impact on water quality (Dragon, 2006).

3.2.0 Hierarchical Cluster Analysis

Hierarchical cluster analysis (HCA) effectively separates water samples into statistically significant groups based on their similarity in multiple chemical and physical parameters (Guler et al., 2002; StatSoft, 1997). Guler et al. (2002) found that a combination of Euclidean distance measurement and Ward linkage method produced the most distinctive clusters in a large regional dataset. Euclidean distance measurement calculates a straight line between samples through multi-dimensional space. The Ward linkage method attempts to reduce the sum of squared deviations from the cluster means (Swan and Sandilands, 1995).

Since most statistical analysis methods assume that input data is normally distributed, data must be normalized and standardized in order to achieve equal weighting of parameters (Guler et al., 2002). Two parameters, alkalinity and pH, were normally distributed. The remaining parameters were log-transformed to better approximate a normal distribution. Standardization of data, which centers values around a mean of zero and scales the variability of each parameter to a similar range, is automatically calculated during statistical analysis in Minitab 14, the statistical software program used for this analysis.

2017-002976-0000746

Hierarchical clustering was conducted on normalized and standardized hydrochemical data from the 620 selected samples using the following variables: alkalinity, calcium, chloride, fluoride, potassium, iron, magnesium, manganese, sodium, sulfate, total dissolved solids, pH, and dissolved methane.

3.3 Evaluation of Spatial Coherence

The spatial distribution of hydrochemical data was evaluated in order to determine if hydrochemical processes or trends have geologic or physiographic significance. A strong correlation between hydrochemical data and geologic factors, such as lithology or structural trends, could suggest that the chemical variations are reliant on the geologic setting. In order to observe spatial trends and correlations, water samples, bedrock geology, surface water, major structural features, and some chemical parameter concentrations were mapped in ArcGIS 9.0. Geologic information was transcribed from maps produced by Tremain and Tyler (1995) and URS (2006). Surface water and municipal features were obtained from Garfield County's GIS department. Gas well pad locations were downloaded from the COGCC.

3.4 Principal Component Analysis

Principal component analysis (PCA) was utilized to reduce the variability of the dataset into fewer variables, or axes, which are composed of linear combinations of the original variables (Shrestha and Kazama, 2007). For instance, if measurements from a large number of samples reveal that fluoride values are consistently equal to half of the chloride value, then one variable can be used to describe the values of both ions. PCA, or other forms of factor analysis, have commonly been used for assessment of water quality (Dragon, 2006; Guler and Thyne, 2004; Hannigan and Bickford, 2003; Lee et al., 2001; McNeil et al., 2005; Shrestha and Kazama, 2007; Subba Rao et al., 2006). PCA was conducted in Minitab 14 using the same variables as in the clustering analysis.

3.5 Inverse Modeling

Inverse modeling was conducted in PHREEQC v2.12 in order to test hypotheses about processes and sources affecting water quality at the study area. PHREEQC uses a mass-balance approach to simulate reactions between minerals, gases, solids and aqueous

2017-002976-0000747

phases that can produce a given solution (Parkhurst and Appelo, 1999). Models are constrained by geologic conditions in order to determine if the natural system can explain the hydrochemical variations observed. After a hypothesis has been formulated of the hydrochemical system, PHREEQC can be used to test the feasibility of the proposed chemical processes and potential anthropogenic contributions (Guler and Thyne, 2004).

Inverse geochemical modeling has been applied to many water chemistry studies, including those which attempt to understand natural processes affecting water quality (Guler and Thyne, 2004; Lecomte et al., 2005), and distinguish between natural and anthropogenic impacts (Mahlknecht et al., 2004; Roy et al., 1999; Thyne et al., 2004; Uliana, 2005). In this study, inverse geochemical modeling was conducted to test natural evolution of water clusters involving dissolution and precipitation of highly soluble, geologically available minerals, and mixing between end member solutions derived from cluster analysis and anthropogenic inputs associated with natural gas production.

3.6 Methods Model

The sequential combination of statistical, spatial, and geochemical analysis utilized in this study was modeled after that of Thyne et al. (2004). Thyne et al. (2004) describe and implement this sequential analysis to comprehensively characterize the hydrochemistry of a watershed in central Colorado. The method is outlined in Figure 3.2.

The method is a robust and objective technique for characterizing hydrochemical facies and natural water evolution, but has also been useful in distinguishing anthropogenic impacts from natural background waters (Thyne et al., 2004). The method is based on the understanding that natural water chemistry primarily results from the composition of the initial precipitation plus chemical reactions that occur between water and the sediment and rocks encountered along its flowpath (Drever, 1997; Guler and Thyne, 2004; Hem, 1985; Thyne et al., 2004).

2017-002976-0000748

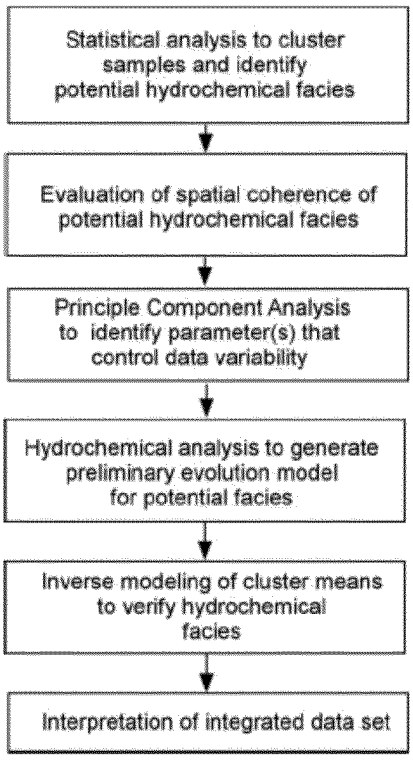

Figure 3.2: Flowchart of methodology steps. From Thyne et al. (2004).

2017-002976-0000749

CHAPTER 4 : CHARACTERIZATION OF HYDROCHEMICAL VARIABILITY

Data variability must be characterized to interpret controls on the hydrochemical system. Characterization using multivariate statistical methods can simplify a complex system by distinguishing major controlling factors and identifying influential processes.

4.1 Characterizing Hydrochemical Variability at the Study Area

Hierarchical cluster analysis was performed on 620 samples and 13 chemical parameters in order to identify multivariate statistical differences between water sample chemistry. The dendogram (Figure 4.1) shows the clustering of samples into two sections, and four major groups (1-4). Nine sub-groups, or clusters, were identified for analysis.

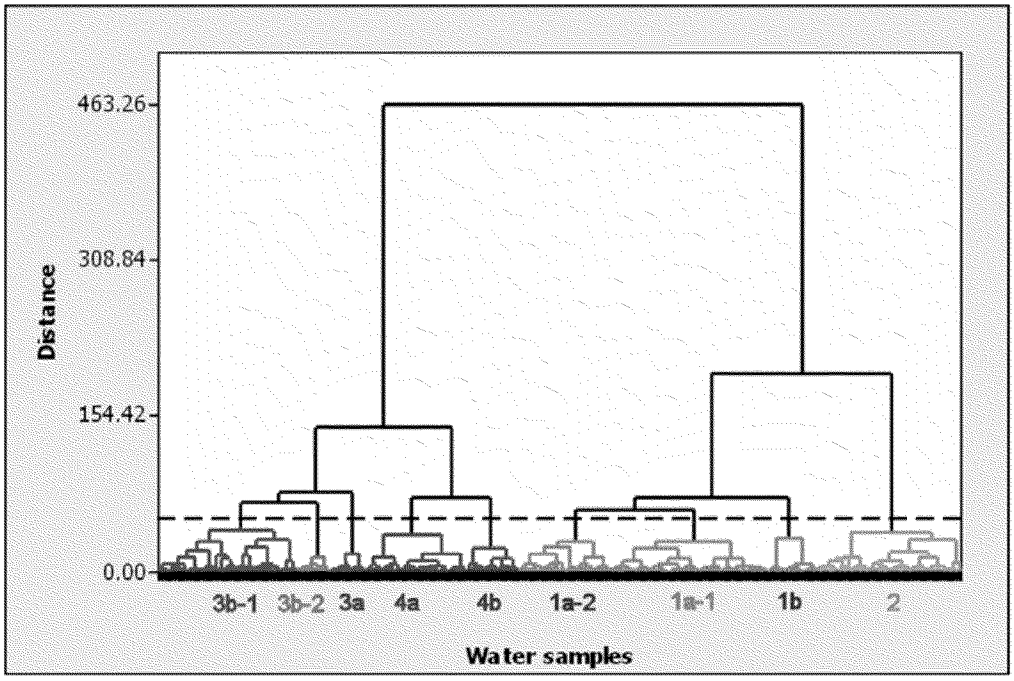

Figure 4.1: Dendogram of hierarchical clustering of 620 water samples. The dashed black line, the phenom line, shows the distance (a measure of degree of similarity) that defines the number of clusters was chosen for analysis.

2017-002976-0000750

Clusters represent groups of samples that are more similar to other samples in the same cluster than to any other sample in the database. The degree of similarity is measured by distance along the y-axis with higher degree of similarity having a lower distance. Mean values of chemical parameters for each cluster are shown in Table 4.1 and plotted in Figure 4.2. Inspection of the mean chemical compositions of clusters allowed for characterization of the main chemical differences between clusters and groups, which can be interpreted as representing distinct hydrochemical facies.

Table 4.1: Mean water chemistry for water clusters. Concentrations in mg/L, except pH in standard units. "Alk" represents alkalinity, as $CaCO_3$. The number of samples in each cluster is indicated by *n*.

Cluster	*n*	Ca	Cl	F	Fe	Alk	K	Mg	Mn	Na	SO_4	TDS	CH_4	pH
		mg/L	*mg/L*	*mg/L*	*mg/L*	*mg/L*	*mg/L*	*mg/L*	*mg/L*	*mg/L*	*mg/L*	*mg/L*	*mg/L*	*s.u.*
1a-1	122	56.3	9.1	0.7	0.2	338.6	3.1	34.8	0.0	53.3	32.4	429.3	0.0	7.7
1a-2	71	77.4	19.6	0.7	0.4	494.2	6.2	55.0	0.0	115.8	129.0	747.5	0.0	7.6
1b	38	56.9	12.5	0.8	1.1	301.2	3.1	27.3	0.1	68.6	63.2	444.8	0.0	8.6
2	112	89.2	16.7	1.1	11.7	454.7	4.5	33.3	1.2	79.5	33.0	542.7	1.8	7.7
3a	28	7.6	208.6	5.2	0.3	244.4	0.6	0.3	0.0	259.6	16.0	655.4	5.7	8.4
3b-1	107	20.7	155.8	3.0	1.6	389.1	4.1	2.7	0.1	445.3	372.7	1280.3	0.8	8.2
3b-2	25	61.6	1052.1	3.9	0.7	200.6	1.9	3.3	0.1	748.2	117.3	2161.6	10.7	7.9
4a	78	52.9	78.1	2.3	0.3	507.0	1.6	25.4	0.0	275.8	181.9	958.8	0.5	7.8
4b	39	159.8	218.6	1.2	5.4	424.2	4.3	72.5	0.5	610.1	1284.7	2636.1	0.5	7.5

4.1.1 Group 1

Group 1 (clusters 1a-1, 1a-2, and 1b) contains waters with lower TDS concentrations. Cluster 1a-1 (122 samples) has a Ca-Na-HCO_3 signature with the lowest mean TDS of all clusters. Cluster 1a-2 (71 samples), has somewhat higher TDS, and has a Na-Ca-HCO_3-SO_4 signature. Cluster 1b (38 samples), shows a similar Na-Ca-HCO_3-SO_4 signature, but with lower TDS and higher pH. Clusters 1a-2 and 1b are similar to the chemistry of cluster 1a-1, however, they show increased sodium and sulfate. All clusters in group 1 have little to no dissolved methane.

4.1.2 Group 2

Cluster 2 (112 samples) comprises group 2, and shows a Ca-Na-HCO_3 signature, with low TDS similar to Cluster 1a-1. However, cluster 2 shows distinctly high iron and manganese concentrations compared to other clusters, and a significant concentration of

2017-002976-0000751

dissolved methane (mean = 1.8 mg/L). Elevated iron, manganese, and methane are all indicators of reducing conditions (Hem, 1985).

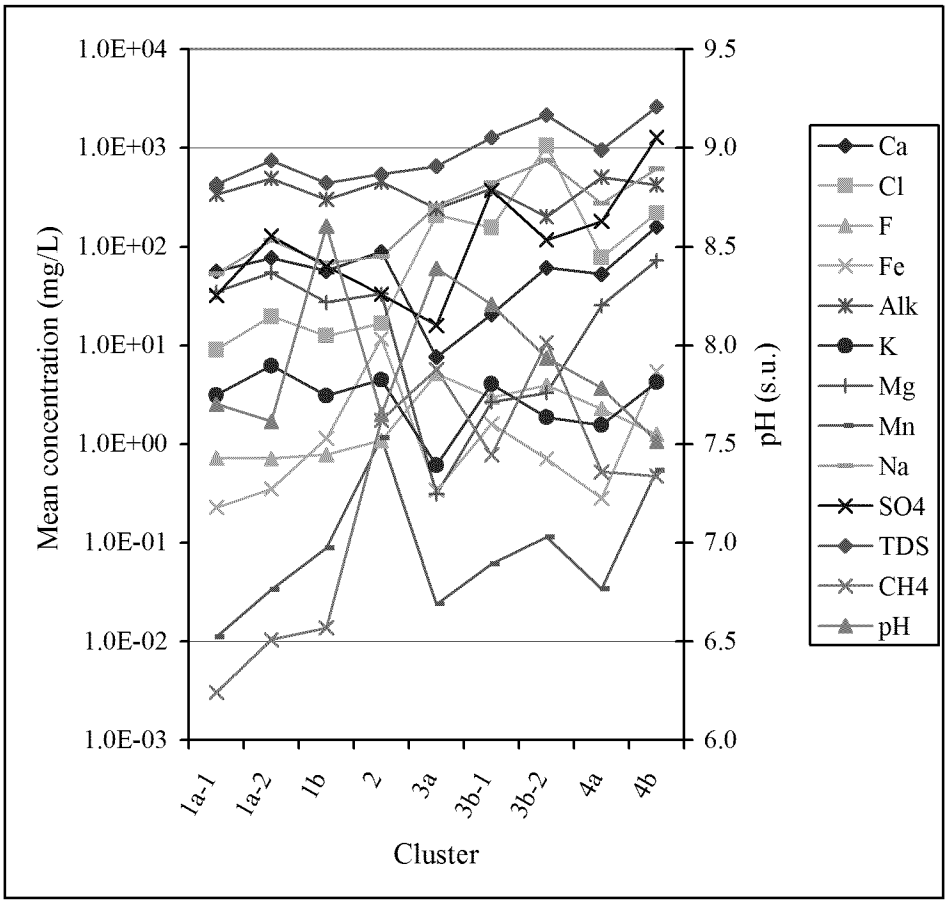

Figure 4.2: Mean concentrations of each of 13 parameters for each cluster. Note the vertical log-scale on left, and secondary axis on right. "Alk" stands for alkalinity.

4.1.3 Group 3

Group 3 contains three clusters that share a Na-Cl component distinct from groups 1 and 2 (Figure 4.2). Cluster 3a (28 samples) has a Na-HCO_3-Cl signature, with moderate TDS. Cluster 3b-1 (107 samples) has a Na-HCO_3-SO_4-Cl signature, with high TDS. This cluster has a higher sulfate component than other clusters in group 3. Cluster 3b-2 (25 samples) has a Na-Cl signature, with high TDS. The most important geologic source of chloride is halite, however, no halite has been observed in the Wasatch Formation near the study area. However, formation water from the gas production zone is Na-Cl-HCO_3

2017-002976-0000752

or Na-Cl in type (Breit, 2002). Cluster 3a, 3b-1, and 3b-2 also have elevated mean dissolved methane values at 5.7, 0.8, and 10.7 mg/L, respectively.

4.1.4 Group 4

Group 4 contains two clusters. Cluster 4a has a Na-HCO_3-SO_4 signature with moderate TDS. Cluster 4b has a Na-SO_4-HCO_3 signature, with high TDS. Cluster 4b has the highest mean sulfate value of all clusters. Both clusters in group 4 have relatively low mean dissolved methane concentrations of 0.5 mg/L.

4.1.5 Piper Diagram

The Piper diagram helps to visualize the similarities and differences in the relative concentrations of major ions between clusters (Figure 4.3). Clusters 1a-1, 1a-2, 1b, and 2 plot close together toward the left of the center diamond, showing the dominance of bicarbonate anion with a mix of cations. Cluster 4a, 3b-1, and 4b show increasing relative sodium and sulfate compared to groups 1 and 2. However, two clusters, 3a and 3b-2, show high relative sodium and relative chloride concentrations greater than 50% of anions.

4.2 Sample Source

Water samples originated from either surface or groundwater sources. Some clusters are composed exclusively of ground or surface waters, while other clusters have samples from both sources. The percent of surface and groundwater samples represented in each cluster is shown in Table 4.2 and Figure 4.4. Overall, group 1 has the highest percentage of surface water samples. Cluster 1b is entirely composed of surface water samples, and closely related clusters 1a-1 and 1a-2 each have 29% and 36% surface water samples respectively. This suggests that group 1 samples represent areas where surface water and groundwater may be significantly connected. Cluster 2 also suggests shared water chemistry between surface and groundwater. Group 3 primarily represents groundwater. Group 4 also has a small proportion of surface water samples, 17% in cluster 4a and 5% in cluster 4b. Of these samples 40% are spring, 13% are pond, and

2017-002976-0000753

47% are river samples. These surface water samples, especially the springs, may be fed by groundwater traveling along natural conduits, such as faults or fractures.

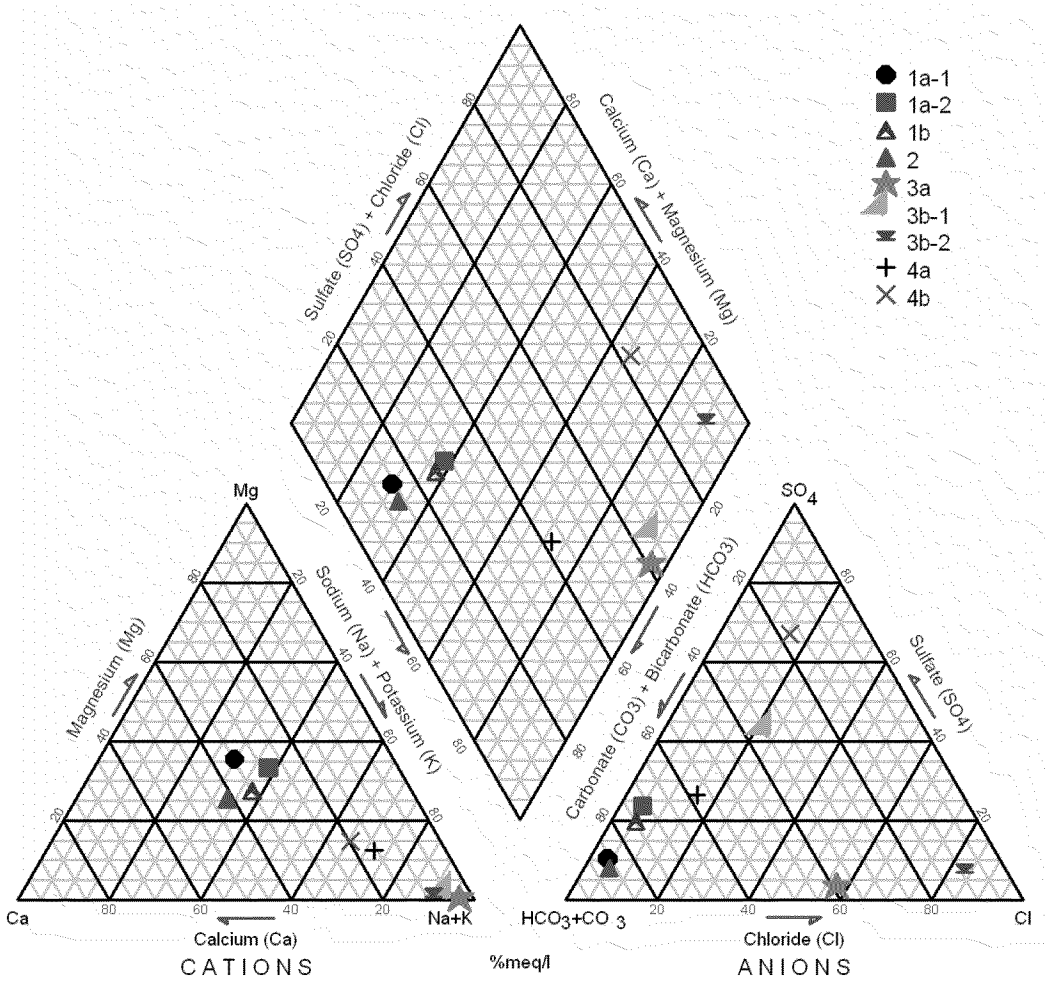

Figure 4.3: Piper diagram showing relative concentrations of major ions by cluster.

Table 4.2: Percentage of surface and groundwater samples by cluster.

Cluster	Groundwater	Surface Water
1a-1	71%	29%
1a-2	63%	37%
1b	0%	100%
2	77%	23%
3a	100%	0%
3b-1	97%	3%
3b-2	100%	0%
4a	83%	17%
4b	95%	5%

2017-002976-0000754

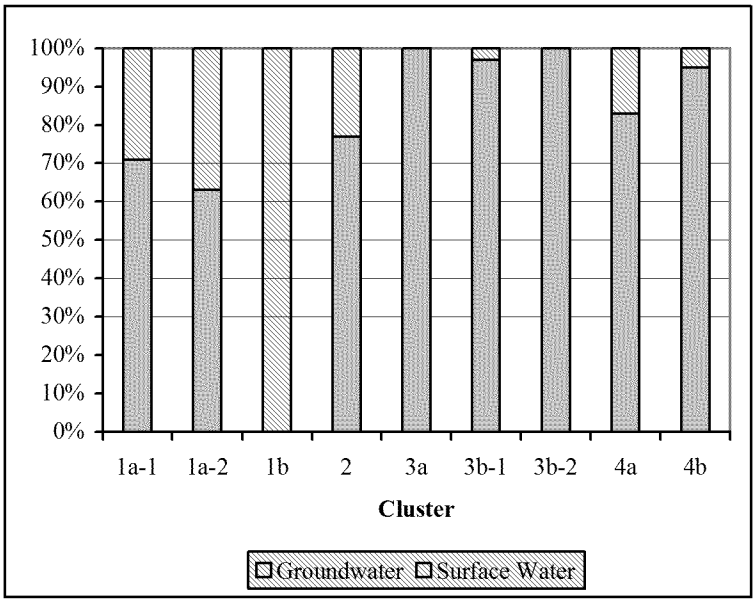

Figure 4.4: Percentage of surface and groundwater samples by cluster.

4.3 Spatial Analysis

Hydrochemical clusters were plotted by group in ArcGIS 9.0 with lithologic contacts and major structural features to determine if water chemistry is correlated with geologic features (Figures 4.5-4.8). Major structural features were derived from Tremain and Tyler (1995) and URS (2006). Lithologic contacts are from URS (2006).

Adequate and impartial spatial coverage over the study area is not attained by the selected samples, especially in the central, southwest, and northern areas. Clusters do not appear to have strong lithologic preferences. All clusters occur in multiple areas, except clusters 2 and 3b-2, which occur only in the Atwell Gulch and Molina-like members, respectively.

Group 1 samples occur more often on the western side of the study area in the uppermost Shire member (Figure 4.5). Group 1 samples are often found on alluvial plains or stream valleys where alluvial aquifers may experience some recharge by stream losses or precipitation. Cluster 1a-2, with higher TDS relative to other group 1 clusters, is located further down flowpaths toward the center of the study area (see section 2.2.3.1).

Cluster 2 samples are strongly grouped on West Divide Creek in the eastern portion of the study area (Figure 4.6). As expected, the main location of these samples

2017-002976-0000755

correlates precisely to the location of the West Divide Creek gas seep since many of these samples were collected in response to the seep. Some cluster 2 samples occur upstream on West Divide Creek or on East Divide Creek, however, deviation from the central location is relatively small.

Group 3 samples are generally found more often on the eastern side of the study area, but are not confined to this area (Figure 4.7). Cluster 3b-2 is found primarily in the Molina member, however, clusters 3a and 3b-1 contain a Na-Cl component similar to cluster 3b-2, and are found in all three members of the Wasatch Formation.

Group 4 samples form a cluster near the nose of the Divide Creek anticline, in the Molina-like member of the Wasatch Formation (Figure 4.8). Cluster 4a samples are generally found on the eastern side of the study area. However, many cluster 4b samples are found in close proximity to traces of major faults and fractures in the central and western portions of the study area, as well as near the nose of the anticline.

Only major structural features were transcribed over the study area. However, the Wasatch Formation and Mesaverde Group have experienced multiple episodes of structural deformation and exhibit local fracture sets in multiple orientations. The Divide Creek anticline may provide enhanced transport pathways along fractures and thinning of the Wasatch Formation due to erosion of the Shire member. Due to the incomplete sample coverage over the area, a strong correlation between cluster chemistry and lithologic units cannot be confirmed. However, cluster 4b does appear to be structurally controlled, and cluster 2 is spatially distinct in the area of the West Divide Creek seep.

4.3.0 Spatial Analysis of Chemical Parameters

Important chemical parameters were investigated spatially over the study area to determine if spatial trends exist. Concentrations of individual parameters were contoured in ArcGIS using the inverse distance method of data interpolation. However, sampling locations show that data is limited in the central and southwestern sections of the study area. TDS concentrations are contoured over the study area in Figure 4.9.

Increasing TDS is a good indicator of water evolution (Drever, 1997). Waters appear less evolved toward the southwest corner of the study area and more evolved in

2017-002976-0000756

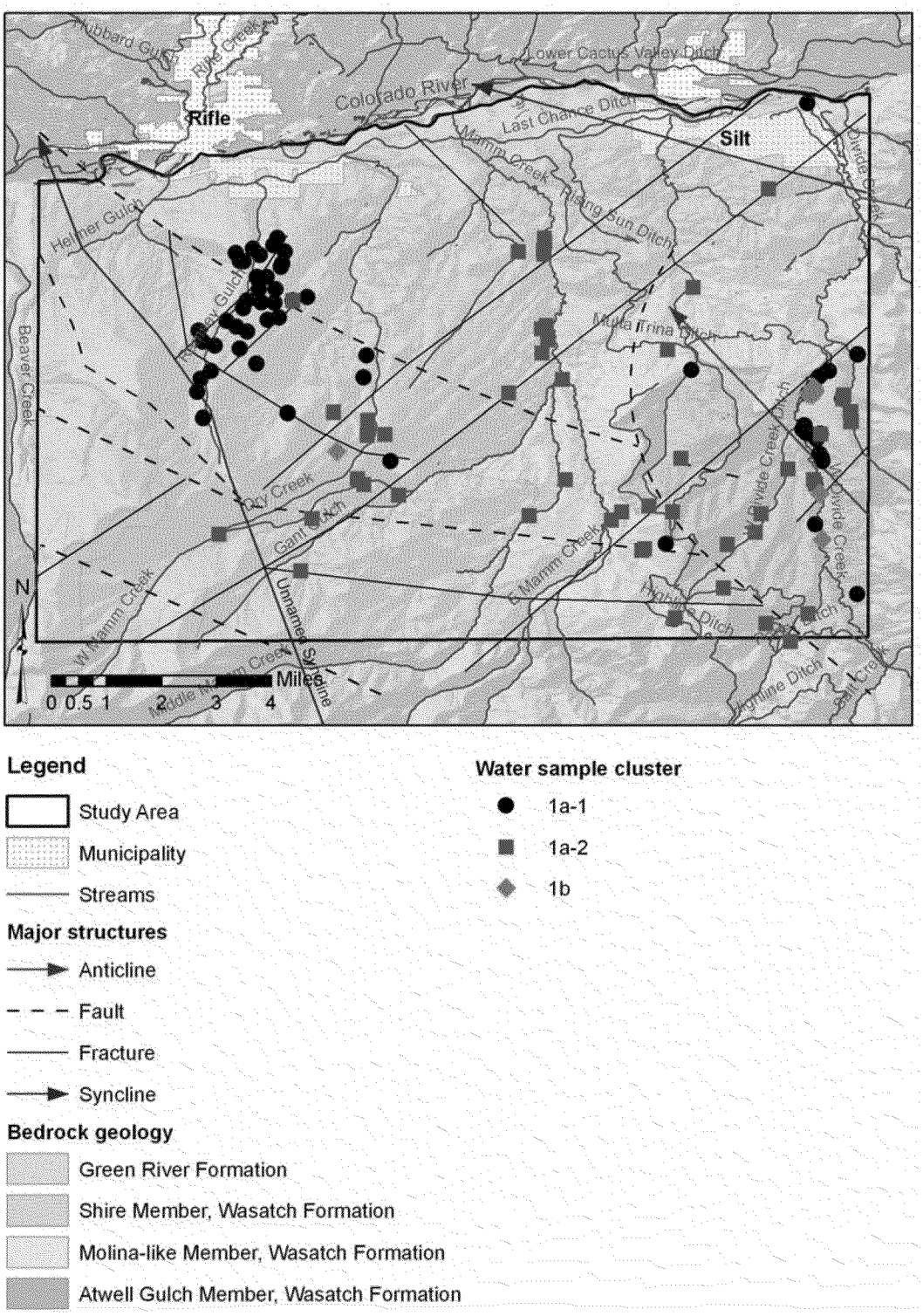

Figure 4.5: Spatial distribution of clusters in group 1 over the study area, with bedrock geology and major structural features. Lithology from URS (2006); structural features modified from Tremain and Tyler (1997) and URS (2006).

2017-002976-0000757

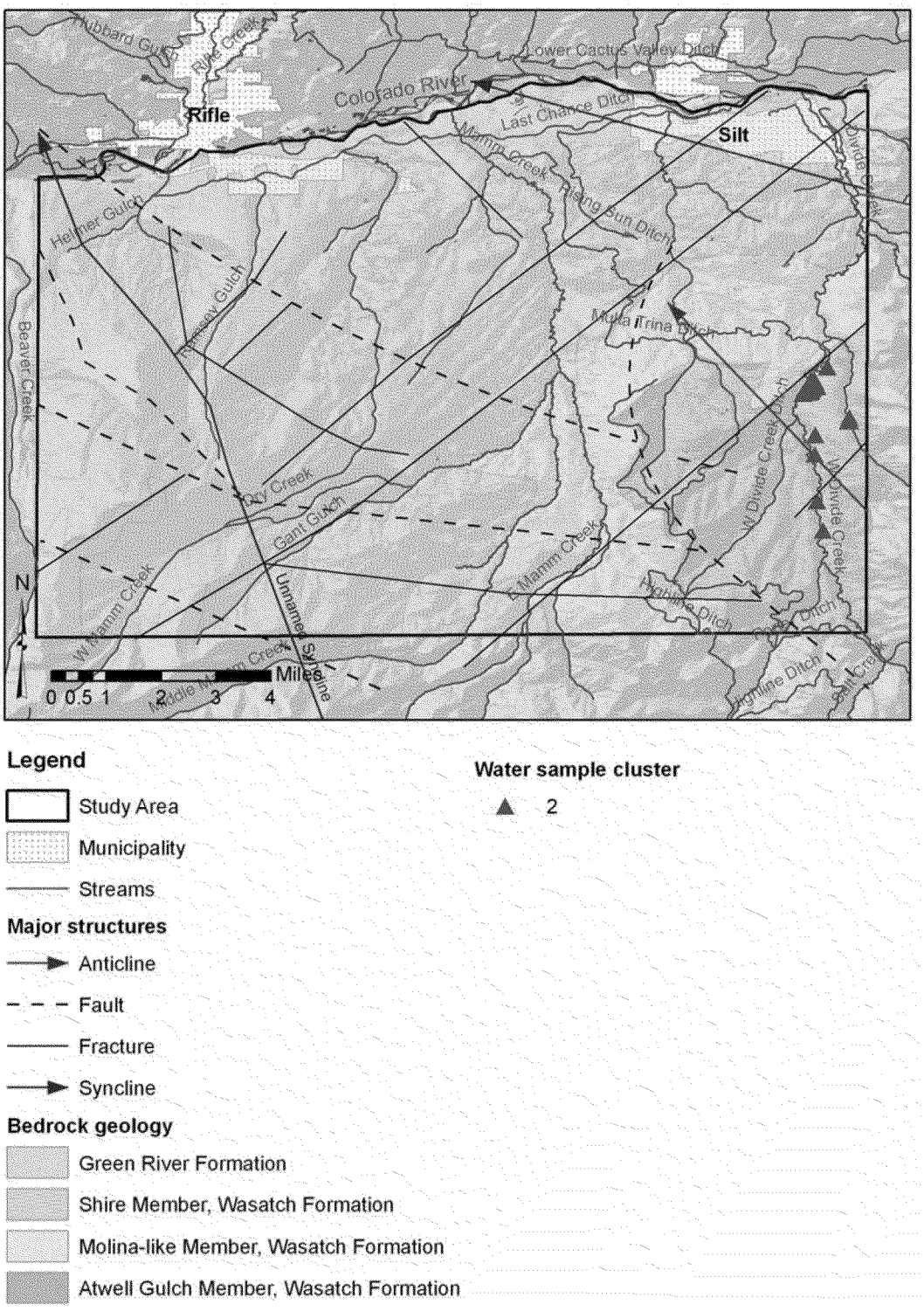

Figure 4.6: Spatial distribution of group 2 over the study area, with bedrock geology and major structural features. Lithology from URS (2006); structural features modified from Tremain and Tyler (1997) and URS (2006).

2017-002976-0000758

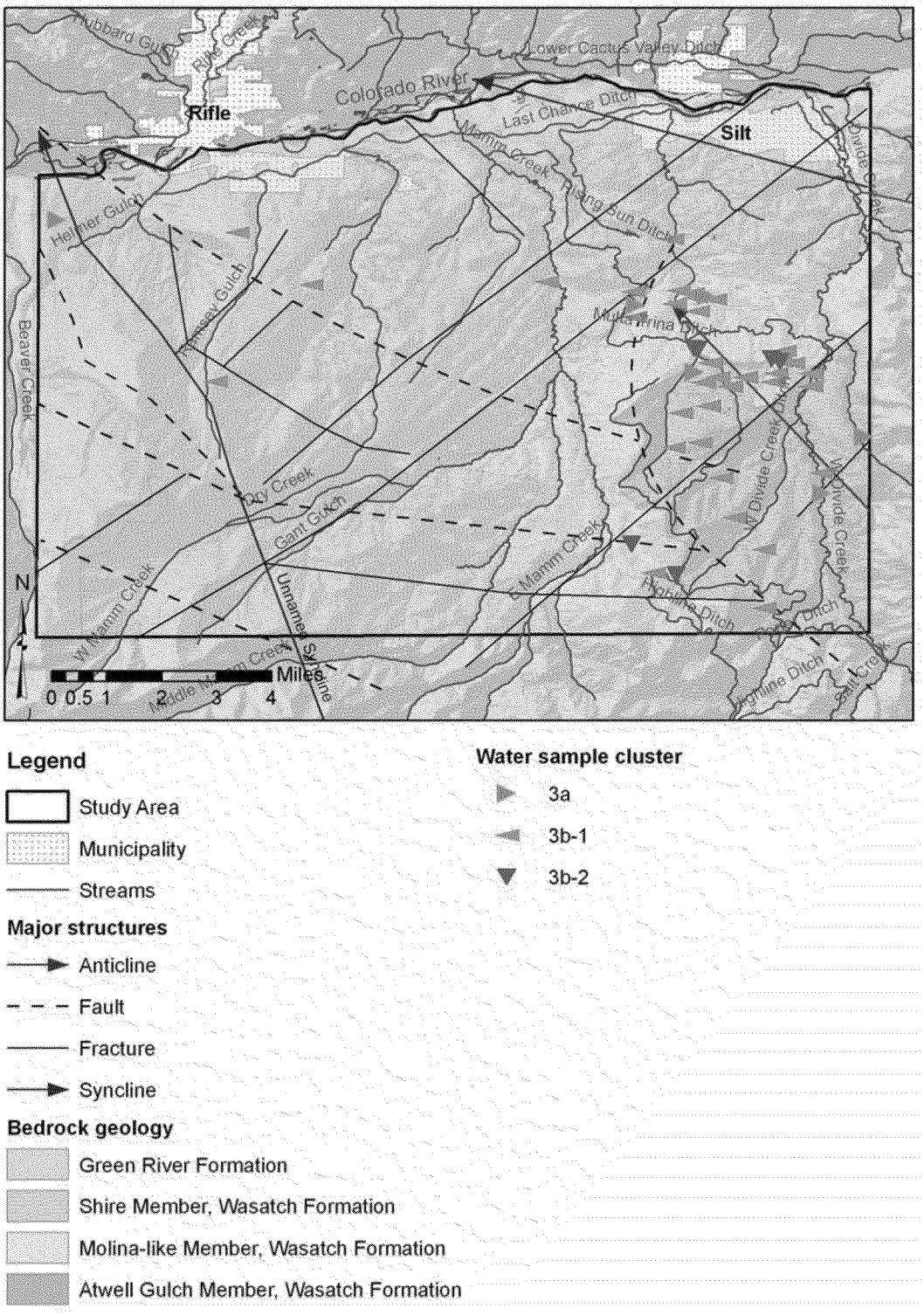

Figure 4.7: Spatial distribution of clusters in group 3 over the study area, with bedrock geology and major structural features. Lithology from URS (2006); structural features modified from Tremain and Tyler (1997) and URS (2006).

2017-002976-0000759

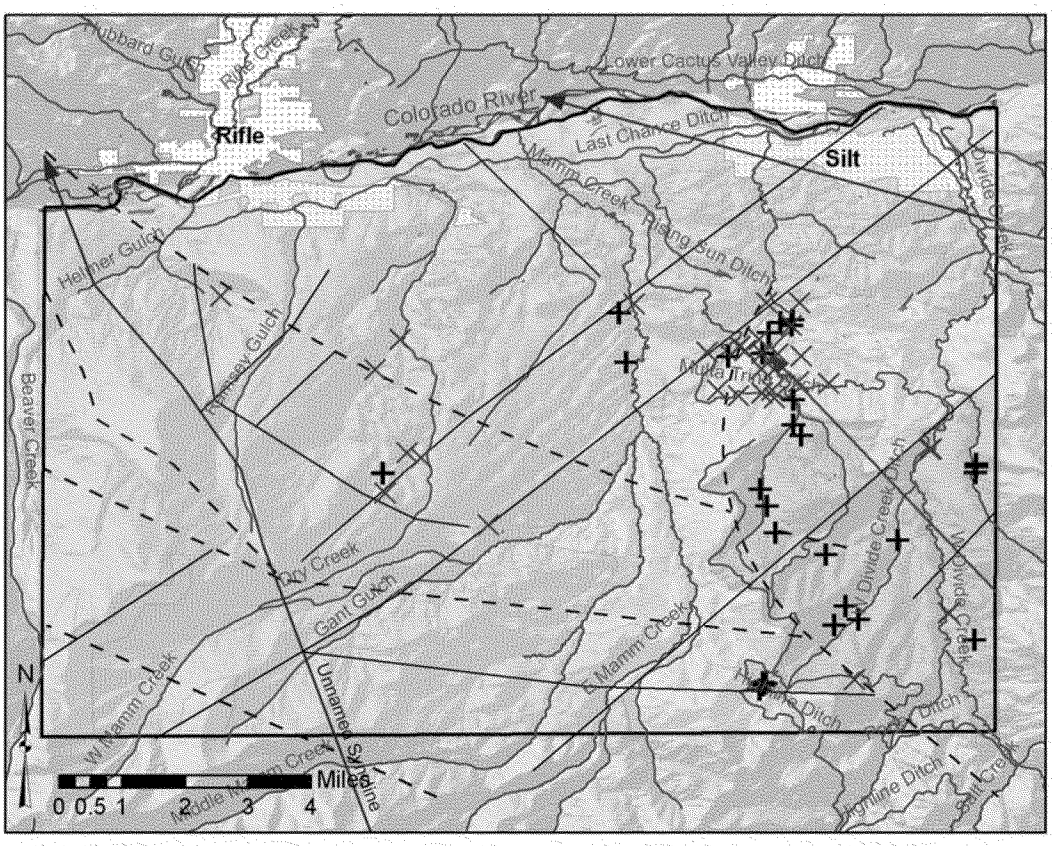

Legend

- Study Area
- Municipality
- Streams

Major structures

- Anticline
- Fault
- Fracture
- Syncline

Bedrock geology

- Green River Formation
- Shire Member, Wasatch Formation
- Molina-like Member, Wasatch Formation
- Atwell Gulch Member, Wasatch Formation

Water sample cluster

- 4a
- 4b

Figure 4.8: Spatial distribution of clusters in group 4 over the study area, with bedrock geology and major structural features. Lithology from URS (2006); structural features modified from Tremain and Tyler (1997) and URS (2006).

2017-002976-0000760

the northeast and eastern portions of the study area, which is likely due in combination to regional flowpath directions and upheaval of older Wasatch members to the ground surface in the vicinity of the Divide Creek anticline. The highest TDS values in the study area occur near the nose of the anticline. Individual points of anomalously high sodium concentrations are typically samples from cluster 4b that correlate with major structural features (see Figure 4.8).

Chloride may be an indicator of impact by formation water, since major geologic sources of chloride are not present in the study area. Chloride concentrations are contoured over the study area in Figure 4.10. Chloride concentrations over the study area show higher chloride in the eastern and northeastern portions of the study area. Samples from cluster 3b-2 show the highest chloride concentrations to the east. Anomalous points with elevated chloride concentrations in the central and west parts of the study area are typically samples from cluster 4b that correlate with major structural features (see Figure 4.8). Some of these samples also show anomalously high TDS concentrations (see Figure 4.9). The occurrence of high chloride concentrations is only moderately cohesive with water evolution trends.

Methane may be an indicator of impact from the gas production interval. Methane concentrations are contoured over the study area in Figure 4.11. Methane is generally very low throughout the central and southwest portions of the study area. To the east and southeast, higher methane concentrations occur, and correlate with group 3 samples. One high methane sample is found on the west side of the study area as well. The occurrence of high methane appears somewhat correlated with high chloride concentrations in group 3 samples, but not with water evolution trends.

4.4 Controls of Dataset Variability

Principal component analysis (PCA) was performed on normalized and standardized data for selected parameters including alkalinity, calcium, chloride, fluoride, iron, potassium, magnesium, manganese, sodium, sulfate, dissolved methane, pH, and TDS. Principal component analysis reduces the variability of the dataset into fewer variables, and the axes derived by the process may represent influential hydrochemical processes or source contributions. The first five principal components account for over

2017-002976-0000761

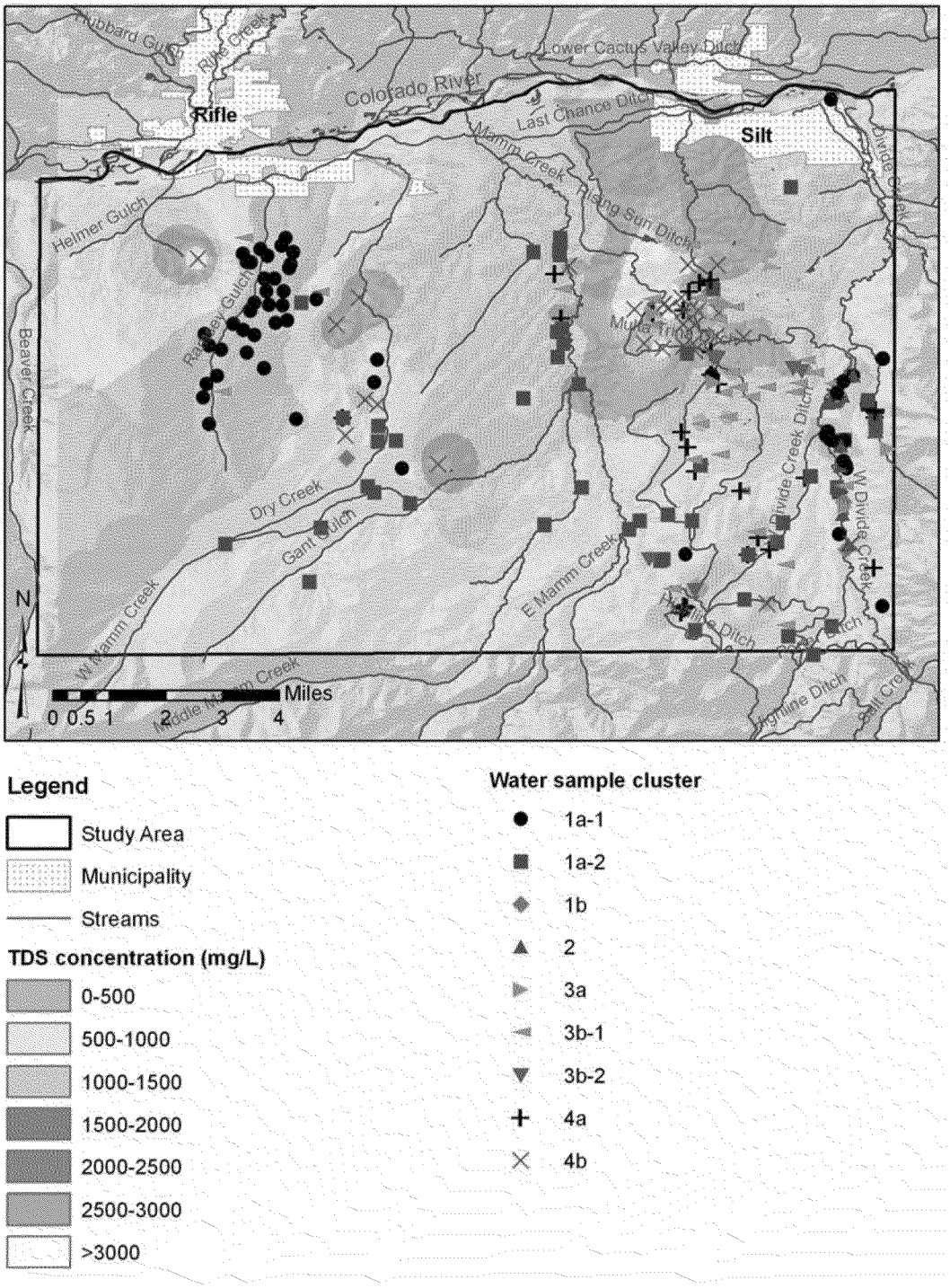

Figure 4.9: TDS concentrations contoured by inverse distance over the study area with water samples plotted by cluster. Note the lack of data points in the southwest, central and northern portions of the study area. Usability of interpolated contours in these areas is limited. Groundwater flow is generally to the north.

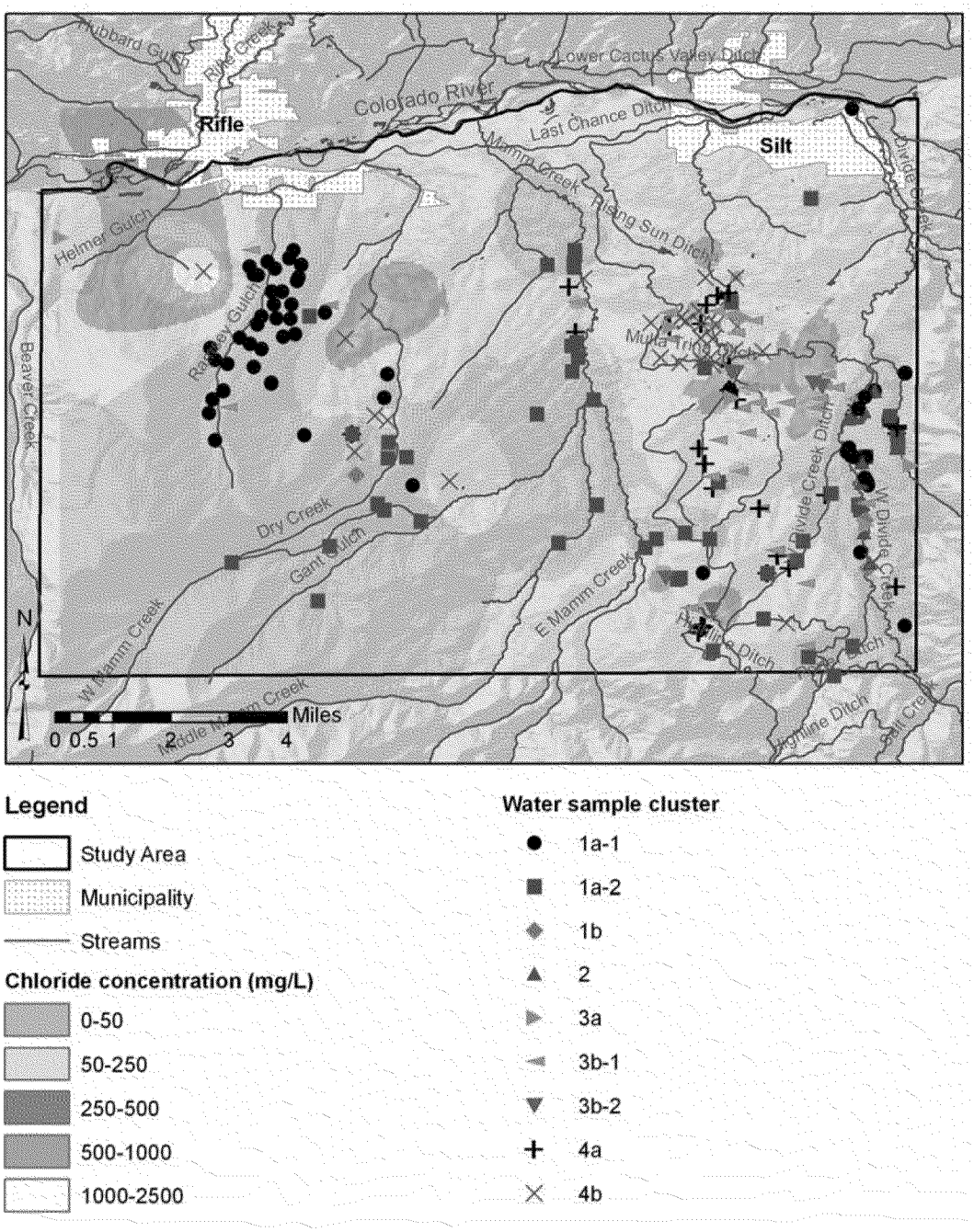

Figure 4.10: Chloride concentrations contoured over the study area with water samples by cluster. Note the lack of data points in the southwest, central and northern portions of the study area. Usability of interpolated contours in these areas is limited.

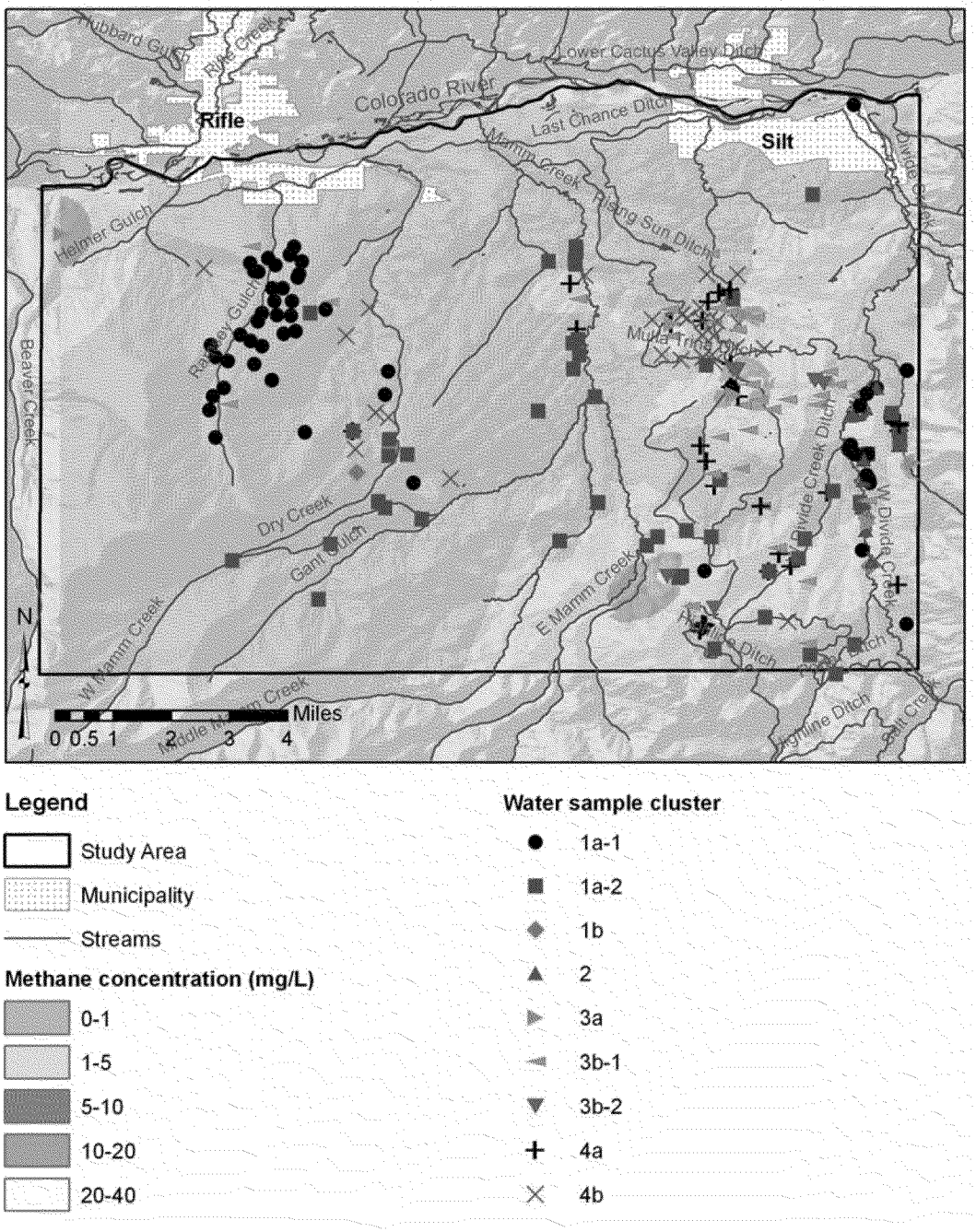

Figure 4.11: Dissolved methane concentrations contoured over the study area with water samples by cluster. Note the lack of data points in the southwest, central and northern portions of the study area. Usability of interpolated contours in these areas is limited.

80% of the total variance in the data. Table 4.3 summarizes the loading of each parameter on the first five principal components, and the proportion of variance explained by each.

Table 4.3: Loading of each parameter on the first five principal components (PC), and the percent of variance explained.

Parameter	PC1	PC2	PC3	PC4	PC5
Alkalinity, as $CaCO_3$	-0.087	-0.296	0.178	-0.563	-0.64
Calcium	-0.282	-0.374	0.045	0.347	0.109
Chlorine	0.395	-0.204	-0.001	0.241	0.147
Fluorine	0.374	-0.021	-0.174	0.05	-0.172
Iron	-0.113	-0.31	-0.465	-0.189	0.117
Potassium	-0.281	-0.253	0.046	-0.099	0.418
Magnesium	-0.383	-0.25	0.163	0.043	0.01
Manganese	-0.076	-0.391	-0.47	-0.107	0.004
Sodium	0.4	-0.254	0.124	-0.044	-0.001
Sulfate	0.192	-0.288	0.43	-0.163	0.145
Methane	0.2	-0.12	-0.452	0.168	-0.22
pH	0.193	0.168	-0.14	-0.615	0.506
TDS	0.312	-0.406	0.212	0.088	0.112
Percent of variance explained by PC	35.1%	18.0%	16.5%	7.3%	6.7%
Cumulative percent of variance explained by PC	35.1%	53.1%	69.6%	76.9%	83.6%

Parameters with a higher loading magnitude control a greater proportion of the principal component. As Table 4.3 shows, control of principal components is typically due to a combination of multiple chemical parameters.

The first principal component contains 35.1% of the dataset's variance, and can be attributed to Na, Cl, F, and TDS inversely coupled with magnesium. Since halite is not present in the study area, the preliminary hypothesis for the principal component is that it represents a Na-Cl component possibly supplied by deeper formation waters from the Williams Fork. The second principal component represents 18.0% of the variance, and is primarily a TDS, Mn, Ca, and Fe component. The preliminary hypothesis for this PC is it represents products of natural weathering (TDS and Ca) and redox indicators (Mn and Fe). The third principal component contains 16.5% of the variance, and can be attributed to Mn, Fe, and dissolved methane, inversely coupled with sulfate. This combination of parameters is the anticipated result of redox reactions involving electron acceptors and an

2017-002976-0000765

organic substrate. A summary of preliminary interpretations for the first three principal components is shown in Table 4.4.

Table 4.4: Summary of preliminary interpretations for the first three principal components.

Principal component	Controlling parameters	Preliminary interpretation
PC1	Na, Cl, F, (-Mg), TDS	Deep formation water
PC2	TDS, Mn, Ca, Fe	Natural evolution and redox reactions
PC3	Mn, Fe, CH4, (-SO4)	Redox reactions

The fourth principal component contains 7.3% of the dataset's variance, and shows the coupled control of alkalinity and pH. The fifth principal component controls 6.7% of the variance, and can be attributed to alkalinity, pH and potassium. Of the first five principal components, none appears to directly represent the expected natural hydrochemical evolution in the study area, that of group 1.

4.4.0 Interaction Between Hydrochemical Clusters

Water samples were plotted by cluster in principal component space to visualize the correlation and degree of continuity between the clusters on principal component axes. Figures 4.11 and 4.12 show the relationships between hydrochemical clusters in principal component space. General overlap of clusters indicates gradational changes in water chemistry throughout the dataset, which may be due to mixing between different source waters in contrast to clearly separated clusters that may indicate distinctly different processes. PC1 (Figure 4.12) distinctly separates group 3, on the right, from groups 1 and 2, on the left, based on Na, Cl, F, and TDS. Clusters 3a and 3b-2 seem to have more unique, end-member compositions, whereas cluster 3b-1 has some transitional samples that extend toward the left, in the vicinity of groups 1 and 2. Group 4, however, has a large variability along the Na-Cl-(-Mg)-F-TDS axis. The PC2 axis separates cluster 1a-1 from 2, and 3a from 3b-2, as well as 4a from 4b.

In Figure 4.13, clusters 3a and 3b-2 plot together in low PC3 and high PC1 space, showing the influence of a Na-Cl source as well as a reducing environment. Cluster 2 is also affected by redox reactions, however, not by the Na-Cl-F-TDS component. Cluster

2017-002976-0000766

1b appears related to cluster 2 in terms of redox indicators. Clusters 1a-1, 1a-2, 4a, and 4b are least affected by redox reactions. Cluster 3b-1, again shows transitional behavior between the other group 3 clusters and group 4.

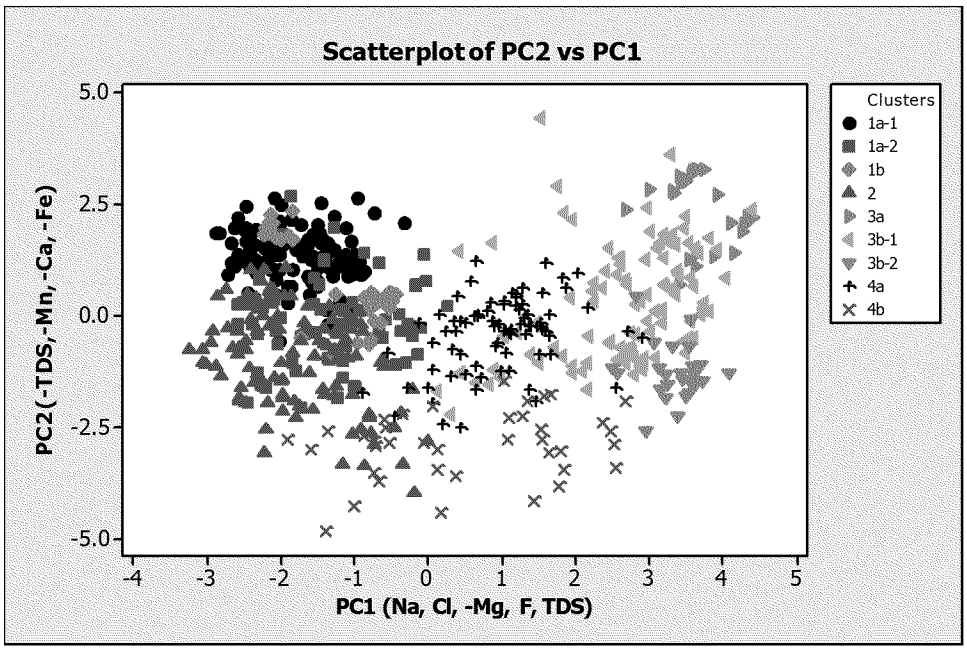

Figure 4.12: Scatterplot of clusters in PC2 vs. PC1 space. The primary parameters controlling each principal component are shown on their respective axes.

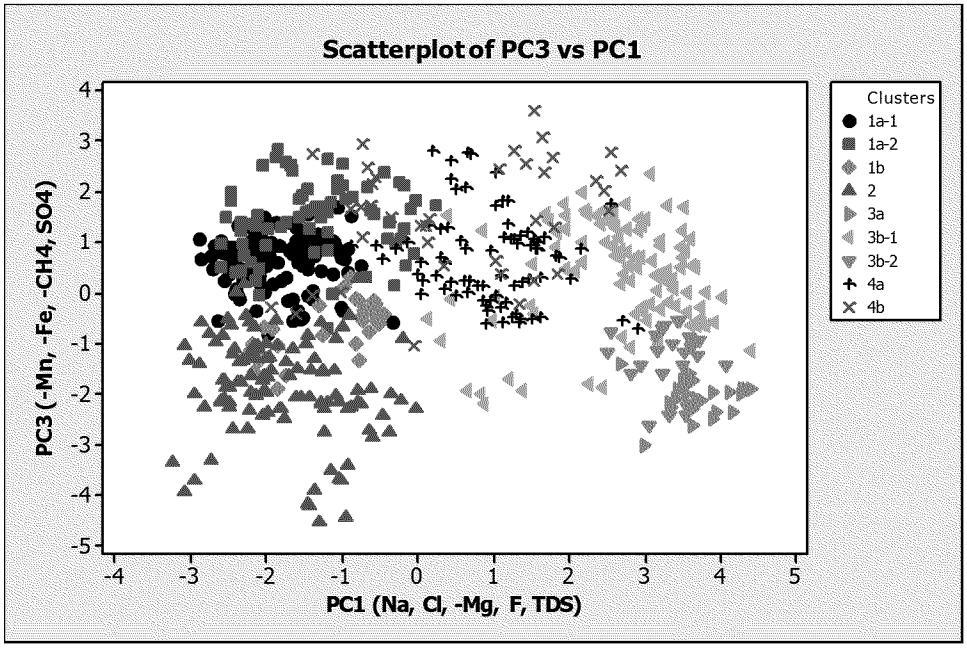

Figure 4.13: Scatterplot of clusters in PC3 vs. PC1 space. The primary parameters controlling each principal component are shown on their respective axes.

2017-002976-0000767

CHAPTER 5: HYDROCHEMICAL CONCEPTUAL MODEL

Characterization of hydrochemical variability leads to the construction of a hydrochemical conceptual model relating chemical characteristics to possible natural and/or anthropogenic causes. This model will be tested in Chapter 6.

5.1 Background Water Chemistry

For this study, "background" water is defined as that which occurs in areas that have experienced little to no oil and gas exploration. However, this definition of "background" does not exclude the effects of other anthropogenic impacts. Background waters are not necessarily less evolved waters, and in the study area they may show both low and high TDS.

Low TDS, background waters can be represented by cluster 1a-1, which shows the lowest salinity, a low chloride concentration, and low dissolved methane. Cluster 1a-1 also represents waters that are less evolved. Cluster 1a-2 is similar to 1a-1, but is slightly more evolved, as it shows higher sodium, sulfate, and TDS. Less evolved background waters occur closer to the edges of the study area, while cluster 1a-2 occurs more often toward the center of the study area, down the hydrological gradient. Figure 5.1 shows that water samples in the study area show a general increase in sodium concentration with TDS, and therefore, sodium concentration can be a good general indicator of water evolution in this area.

Sodium may be gained from cation exchange reactions with clay minerals in mudstones of the Wasatch Formation (Hem, 1985). Cluster 1b represents only surface water, and shows a similar chemical composition to cluster 1a-1. The close geochemical relationship between these clusters also indicates the close hydrological coupling between the groundwater and surface water at the sample locations.

2017-002976-0000768

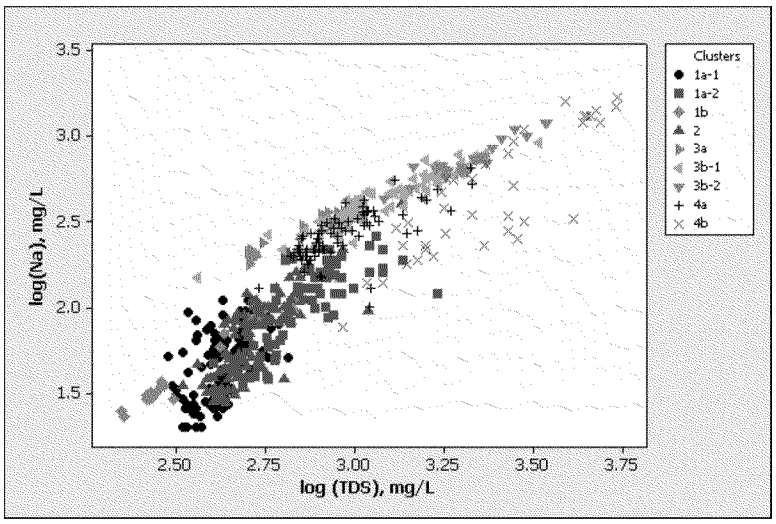

Figure 5.1: Log-log plot of sodium versus total dissolved solids (TDS) concentration. Points symbolized by cluster.

Group 4 is tentatively identified as characterizing high TDS background waters. Cluster 4a and 4b show elevated sodium and sulfate levels compared to other clusters, which may be due to progression of water-rock interactions during longer residence times, such as pyrite oxidation, dissolution of gypsum, or cation exchange. Longer contact time is consistent with the high proportion of groundwater samples in those clusters. Cluster 4b appears to be structurally controlled (see Figure 4.8), which suggests that its chemistry could be due to upward migration of high TDS, groundwater along natural pathways. Alternatively, since clusters 4a and 4b (as well as clusters 3b-1, 1a-2, and 1a-1) also show slightly elevated mean nitrate levels (Table 5.1), they may be impacted by another anthropogenic source, such as irrigation return flow or septic tank effluent (Hem, 1985). However, testing anthropogenic sources, other than those related to natural gas production is not part of the scope of this project.

5.2 Impacted Water Chemistry

The third principal component shows the control of redox reactions on clusters 2, 3a, 3b-1, and 3b-2, and the first principal component distinctly separates group 3 clusters from low TDS background waters on the basis of Na, Cl, (-Mg), F, and TDS. There is some overlap between group 4 samples and group 3 samples, which may indicate coexisting hydrochemical controls or significant mixing.

2017-002976-0000769

Table 5.1: Mean nitrate concentrations by cluster.

Cluster	Nitrate *mg/L*
1a-1	4.3
1a-2	8.8
1b	0.1
2	0.6
3a	0.1
3b-1	14.4
3b-2	1.2
4a	12.6
4b	5.9

The spatial correlation of cluster 2 samples with the West Divide Creek seep identifies this cluster's distinctive water chemistry as representing at least one type of impact by thermogenic methane gas and drilling fluids on surface and groundwater (COGCC, 2006). Cluster 2 shows elevated iron, manganese, and methane, however, its major ion chemistry is similar to background water quality, which suggests that the only impact incurred was loading of natural gas and organic compounds into normal background water.

A plot of sulfate concentration versus TDS (Figure 5.2) shows that some samples from cluster 2, as well as clusters 3a, 3b-1, and 3b-2, appear to have depleted sulfate, consistent with sulfate-reduction redox reactions. This result correlates with the combined control of multiple redox indicators on the third PC (see section 4.4).

Group 3 samples are distinguished from other clusters by PC1, indicating relatively elevated Na, Cl, F, and TDS, and in some cases, by the redox indicators represented by PC3. Clusters 3a and 3b-2 show a distinctive Na-Cl signature, as well as high mean dissolved methane concentrations. Evaporite minerals, such as halite, are the most important geologic sources of chloride, however, since halite is not present in the lithology of the Wasatch Formation, the only known alternate source of chloride in the study area is the formation water of the Williams Fork Formation (Hem, 1985; URS, 2006). The source of dissolved methane in groups 2 and 3 may also be natural gas reservoirs of the Williams Fork Formation (primarily thermogenic type), CO_2-reduction of marine organic material (biogenic type), or bacterial fermentation in the shallow subsurface (biogenic type). However, since the occurrence of dissolved methane is

2017-002976-0000770

coupled with the chemical signature of the formation water from the gas-producing interval in group 3, the preliminary hypothesis is that both signatures are derived from the same mechanism. Since group 3 samples do not appear to be structurally controlled, they suggest that formation or produced water from the Williams Fork may have migrated into the shallower portions of Wasatch Formation assisted by vertical conduits provided by natural gas wells with ineffective cementation or casing.

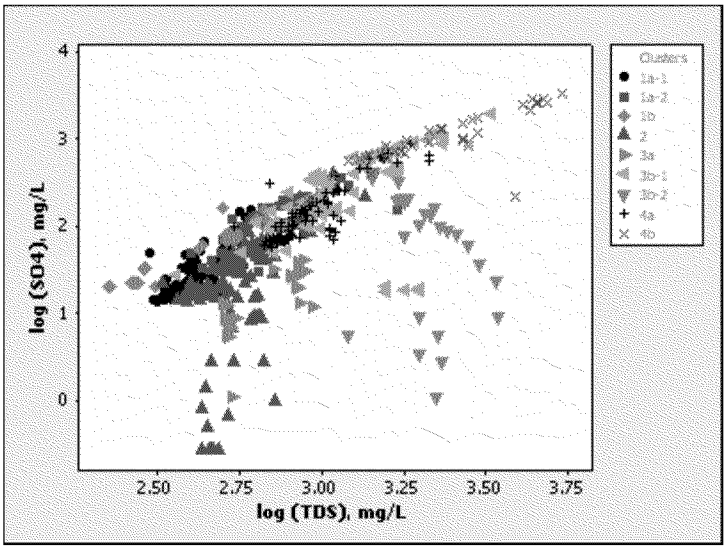

Figure 5.2: Log-log plot of sulfate versus TDS concentration. Points symbolized by cluster.

Figure 5.3 shows mean values by cluster for sodium versus TDS, including two samples of produced water from the Williams Fork Formation of Na-Cl and Na-Cl-HCO_3 type (see Table 6.8). Assuming conservative mixing, a mixing line between produced water compositions and low TDS background water (cluster 1a-1) shows that all clusters fall reasonably well onto this trend. Clusters 3a, 4a, and 3b-1 show slightly elevated sodium from the mixing line, which could indicate the influence of cation exchange reactions with clay minerals in the Wasatch Formation.

Figure 5.4 shows the relationship between the mean chloride and TDS concentrations by cluster. Again, a conservative mixing curve between produced waters (PW-A and PW-B) and low TDS background water (cluster 1a-1) indicates good correlation with most observed clusters. Figures 5.3 and 5.4 suggest that mixing with

2017-002976-0000771

produced water may be an important process that influences the hydrochemical variability of samples in the study area.

The complex water chemistry of the area suggests that multiple natural processes, such as water-rock interaction and cation exchange, as well as anthropogenic inputs from natural gas production, including methane gas and produced water may influence hydrochemistry in the study area. This hypothesis will be tested in Chapter 6.

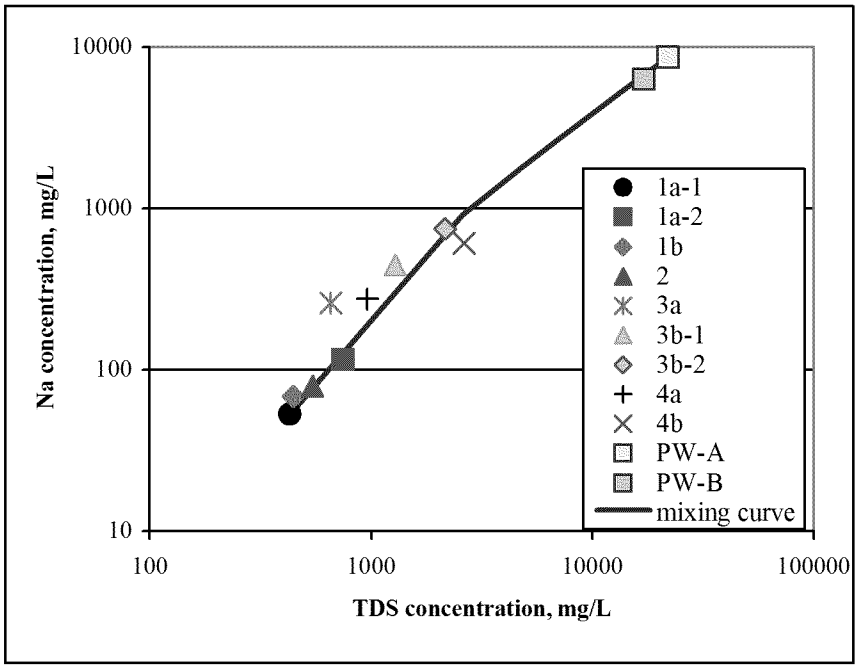

Figure 5.3: Plot of mean sodium versus TDS concentrations, with conservative mixing curve. PW-A and PW-B are produced water compositions from the study area.

2017-002976-0000772

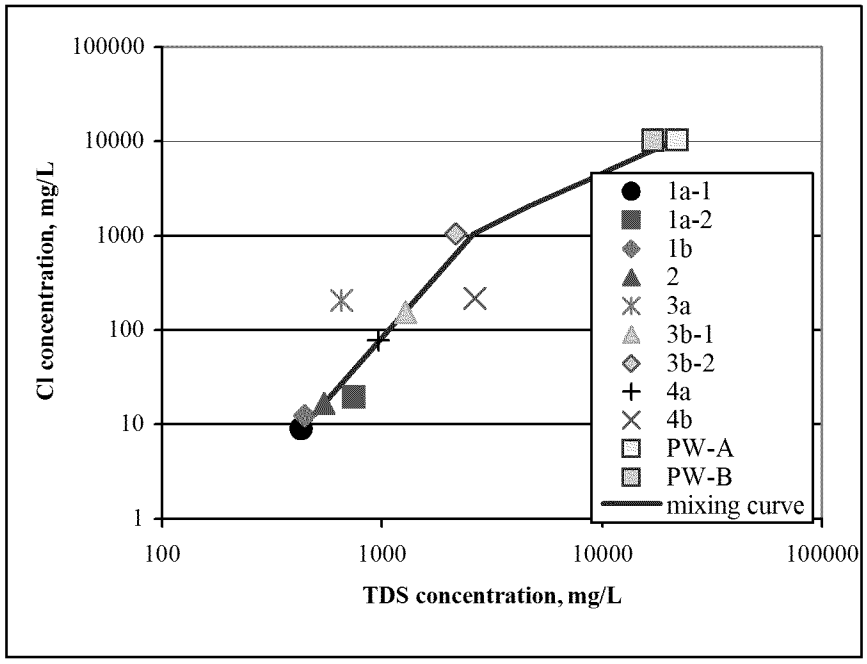

Figure 5.4: Log-log plot of mean molar sulfate-chloride ratio versus chloride concentration for each cluster. PW-A and PW-B are produced water compositions. The dashed line indicates hypothetical mixing.

CHAPTER 6: TESTING THE HYDROCHEMICAL CONCEPTUAL MODEL

In order to test the hydrochemical conceptual model, regional water quality was considered, temporal and spatio-temporal trends and relationships were investigated, and geochemical modeling was conducted. Each of these analyses provides additional information that helps determine whether impact by natural gas production has occurred in the study area.

6.1 Establishing a Regional Context for the Observed Hydrochemistry

Studies completed by S.S. Papadopulos and Associates, Inc. (SSPA) and Cordilleran Compliance Services, Inc. in the spring of 2007 provide insight into regional water quality conditions in areas near the study area that have experienced little to no petroleum development. SSPA (2007) studied the area north of the Colorado River, between the towns of New Castle and Rifle. A portion of this area lies directly north of the study area. Cordilleran Compliance Services, Inc. (2007) studied the Battlement Mesa area, directly southwest of the study area.

6.1.1 SSPA Dataset

SSPA conducted a baseline water quality study on data collected by the COGCC between 1996 and 2005, and conducted additional water quality sampling of 70 groundwater supply wells in 2006. Samples were analyzed for major and minor ions, physical parameters, benzene, toluene, ethylbenzene, and xylene (BTEX), methyl-tertiary-butyl-ether (MTBE), dissolved methane, some stable isotopes, and some gas composition parameters. Their study area has experienced "little previous drilling activity and has no producing oil and gas wells" (S.S. Papadopulos & Associates, 2007).

The 70 groundwater samples collected by SSPA were characterized in this study by hierarchical clustering (see Appendix C). Clustering was conducted based on normalized and standardized data for pH, bicarbonate, calcium, chloride, fluoride,

2017-002976-0000774

magnesium, manganese, sodium, sulfate and TDS. Potassium and iron were removed since they have greater than 40% censored values (50% and 81%, respectively). Other parameters with censored values include chloride (4%), fluoride (19%), and manganese (31%), which were estimated according to Sanford et al. (1993) (see section 3.1.3). Clustering in Minitab 14 was conducted using Ward linkage method and Euclidean distance measurement (see section 3.2.0).

Clustering produced two main clusters (Figure 6.1). One cluster, SSPA 1 (31 samples), has a moderate TDS, Na-HCO_3-SO_4 signature. SSPA 2 (39 samples) shows a more evolved signature, with high TDS, and a Na-SO_4-HCO_3 type (see Table 6.1).

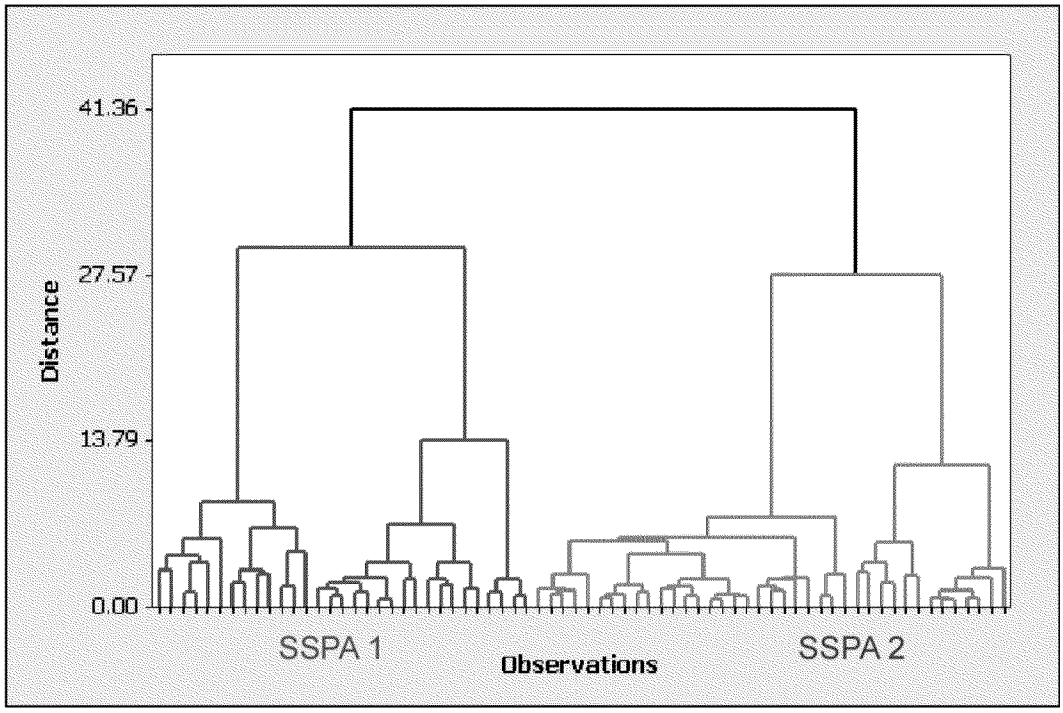

Figure 6.1: Dendogram showing hierarchical clustering of 70 groundwater samples. Group SSPA 1 is to the left, and SSPA 2 is to the right.

Principal component analysis shows that the first principal component, which controls 42.3% of the variance of the dataset, is primarily a Na, TDS, SO_4, and Cl signal. This principal component seems to represent the transition between less evolved waters to more evolved waters. The second principal component controls 29.2% of the dataset variance, and shows a Ca, Mg, and inversely related pH signal. The coupling of Ca and Mg may represent natural water evolution reactions, such as cation exchange. Unlike the

2017-002976-0000775

data from the study area where there was a distinct Na-Cl signal (see section 4.4), no sodium-chloride type waters were found in the SSPA study area north of the Colorado River (S.S. Papadopulos & Associates, 2007). Additionally, no dissolved methane, BTEX, or MTBE were detected above reporting limits in any of the samples (S.S. Papadopulos & Associates, 2007).

Table 6.1: Mean water chemistry for water clusters. Concentrations in mg/L, except pH in standard units. The number of samples in each cluster is indicated by *n*.

Cluster	*n*	Ca	Cl	F	HCO_3, as $CaCO_3$	Mg	Mn	Na	SO_4	TDS	pH
		mg/L	*mg/L*	*mg/L*	*mg/L*	*mg/L*	*mg/L*	*mg/L*	*mg/L*	*mg/L*	*s.u.*
SSPA 1	31	54.0	72.9	1.1	342.6	26.3	0.0	258.0	310.9	950.0	7.8
SSPA 2	39	122.8	147.6	0.7	440.3	76.5	0.1	367.9	710.8	1688.5	7.4

6.1.2 Battlement Mesa Dataset

Cordilleran Compliance Services, Inc. has performed annual water quality sampling in the Battlement Mesa area of Garfield County since 2004, which lies directly to the southwest of the study area. PRESCO, Inc. began natural gas drilling activities in this area in the fall of 2005 (Cordilleran Compliance Services, 2007). Data previously collected by other agencies was reviewed in addition to sampling efforts conducted annually from 2004 – 2006. Previously collected data includes: samples from 1969 collected by the USGS, samples from 1974-1977 collected by the Environmental Protection Agency (EPA), and samples from 1997-1999 collected by the COGCC. Cordilleran Compliance Services, Inc. (2007) presented statistical information for each of the four datasets, including major and minor ions, and physical parameters. Analyses were also completed for radionuclides, volatile organic compounds (VOCs), and bacteria (Cordilleran Compliance Services, 2007). Dataset means are shown in Table 6.2.

Water types found in the Battlement Mesa area are consistently Na-Ca-HCO_3-SO_4, or Na-HCO_3-SO_4 type with relatively low TDS compared to the Mamm Creek field area. COGCC analyzed for VOCs, including BTEX, MTBE, and methane in the 1997-1999, and Cordilleran Compliance Services, Inc. analyzed these parameters annually from 2004 – 2006. With the exception of a few very low level BTEX detections, these

2017-002976-0000776

compounds were generally not detected in water samples from the Battlement Mesa area (Cordilleran Compliance Services, 2007).

Table 6.2: Mean water chemistry for water sampling events. Concentrations in mg/L, except pH in standard units. The number of samples in each cluster is indicated by *n*. ND indicates no data.

Source	n	Ca	Cl	HCO_3/ Total Alkalinity	K	Mg	Na	SO_4	TDS	pH
		mg/L	*mg/L*	*mg/L*	*mg/L*	*mg/L*	*mg/L*	*mg/L*	*mg/L*	*s.u.*
BM 1969	13-37	59.4	11.2	380.1	3.0	26.7	83.8	137.0	485.0	7.9
BM 1974-77	25	28.4	6.8	258.8	2.2	26.4	42.1	36.2	312.3	ND
BM 1997-99	57	51.7	8.6	323.4	2.6	36.8	65.0	76.1	394.7	7.9
BM 2004-06	48	52.6	6.1	268.0	2.5	36.6	53.2	113.9	462.5	7.9

6.1.3 Comparison with the Study Area

The nine hydrochemical clusters, or water facies, from the study area were compared to the two SSPA clusters from north of the Colorado River, and to the means of three sampling events (1969, 1997-99, and 2004-06) from the Battlement Mesa area. The sampling event from 1974-77 completed in the Battlement Mesa area was not included in the comparison due to lack of pH data.

Hierarchical clustering was conducted on the means of the 14 groups of data in order to determine regional similarities and differences in hydrochemistry. Clustering was conducted with normalized and standardized common parameters, including bicarbonate, calcium, chlorine, potassium, magnesium, sodium, sulfate, TDS, and pH. The resulting dendogram is shown in Figure 6.2.

The dendogram shows two major groups, waters on the left are generally lower TDS clusters, with less evolved signatures. Cluster 1a-1 from the study area is most similar to the low TDS waters from the Battlement Mesa area, which provides runoff water to the study area. This cluster, as well as the Battlement Mesa hydrochemistry, represents a regional background water composition. Cluster 1b is closely related to this background signature. Other clusters, such as clusters 1a-2 and 2, form a different subgroup due to their somewhat elevated TDS levels, and more evolved signatures including higher sodium, bicarbonate, and sulfate. The major group on the right side of

2017-002976-0000777

Figure 6.2 includes clusters with relatively elevated TDS, sodium, sulfate or chloride. The clusters SSPA 1 and SSPA 2 represent background water quality for the area north of the Colorado River since this area has experienced little to no petroleum activity. Background water chemistries of SSPA 1 and SSPA 2 are most similar to clusters 4a and 4b, which suggests that these clusters are consistent with an elevated TDS regional background water quality. The source of the elevated TDS (primarily Na and SO_4) may be due to mixing of shallow groundwater with deep groundwater or local anthropogenic impacts other than petroleum development.

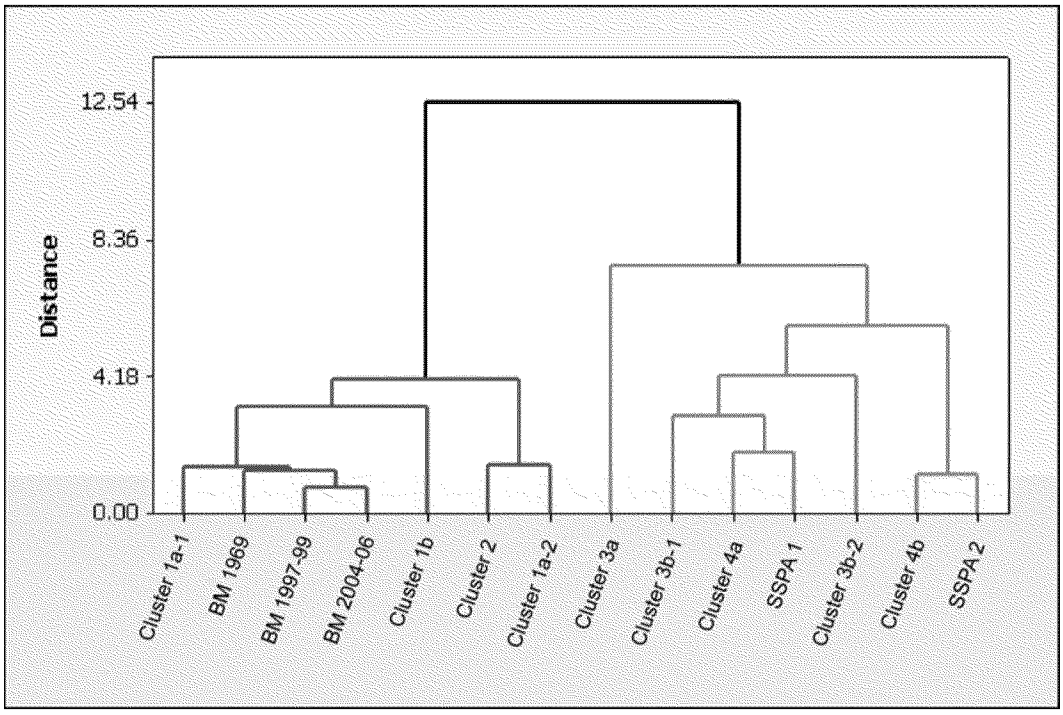

Figure 6.2: Dendogram of 9 clusters from the study area (1a-1, 1a-2, 1b, 2, 3a, 3b-1, 3b-2, 4a, and 4b), 2 clusters from the SSPA study (SSPA 1 and SSPA 2), and means of 3 datasets from Battlement Mesa area (BM 1969, 1997-99, and 2004-6).

Clusters in group 3 seem unique from regional water quality. Cluster 3b-1 is somewhat similar to Cluster 4a and SSPA 1, which may be due to its transitional water chemistry (see Figures 4.12 and 4.13). Clusters 3b-2 and 3a are most dissimilar from regional higher TDS background waters, which is likely due to their Na-Cl component.

2017-002976-0000778

6.2 Temporal Analysis

Data was not available in adequate intervals from the same sites in order to produce useful time-series analysis. However, cluster membership was evaluated over time to distinguish trends in water types in the study area. This method, however, assumes adequate spatial coverage of sampling each year, which is not achieved by the selected samples. Methane, a primary constituent of the West Divide Creek seep, was also investigated over time.

6.2.1 Cluster Membership Over Time

Considering the number of samples belonging to each group over time will help determine whether groups and clusters have any temporal significance. Data was compiled for the years 1997 – 2005. Since the years 1998 – 2000 had no samples, and 1997 and 2001 have only 5 and 1 samples, respectively, samples taken prior to 2002 were combined with 2002 for temporal analysis. Table 6.3 shows the number of samples taken by year. Samples are plotted spatially by cluster and year in Figures 6.3 – 6.6.

Table 6.3: Number of water samples in selected database by year.

Year	Total water samples in selected database
1997	5
1998	0
1999	0
2000	0
2001	1
2002	37
2003	102
2004	249
2005	266

Although sampling did not occur repetitively at standard sampling locations, Figures 6.3 – 6.6 are of some interest. Cluster 2 occurs in 2004 and 2005 in the vicinity of the West Divide Creek seep, however, other samples belonging to cluster 2 occur in the pre-2002 through 2002 time frame (Figure 6.3). These samples occur further to the south, near West Divide Creek. The occurrence of cluster 2 samples may suggest that impact due

2017-002976-0000779

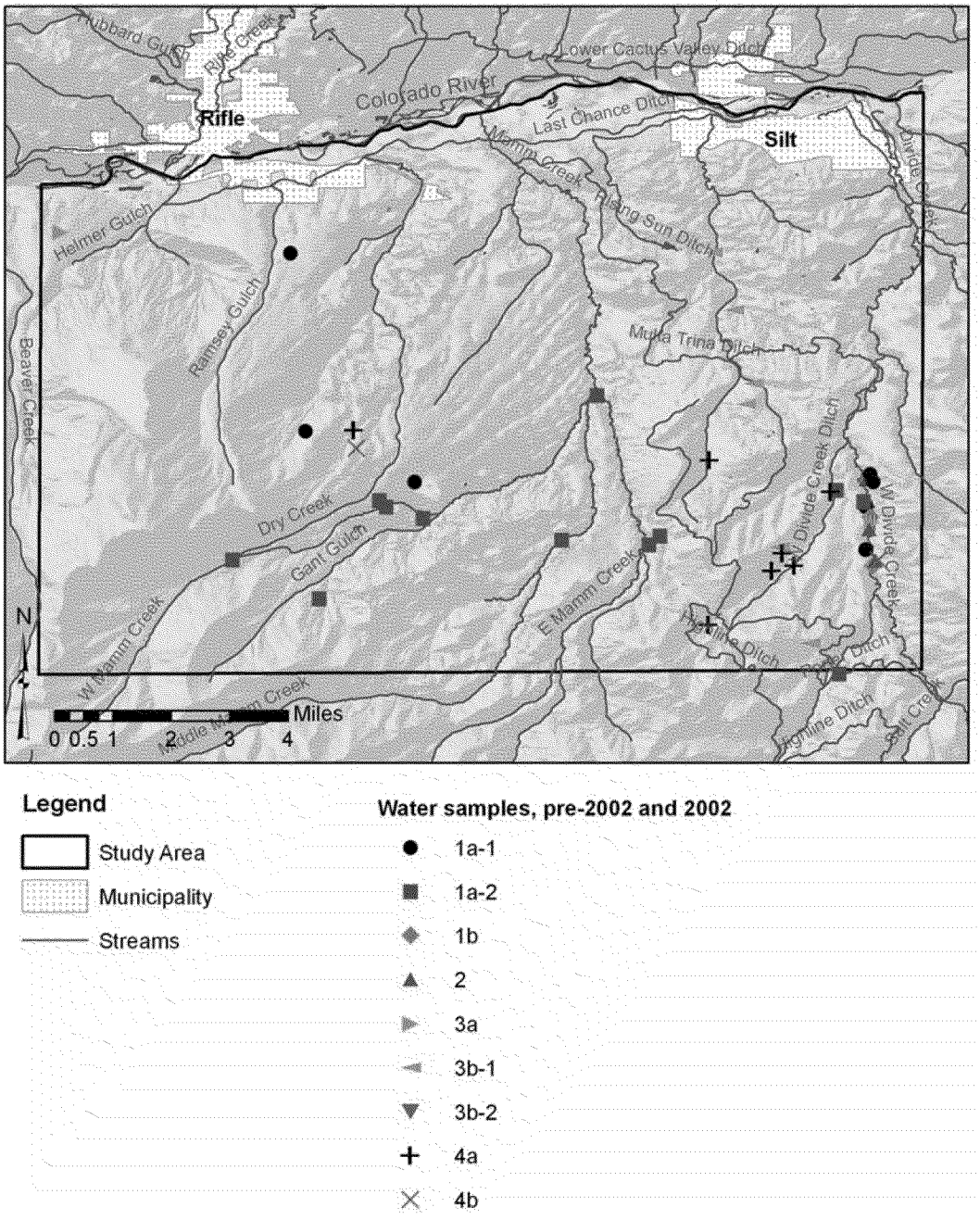

Figure 6.3: Water samples taken in 1997, 2001, and 2002 plotted by cluster.

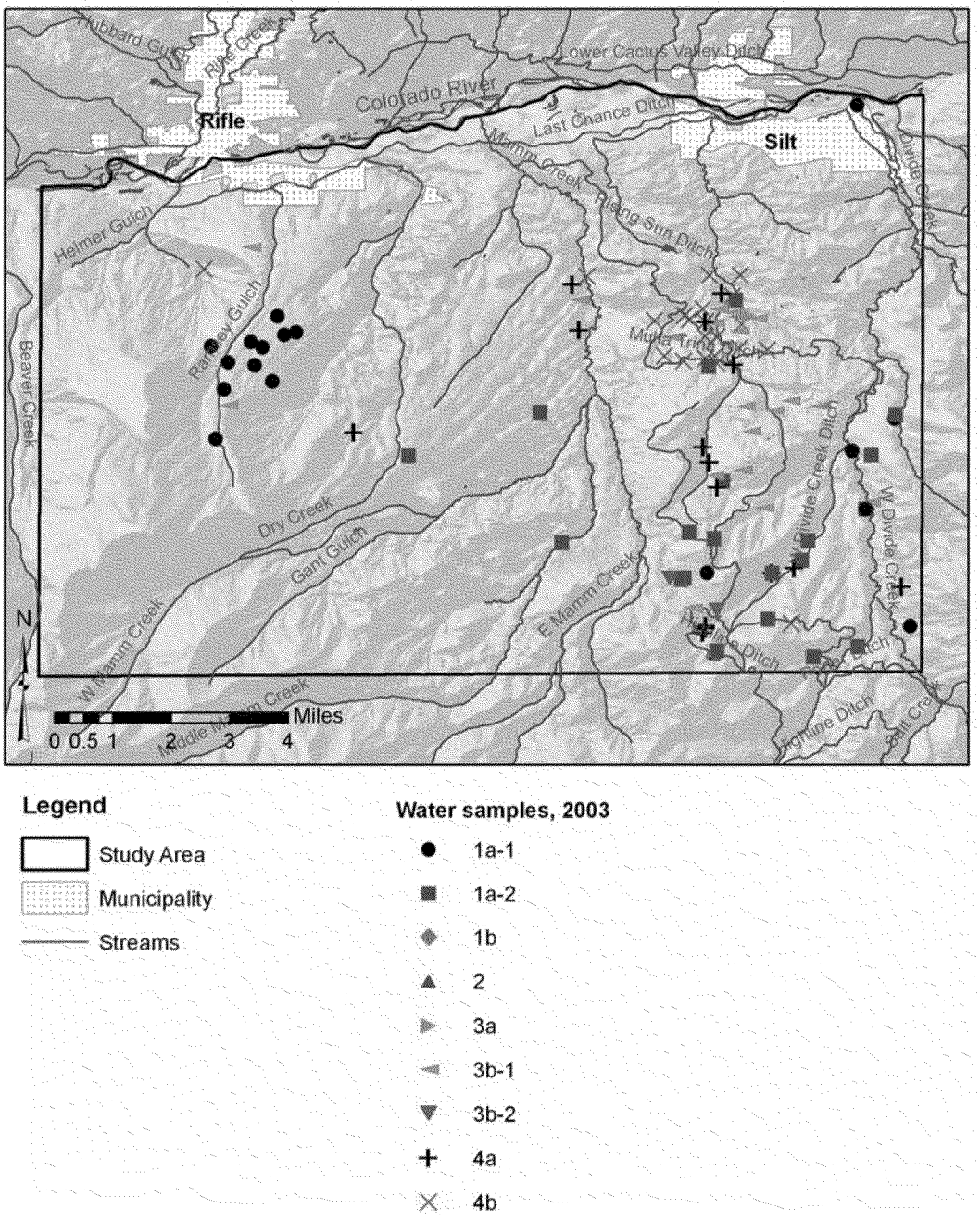

Figure 6.4: Water samples taken in 2003 plotted by cluster.

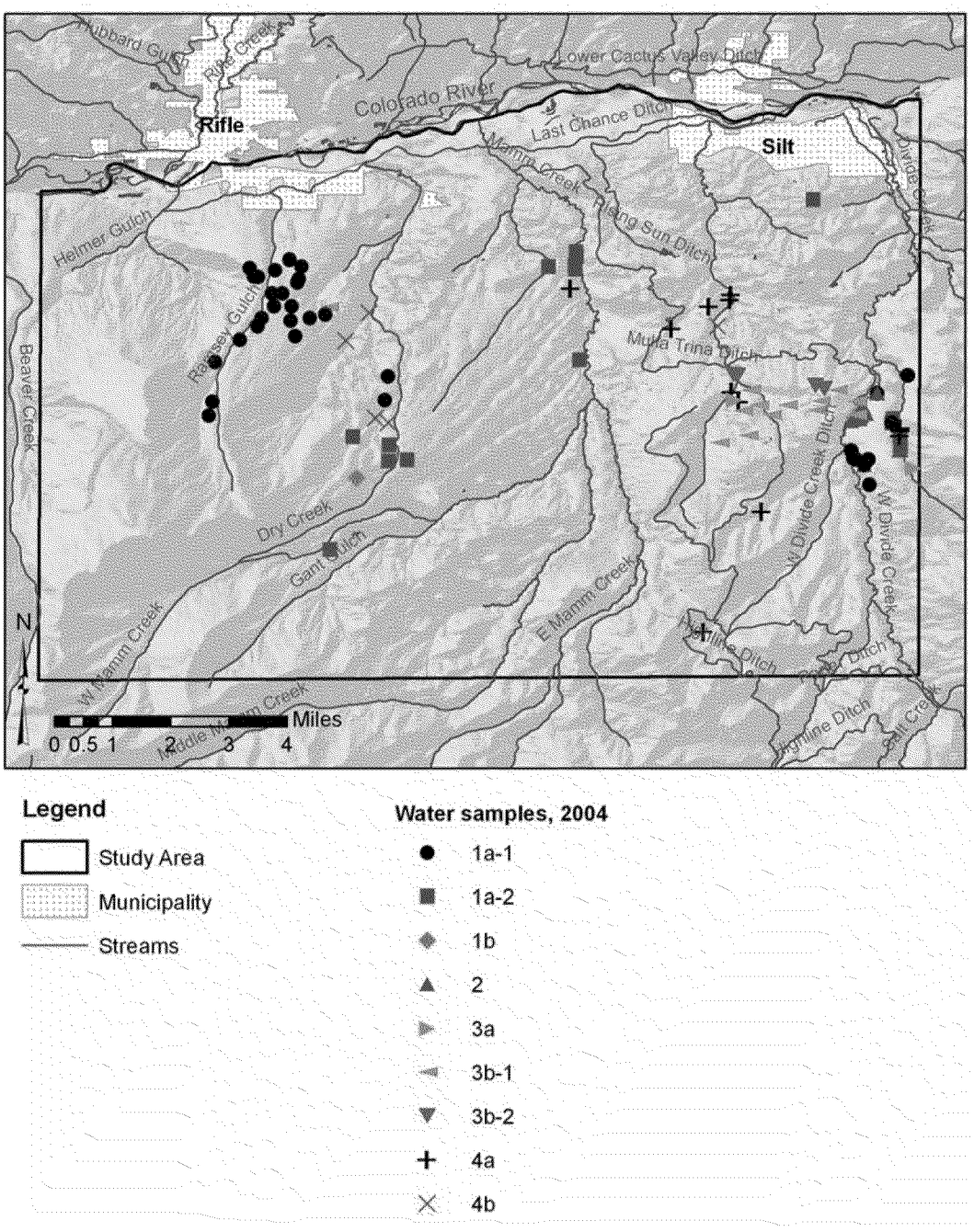

Figure 6.5: Water samples taken in 2004 plotted by cluster.

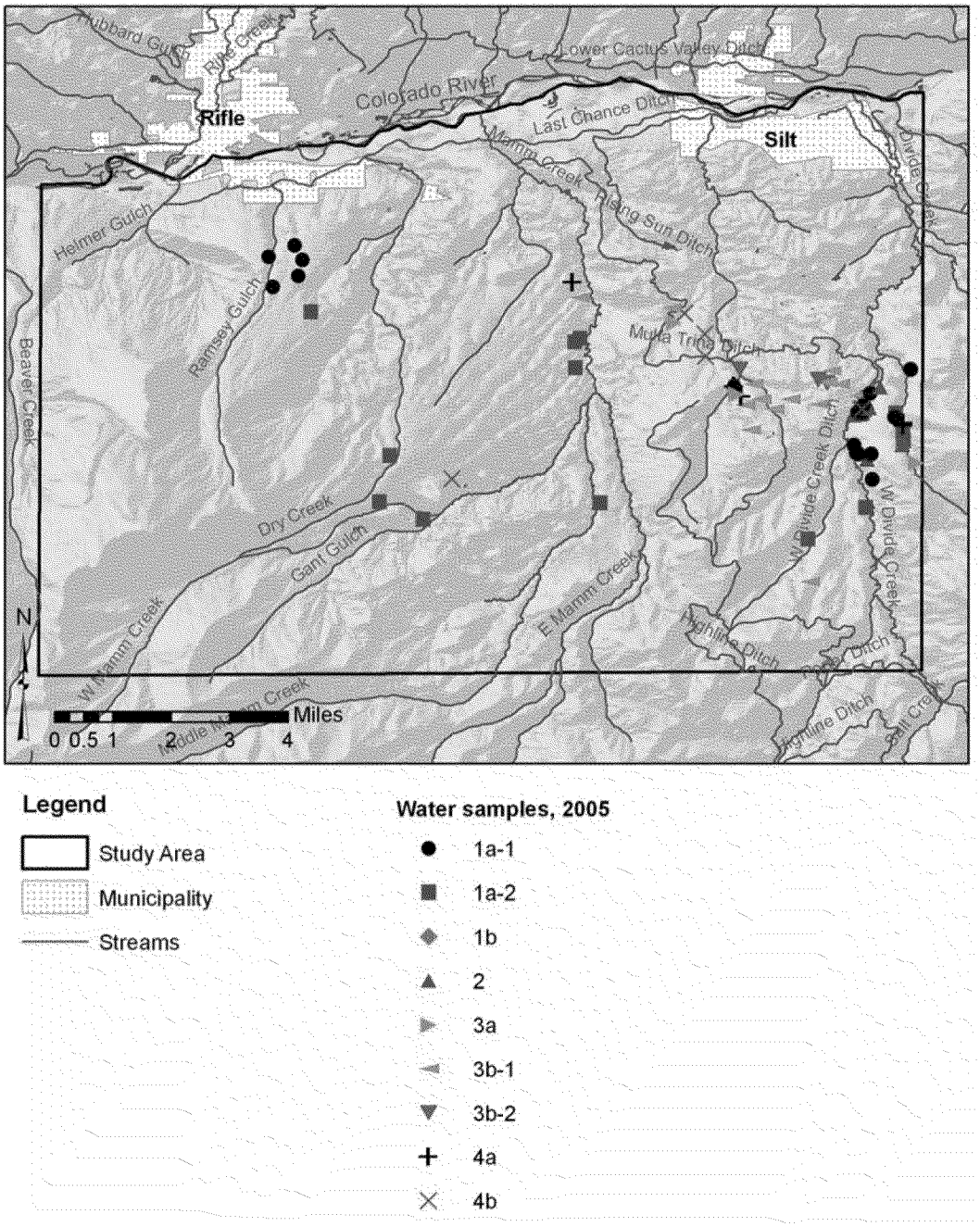

Figure 6.6: Water samples taken in 2005 plotted by cluster.

to methane gas and drilling fluids may have occurred previously in other locations in the study area, or that other factors may be causing a similar localized reducing environment. Cluster 3b-2 (showing the strongest Na-Cl component) was observed first in 2003 in the southeastern portion of the study area, before the West Divide Creek seep that occurred in April of 2004 (Figure 6.4). In 2004 and 2005, it persists in the eastern portion of the study area, to the west-northwest of the West Divide Creek seep. Cluster 3b-2 is accompanied spatially by cluster 3b-1. Cluster 4b occurs in large number in 2003, which may be due to the particular sampling locations that year (Figure 6.4). The percentage of samples by year belonging to each of the nine clusters is tabulated in Table 6.4.

Table 6.4: Cluster and group membership over time.

Year:	2002	2003	2004	2005
1a-1	16%	18%	23%	27%
1a-2	30%	20%	9%	17%
1b	5%	0%	8%	7%
2	8%	0%	19%	8%
3a	5%	1%	6%	4%
3b-1	14%	21%	14%	19%
3b-2	0%	2%	6%	4%
4a	16%	17%	12%	11%
4b	5%	23%	2%	4%
Group 1	51%	38%	40%	51%
Group 2	8%	0%	19%	8%
Group 3	19%	24%	26%	27%
Group 4	21%	30%	14%	15%

Membership over time by cluster does not reveal any notable trends. This may be due to inadequate spatial coverage of samples and non-standard sampling locations. Also, sampling in 2005 includes only about half of the year. Membership by group does show some general trends over time, and since groups represent sets of clusters with statistically similar chemistries, this interpretation is of some interest. The percentage of samples in group 1 is lower for the years 2003 – 2005 than in 2002. The percentage of samples in group 2 increases over time, which is likely due to increased sampling near the West Divide Creek seep during 2004 and 2005. Group 3 appears to be increasing in percentage over time, especially when it is considered that 2005 is only a partial sampling

2017-002976-0000784

year. The percentage of samples in group 4 increases from 2002 – 2003, however decreases thereafter. These trends seem to indicate that impacted samples from groups 2 and 3 become more a significant fraction of the total over time since 2002.

6.2.2 Occurrence of Methane Over Time

In order to evaluate the occurrence of methane, a potential indicator of impact by natural gas production, the original database was accessed to obtain a larger number of measurements to achieve the best spatial and temporal coverage possible with the available data. A total of 2189 dissolved methane measurements from 439 sites were evaluated for temporal trends (see Appendix D). Samples were taken each year between 1997 and 2005, however, the six values taken in 1998 were removed due to inaccurate recording, and the four values from 2000 were removed based on the low number of data points. Means of dissolved methane concentrations by year were calculated for the log-normally distributed data, and are shown in Table 6.5.

Table 6.5: Number of dissolved methane measurements (n) taken by year, with mean of the log-value and standard deviation.

Year	n	Mean, log(value)	Standard Deviation
1997	34	-2.962	0.3827
1999	17	-2.398	1.319
2001	41	-2.025	1.647
2002	100	-2.451	1.462
2003	143	-1.822	1.48
2004	921	-1.505	1.479
2005	923	-1.713	1.377

Mean dissolved methane concentrations are plotted by year in Figure 6.7. A strong positive correlation exists between mean dissolved methane concentrations and year. The number of new wells drilled each year in the study area has been increasing since 1998 (Figure 6.8). Note that data for the year 2005 only includes approximately half of the year. Drilling activity sharply increased in 2003. Mean dissolved methane concentrations also show a strong positive correlation with the cumulative number of wells and new wells drilled by year in the study area (Figures 6.9 and 6.10).

2017-002976-0000785

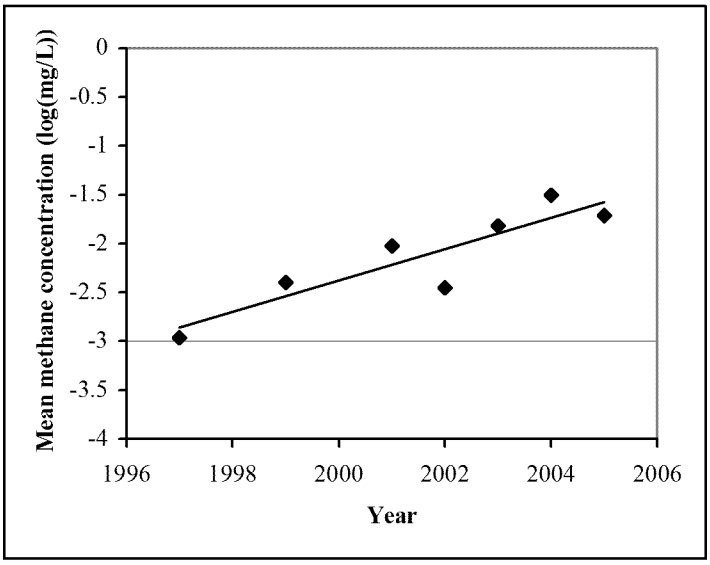

Figure 6.7: Log of mean dissolved methane concentrations (mg/L) by year. R^2=0.80.

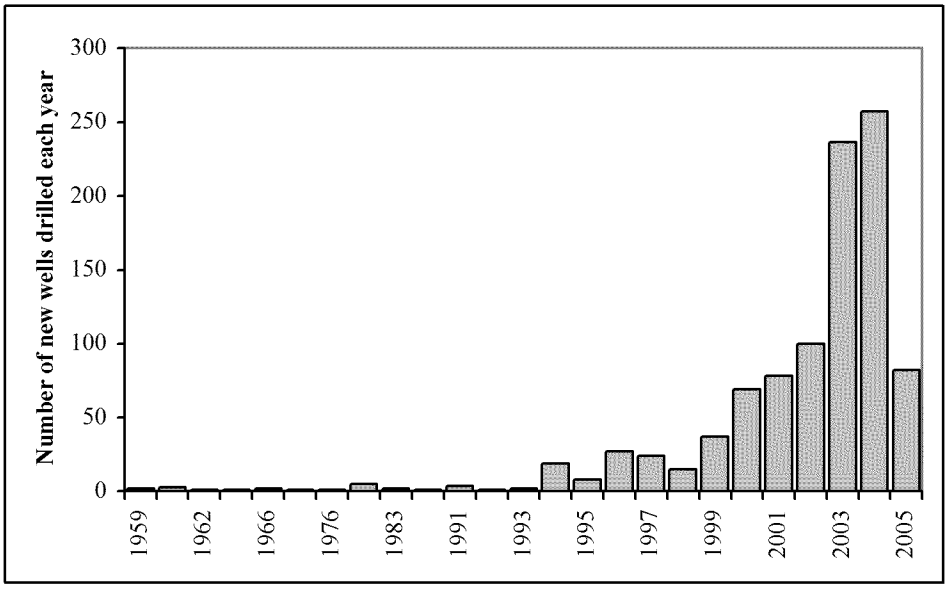

Figure 6.8: Number of new gas wells drilled by year.

2017-002976-0000786

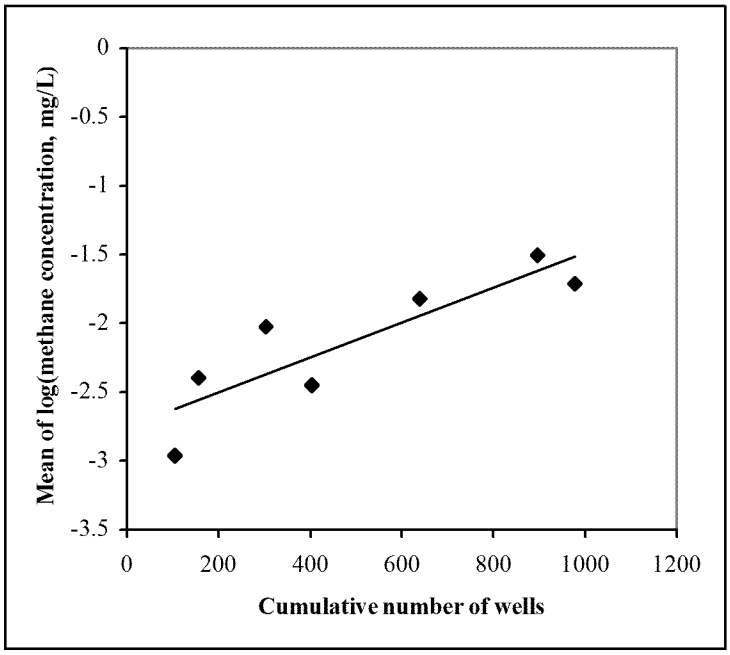

Figure 6.9: Mean methane concentration by year versus cumulative gas wells present in the study area that year. R^2=0.76.

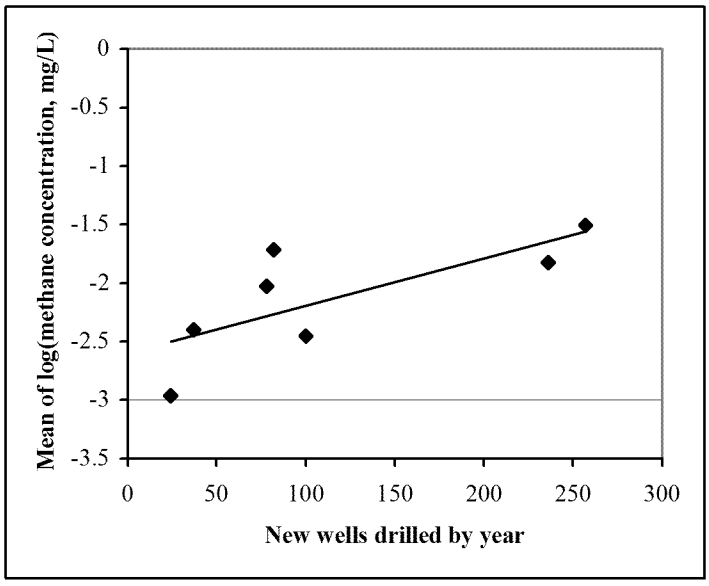

Figure 6.10: Mean methane concentration by year versus new natural gas wells drilled in the study area that year. R^2=0.55.

Next, in order to minimize the effect of differences in sampling events each year, the percent of samples with methane concentrations greater than 1 mg/L by year were plotted (Figure 6.11). Years before 2002 were not included since substantially fewer samples were taken during those years. This plot also shows an increase in the percentage

2017-002976-0000787

of samples with high methane concentrations over the years when drilling activities increased greatly. This suggests that rising dissolved methane levels and occurrences is correlated with increasing drilling activity. If confirmed, this may indicate that gas wells may be providing enhanced vertical pathways for upward movement of deep formation or produced water.

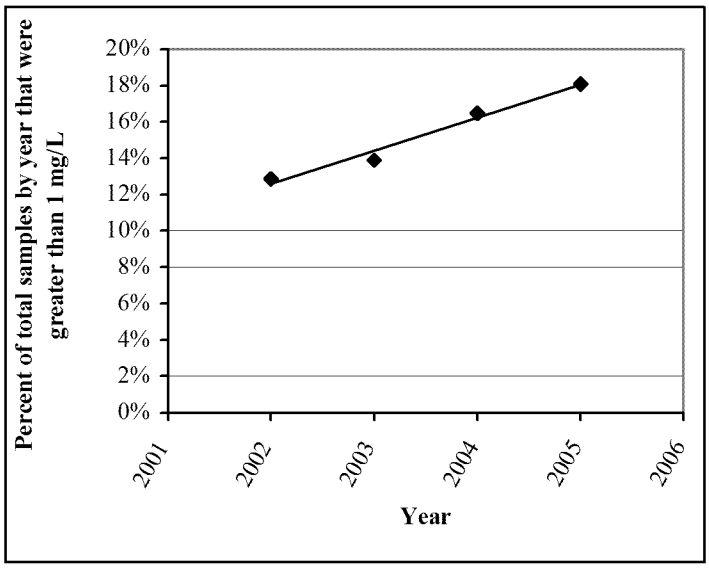

Figure 6.11: Percent of water samples by year with methane concentrations greater than 1 mg/L. R^2=0.98.

If the growing occurrence of methane is due to enhanced vertical migration from the Williams Fork Formation caused be gas well drilling, then other components of the formation water should also by increasing in occurrence over time. The primary source of chloride in the study area is the Williams Fork Formation water. To analyze chloride concentrations over time, 1433 chloride measurements were extracted from the original database (see Appendix D). The percentage of water samples with chloride concentrations greater than 250 mg/L is shown in Figure 6.12.

The occurrence of high concentrations of chloride in the study area also increases over the years during which gas drilling activities increased greatly. This suggests that the increased natural gas production may control both chloride and methane occurrence.

2017-002976-0000788

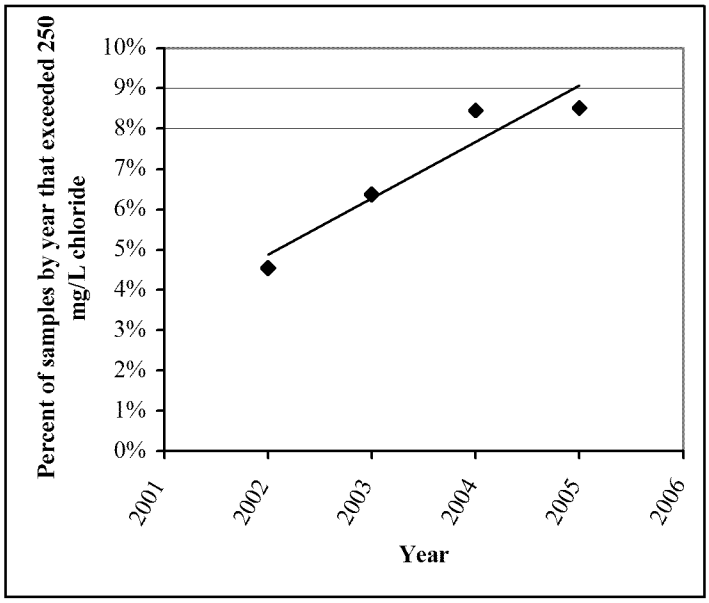

Figure 6.12: Percentage of water samples by year with chloride concentrations greater than 250 mg/L. R^2=0.90.

6.2.2.0 Source of Methane

Stable isotope ratios for carbon and hydrogen are a common method used to try to distinguish the source of methane (Scott et al., 1994). Stable isotope ratios were available for the West Divide Creek seep and associated seeps, production gas (4 samples), bradenhead gas (13 samples), and some water wells (211 samples). However, of the 211 water samples with methane isotope information, less than 27% were associated with samples chosen for hydrochemical analysis. Therefore, establishing any significant correlation with hydrochemical clusters was difficult. A diagram showing the aforementioned data plotted with general zones typically representing thermogenic, CO_2-reduction, and fermentation sources of methane is shown in Figure 6.13.

Surface ponds, some cluster 2 samples, and other water samples plot in and near the fermentation source zone. Production gas, bradenhead gas, and seep gas plots in the thermogenic source zone. Also in the thermogenic zone are most of the samples from cluster 2, and most of the samples from cluster 3b-1, indicating a composition very similar to natural gas from the production interval. Additional water samples that were not included in the cluster analysis also plot in the thermogenic zone, indicating a significant effect of thermogenic methane on water resources. Other water samples not clustered and samples from cluster 3b-2 plot at a similar δD value, but have more

2017-002976-0000789

depleted $\delta^{13}C$ signatures extending into the CO_2-reduction source zone. This may suggest another source of methane from reduction of CO_2 associated with natural gas and significant mixing between the two sources.

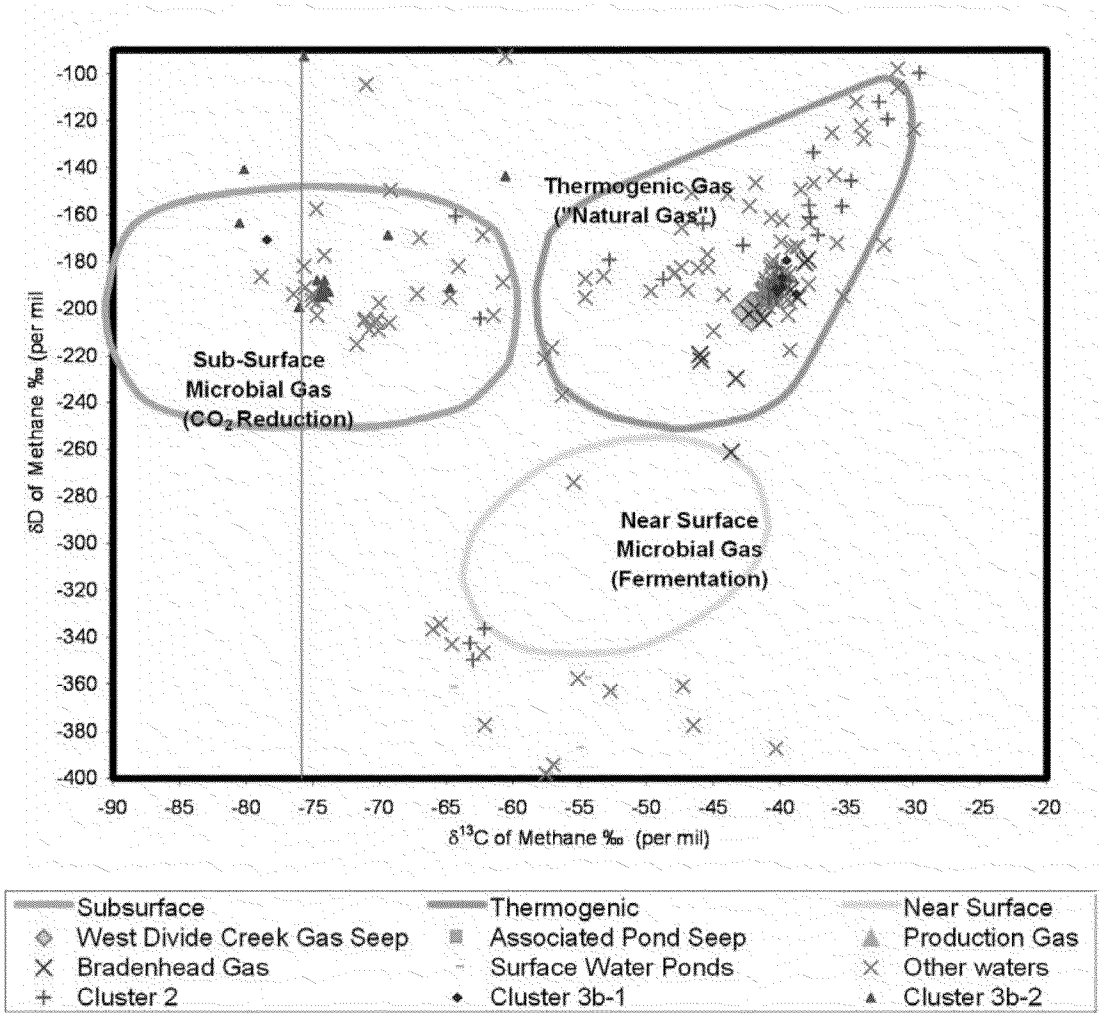

Figure 6.13: Isotopic ratios in methane from different sources in the study area, including water samples from clusters 2, 3b-1, 3b-2, and water samples of unknown cluster. Vertical orange line shows the δC^{13} values predicted for CH_4 derived from CO_2-reduction of CO_2 sourced from the Williams Fork.

Although natural gas accumulations can contain both thermogenic and biogenic gas, natural gas from the Williams Fork Formation contains primarily thermogenic gas (Johnson and Rice, 1990). In addition, the Williams Fork Formation contains a relatively high percentage of CO_2, up to 22% by volume (Johnson and Rice, 1990). CO_2-reduction processes that produce methane with δD ratios between –250 and –170 per mil are

2017-002976-0000790

dominant in marine sediments (Hoefs, 2004), such as the Williams Fork or underlying units. A mean of 27 CO_2 samples shows that an average value of $\delta^{13}C$ of CO_2 from the Williams Fork Formation is –11.0 per mil. Methane produced by reduction of this CO_2 would have a $\delta^{13}C$ value of –76.0 per mil, since the fractionation factor for this process is approximately –65 per mil (Scott et al., 1994). In Figure 6.13, the vertical orange line denotes the predicted $\delta^{13}C$ values for methane produced from Williams Fork sourced CO_2. If this is the origin of the methane with isotopically depleted carbon, these samples could also indicate impact to groundwater from deeper sources.

6.2.3 Spatial Buffering

If geologic features cannot fully explain the spatial distribution of hydrochemical clusters, the potential impact of natural gas drilling activities in the area should be considered. Water samples are shown with gas well locations by year in Figure 6.14. Gas well locations were obtained from the COGCC, and include producing, abandoned, and shut-in wells, in addition to wells waiting on completion as of December 2006 (COGCC, 2006).

Average depths of gas wells producing from the Williams Fork Formation in the study area are 6000 – 8000 ft below ground surface (URS, 2006). The potential for gas well boreholes to provide increased vertical connectivity has been recognized as an important process in other studies (Van Stempvoort et al., 2005), and must be considered at the study area. Figure 6.14 shows that gas wells occur over the entire study area, and are especially dense in the central region. This region, however, has few to no water quality samples.

The proximity of water samples to gas wells, "problem" wells, and major faults and fractures was analyzed using the spatial analyst tools in ArcGIS 9.0. If a certain hydrochemical signature is found preferentially near gas wells, this could either suggest that leaking produced water, crude product, or drilling fluids are contributing to the signature, or that wells are providing enhanced pathways for vertical migration of formation water. If a certain hydrochemical signature is found preferentially near major faults and fractures, this may indicate a geologic control. "Problem" wells are defined as: (1) wells which could not achieve less than 100 psi bradenhead pressure after release, or

2017-002976-0000791

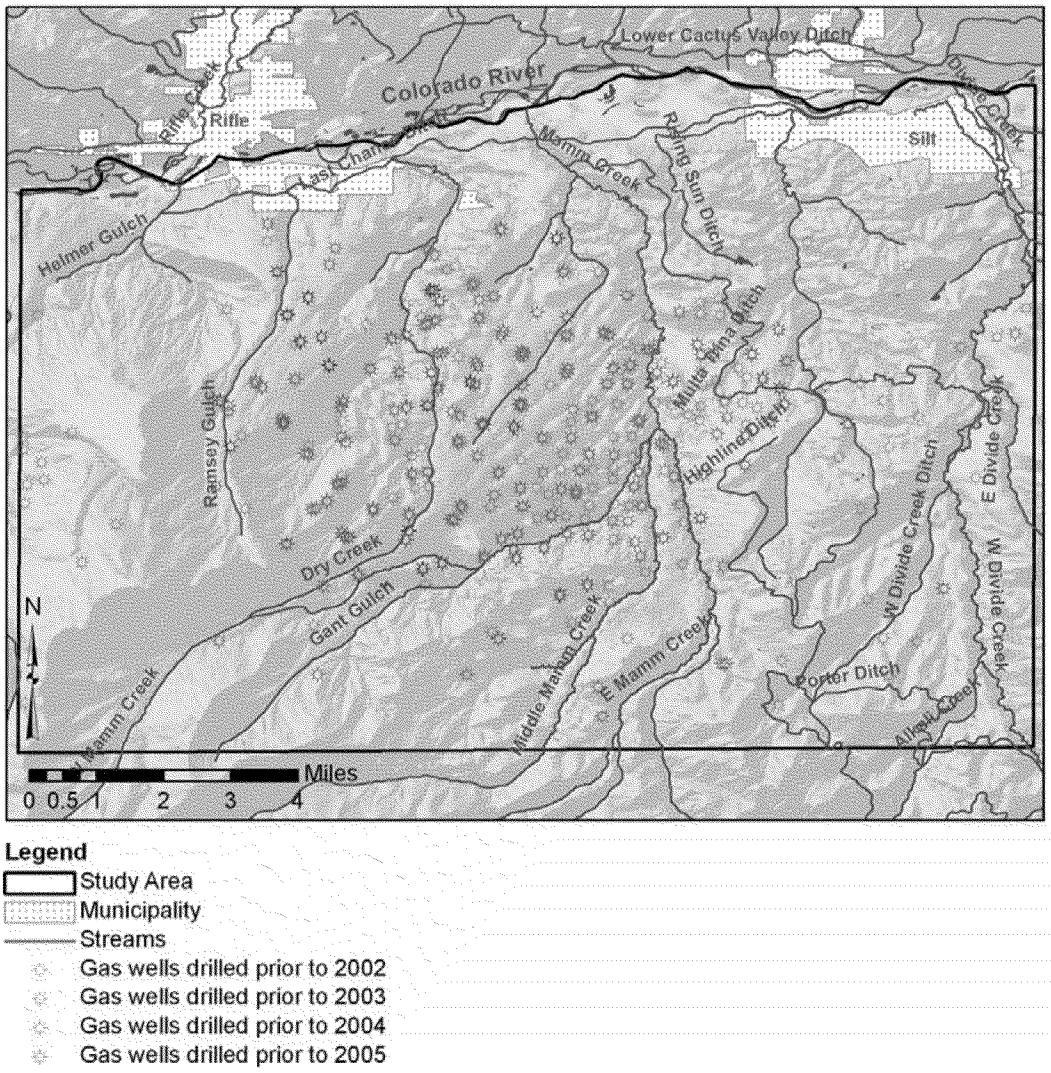

Figure 6.14: Locations of gas wells, not including proposed locations. Gas wells data from COGCC (12/2006).

(2) wells which regained bradenhead pressures of at least 100 psi within 4 months of successful release. Limited bradenhead data was available (see Appendix E). Bradenhead pressure builds up in the well annulus either due to leaking gas from the well casing or infiltration of gas from other subsurface units (URS, 2006). Wells with high or persistent bradenhead pressures often indicate completion or cementation problems (URS, 2006). The location of problem wells is shown in Figure 6.15. Problem wells occur preferentially near the eastern portion of the study area, and coincide with the location of the Divide Creek anticline. Increased fracturing near the anticline may cause a higher

incidence of well drilling and completion problems, which in turn may affect water resources in this area.

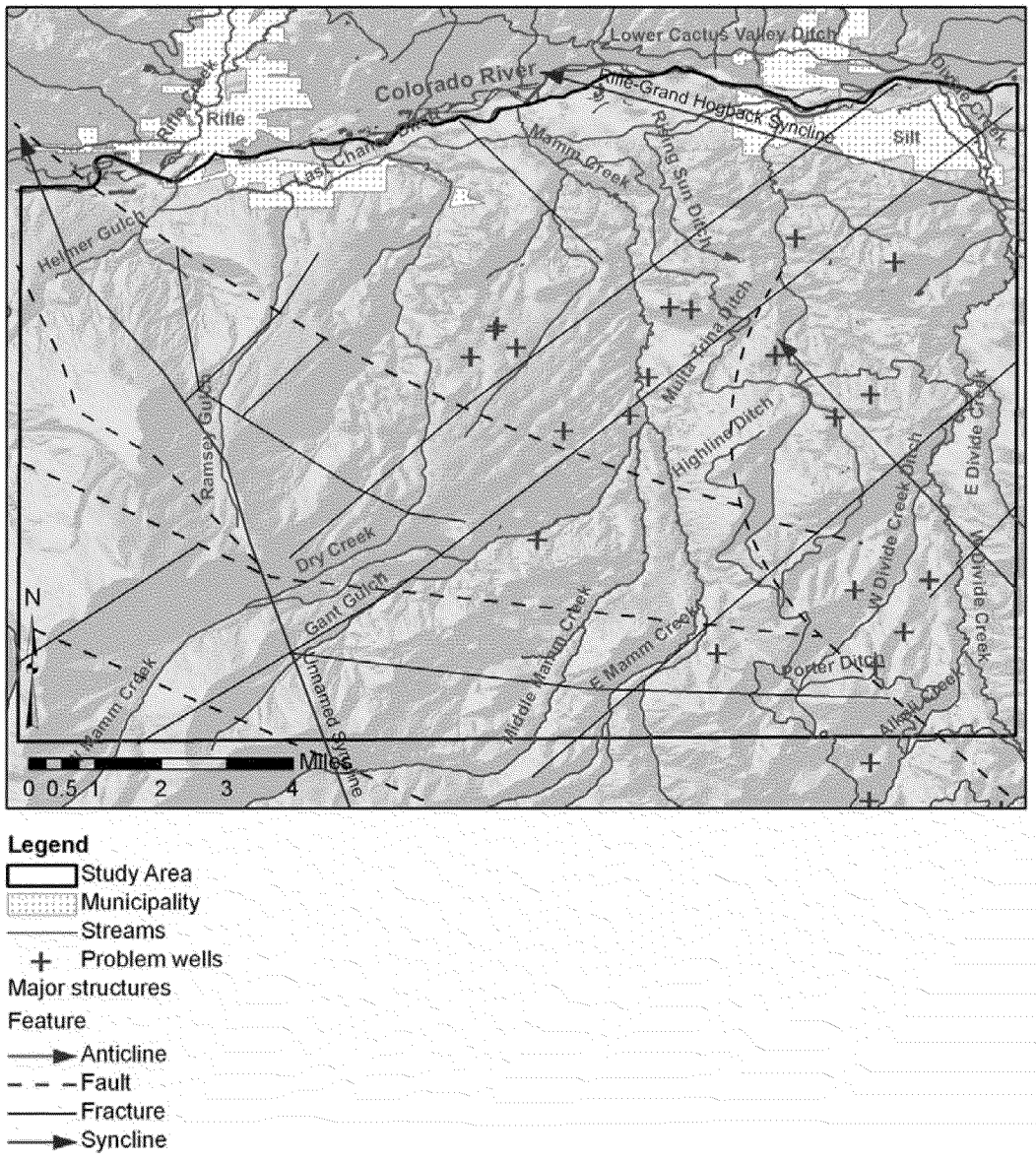

Figure 6.15: Location of problem gas wells.

Spatial buffering was conducted by separating water samples and gas wells by year. Water samples from a given year were buffered against only those gas wells that had a completion or drilling start date of an earlier year. Buffering was conducted using a projected UTM coordinate system in order to minimize distance distortions. Calculations were done to distances up to 3,500 ft, since the West Divide Creek seep involved

2017-002976-0000793

transport of methane gas along a fracture for approximately 3,800 ft (URS, 2006) Samples occurring more than 3,500 ft away from gas wells or major fractures may still be impacted by these features, as was seen in the West Divide Creek seep. However, a spatial relationship between a certain hydrochemical signature and a certain feature may indicate preferential control. The proximity of water chemistries, or clusters, to other features is also influenced by the groundwater flow direction and dispersion, which were not considered in the buffering exercise. The proximity of water samples to gas wells by year, problem wells, and major structural features are tabulated by cluster in Table 6.6.

There appears to be a trend when comparing distances between water samples and gas wells versus major faults and fractures. Clusters 3a, 3b-1, 3b-2, and 4a seem more likely to occur near gas wells than structural features. This is especially true in 2004 and 2005, those years that show the impacts of increased natural gas drilling by other measures such as elevated methane and chloride in groundwater samples (see Figure 6.8).

When comparing the proximity of water samples to problem wells and structural features, samples from clusters 3a, 3b-2, and 4a are more likely to be close to problem wells than structural features, especially cluster 3b-2. Samples from cluster 3b-1 appear relatively close to both problem wells and structural features, whereas the location of cluster 4b samples is more correlated with structural features than problem wells.

6.2.4 Benzene Analysis

Multiple parameters were not used for statistical analysis since greater than 40% of the data was censored. However, benzene was of particular interest to this study due to the natural gas and oil drilling done in the area currently and historically. Benzene is associated with drilling fluids and produced water (Kharaka and Otton, 2003; Veil et al., 2004). Censored benzene values (72%) were estimated according to Sanford et al. (1993) (see section 3.1.3), which reasonably estimates 60% of the values at 80% censored. The mean values for benzene by cluster are shown in Table 6.7.

Benzene concentrations above the method detection limit are strongly correlated with the hydrochemistry of cluster 2. Many of the samples in cluster 2 were taken from the site of the seep where as much as 115MMcf of gas and associated petroleum components were vented through the streambed (COGCC, 2004).

2017-002976-0000794

Table 6.6: Percentage of samples by cluster that occur within a certain distance of gas wells, problem wells, and major structural features.

Buffered against:	Distance:	Cluster: 1a-1	1a-2	1b	2	3a	3b-1	3b-2	4a	4b
Gas wells drilled prior to 2002	*Total number of samples in 2002*	*6*	*11*	*2*	*3*	*2*	*5*	*0*	*6*	*2*
	1500 ft	17%	45%	50%	0%	0%	40%	-	67%	50%
	2500 ft	50%	55%	50%	33%	0%	40%	-	67%	100%
	3500 ft	50%	55%	50%	33%	0%	40%	-	67%	100%
Gas wells drilled prior to 2003	*Total number of samples in 2003*	*18*	*20*	*0*	*0*	*1*	*21*	*2*	*17*	*23*
	1500 ft	44%	40%	-	-	0%	14%	0%	59%	39%
	2500 ft	66%	55%	-	-	0%	19%	0%	71%	57%
	3500 ft	66%	60%	-	-	0%	43%	50%	76%	83%
Gas wells drilled prior to 2004	*Total number of samples in 2004*	*58*	*23*	*19*	*48*	*16*	*35*	*15*	*30*	*5*
	1500 ft	29%	43%	5%	10%	63%	40%	0%	23%	80%
	2500 ft	52%	87%	5%	13%	100%	60%	87%	53%	100%
	3500 ft	71%	87%	5%	13%	100%	69%	87%	93%	100%
Gas wells drilled prior to 2005	*Total number of samples in 2005*	*39*	*16*	*17*	*61*	*9*	*43*	*8*	*24*	*9*
	1500 ft	31%	63%	0%	11%	44%	70%	100%	21%	78%
	2500 ft	90%	88%	71%	72%	100%	86%	100%	67%	100%
	3500 ft	100%	100%	100%	100%	100%	100%	100%	100%	100%
Problem wells identified in 2004	*Total number of samples in 2005*	*39*	*16*	*17*	*61*	*9*	*43*	*8*	*24*	*9*
	1500 ft	0%	0%	0%	0%	0%	23%	0%	0%	11%
	2500 ft	3%	25%	0%	0%	44%	56%	75%	42%	22%
	3500 ft	3%	31%	0%	0%	67%	65%	100%	46%	67%
Major faults and fractures	*Total number of samples in all years*	*122*	*71*	*38*	*112*	*28*	*107*	*25*	*78*	*39*
	1500 ft	51%	41%	97%	88%	54%	26%	4%	23%	56%
	2500 ft	62%	63%	97%	96%	57%	37%	20%	32%	72%
	3500 ft	85%	96%	100%	100%	57%	73%	36%	40%	92%

2017-002976-0000795

Table 6.7: Mean concentrations of benzene by cluster.

Cluster	Mean benzene concentration (ug/L)	Number of samples	Percent measured or estimated	Percent above detection limit
1a-1	0.06	122	100%	0%
1a-2	0.05	71	99%	0%
1b	0.12	38	100%	3%
2	35.64	112	100%	33%
3a	0.07	28	100%	0%
3b-1	0.32	107	96%	6%
3b-2	0.25	25	96%	12%
4a	0.98	78	97%	0%
4b	0.06	39	100%	0%

6.2.4.0 Reactive Transport

High benzene concentrations, in the case of the West Divide Creek seep, indicated leakage of crude petroleum product or drilling fluids. If the sodium-chloride signature associated with group 3 is also associated with impact by natural gas, it could be expected to contain significant concentrations of benzene. Group 3 samples show an average benzene concentration between 0.1 – 0.3 ug/L. Reactive transport of benzene was modeled with PHREEQC v2.12 in order to determine how long benzene would remain detectable in solution during subsurface transport through a sandstone body of the Wasatch Formation. Fracture flow may introduce additional permeability not included in the following model.

A geochemical model developed by Dodds (2003) was utilized to simulate one-dimensional transport of benzene, with simultaneous sorption, biodegradation and volatilization. The model assumes a homogeneous, isotropic material, laminar flow and an incompressible fluid, due to its dependence on Darcy's law. Biodegradation is assumed to not affect sorption. The contaminant input is modeled as a continuous source, and it is assumed that there is no free phase of the component present. Equilibrium is assumed between the aqueous and gas phases, as well as between aqueous and surfaces (sorption).

The hydraulic conductivity and effective porosity for a general sandstone were assumed for the Wasatch Formation based on general ranges compiled by Schwartz and

2017-002976-0000796

Zhang (2003). An approximate hydraulic gradient of 0.04167 m/m was calculated based on potentiometric surface maps produced by URS (2006). An initial benzene concentration of 12,000 ppb was derived from a produced water sample from the study area. A total time of approximately 2 years was chosen as a period of time over which a significant number of new gas wells have been drilled and a succession of water samples have been taken. Dispersivity was calculated as 10% of the column cell length. Mean, minimum and maximum partitioning coefficients for benzene were calculated by Dodds (2003). A median, minimum and maximum biodegradation factor was obtained from a literature review conducted by Bedient et al. (1999). Three scenarios were modeled: a best-case scenario involves minimum transport and maximum degradation, a worst-case scenario involves maximum transport and minimum degradation, and a median-case involves median transport and partitioning parameters and is likely the most realistic case. Input parameters for are shown in Table 6.8.

Table 6.8: Input parameters for reactive transport modeling of benzene under site conditions. Henry's law constants written as inverse.

Parameter	Units	Best-case	Median-case	Worst-case
Hydraulic conductivity, sandstone	m/s	3.00E-10	3.00E-06	6.00E-06
Effective porosity	%	5.0%	17.5%	30.0%
Average linear groundwater velocity	m/s	2.50E-10	7.14E-07	8.33E-07
Biodegradation rate	day^{-1}	2.5	0.003	0
f_{oc}	%	1.00%	0.10%	0.01%
Log K_{oc}		3.01	1.932	1.31
Log K_h		0.597	0.724	0.91

Results for reactive transport modeling of the three scenarios are shown in Figures 6.16 – 6.18. The worst-case scenario shows that after two years, benzene travels more than 50 meters, and is still present above the detection limit of 1 ppb. The median-case scenario shows that benzene degrades to below 1 ppb at a distance of approximately 44 meters from the source. The best-case scenario shows only very low levels of benzene close to the source after 2 years. However, the degradation rate of 2.5 day^{-1} used in this model is probably unrealistic for a groundwater aquifer.

2017-002976-0000797

These results show that benzene levels of less than 12 ppb, a thousand-fold reduction, may still be present after a period of 2 years. However, even the worst-case scenario shows that benzene at this or lower concentrations could travel on the order of 60 meters before being degraded to undetectable concentrations. This suggests that low levels of benzene may be detected in impacted samples within 40-60 meters of a significant benzene source under conditions that maximize transport. However, benzene may not be found in impacted samples over 40 meters from the source depending on the actual site conditions. Only two water samples in the selected database lie within 40 meters of a gas well, which may be a potential source. This suggests that the sample density obtained by selected samples in the study area is not optimal for detection of potential leaks by benzene concentration. It is also evident that the occurrence of the West Divide Creek seep was dependent on substantial fracture pathways that maximized transport of contaminant material.

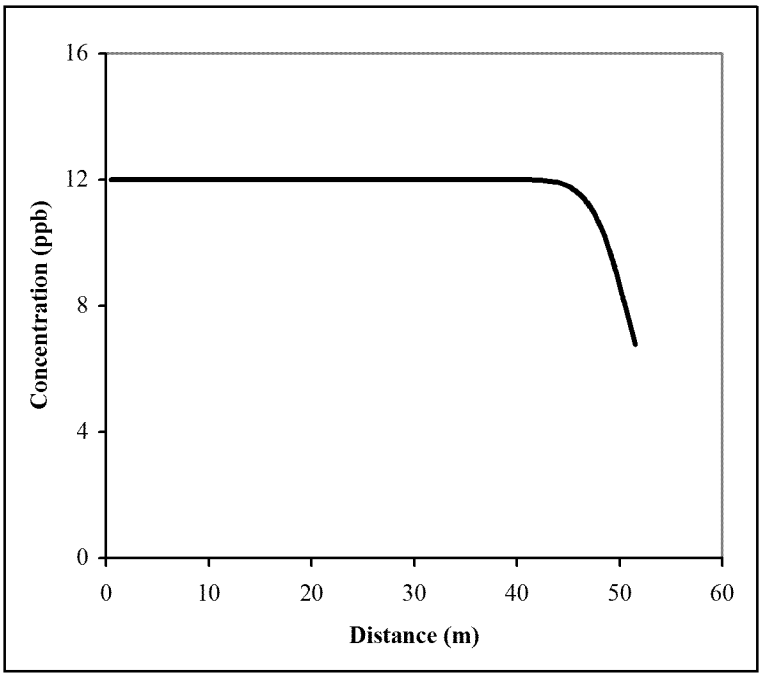

Figure 6.16: Worst-case model of reactive transport of benzene concentration with distance from a continuous source after 2 years. Source is 12,000 ppb benzene.

2017-002976-0000798

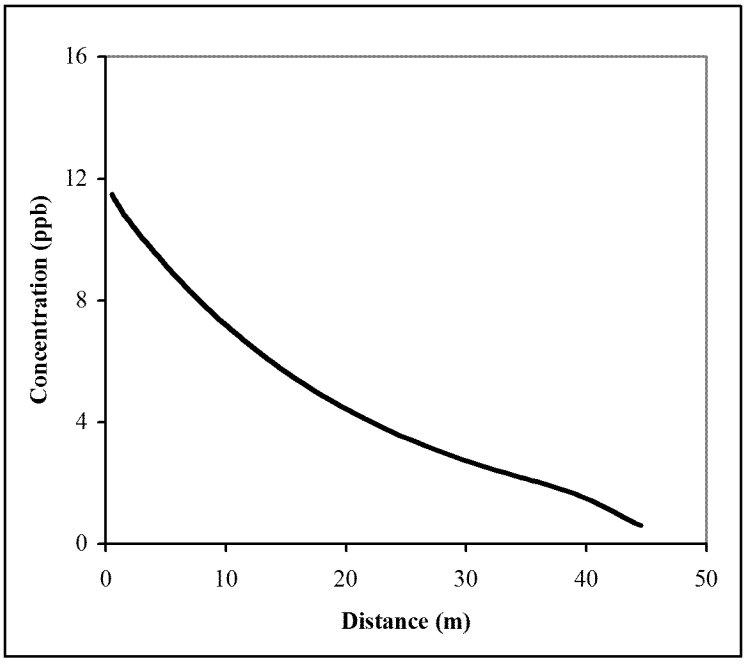

Figure 6.17: Median-case model of reactive transport of benzene concentration with distance from a continuous source after 2 years. Source is 12,000 ppb benzene.

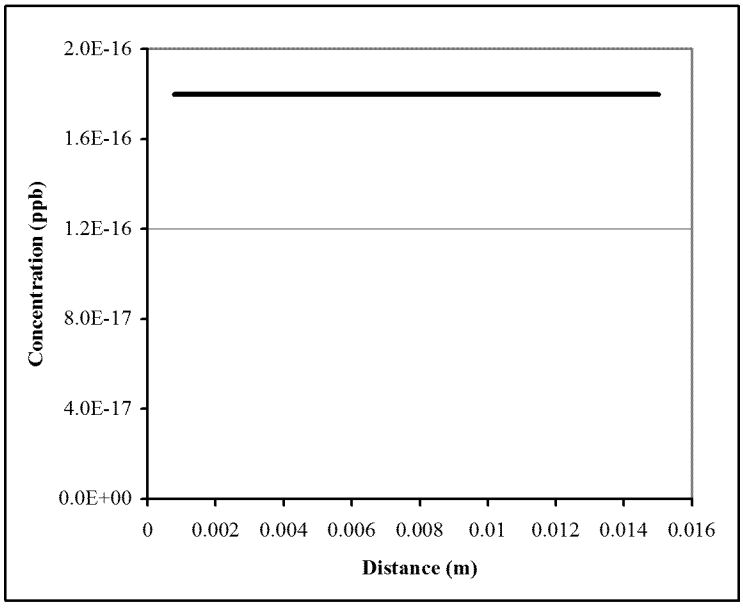

Figure 6.18: Best-case model of reactive transport of benzene concentration with distance from a continuous source after 2 years. Source is 12,000 ppb benzene.

These results show that benzene levels of less than 12 ppb should be realistically expected after a period of 2 years. However, even the worst-case scenario shows that benzene travels on the order of 60 meters under site conditions. This suggests that low

2017-002976-0000799

levels of benzene may be detected in impacted samples within 40 meters of a significant benzene source. However, at distances greater than 40 meters, benzene may not be found in impacted samples. Only 2 water samples in the selected database lie within 40 meters of a gas well, which may be a potential source. This suggests that the sample density obtained by selected samples in the study area is not optimal for detection of potential leaks by benzene concentration. It is also evident that the occurrence of the West Divide Creek seep was dependent on substantial fracture pathways for increased transport of contaminant material.

6.3 Inverse Geochemical Modeling

Based on earlier analysis, mixing between produced water and background water may be an important control on water chemistry. If cement and surface casing installation is not completed properly, the well annulus may provide a vertical conduit for the migration of produced water. The complex fracture system of the Wasatch Formation may provide some lateral dispersion and mixing with in situ water. Therefore PHREEQC was employed to help test the hypothesis developed in section 5.2. Only models that are consistent with geologic constraints on mineralogy and local flow regimes were considered.

Inverse geochemical modeling was conducted to test the possibility of background water mixing with produced water and natural processes, such as mineral precipitation/dissolution and cation exchange, on the observed water chemistry. The chemistry of cluster 1a-1 was used as an end-member, representing low TDS, background water. Produced water was tested as a source input for mixing. Produced water samples represent the major ion chemistry of the formation water of the Williams Fork Formation. Two produced water samples taken in Mamm Creek field, retrieved from the USGS Produced Water Database, were tested in inverse models (Breit, 2002).

Natural evolution would include background water and its reaction with aquifer minerals. Mineral phases were constrained to highly soluble, sedimentary minerals, such as gypsum, dolomite, and calcite, in order to simplify the model. Halite was not included, since it is not found in the lithology of the area. Carbon dioxide gas was added to achieve equilibrium with atmospheric pressure, since samples are both surface water and

2017-002976-0000800

groundwater. Phases that included chemical parameters that were not measured in the water analyses could not be included (i.e. aluminosilicate minerals). Cation exchange reactions were allowed, since they can be an important process that controls the dissolved concentrations of calcium, magnesium, and sodium, where clay minerals are present (Hem, 1985). This process allows dissolved cations to exchange on clay surfaces.

6.3.1 Model Input

Input solutions had charge balance errors from 0.78 to 12.83%, since clusters are an average of multiple samples with multiple parameters. Charge balance error was corrected by adjusting the bicarbonate value to balance the solution in PHREEQC. Altering the bicarbonate concentration for the purpose of charge balance is a reasonable technique for waters with near neutral pH (Hem, 1985). Input solutions are tabulated in Table 6.9.

Table 6.9: Input solutions for inverse modeling in PHREEQC.

		pH	Ca	Cl	HCO_3	Mg	Na	SO_4
		s.u.	*mg/L*	*mg/L*	*mg/L*	*mg/L*	*mg/L*	*mg/L*
Background Waters:	Battlement Mesa, average	7.9	52.6	6.09	333.9	36.57	53.2	113.9
	Cluster 1a-1	7.7	56.3	9.1	449.8	34.8	53.3	32.4
Produced Waters:	A	8.4	84	10400	5369.2	17	8695	74
	B	7.9	329	10200	212.4	3	6331	45
Clusters:	1a-2	7.6	77.4	19.6	656.4	55.0	115.8	129.0
	1b	8.6	56.9	12.5	378.9	27.3	68.6	63.2
	2	7.7	89.2	16.7	603.9	33.3	79.5	33.0
	3a	8.4	7.6	208.6	333.2	0.3	259.6	16.0
	3b-1	8.2	20.7	155.8	519.7	2.7	445.3	372.7
	3b-2	7.9	61.6	1052.1	235.5	3.3	748.2	117.3
	4a	7.8	52.9	78.1	676.5	25.4	275.8	181.9
	4b	7.5	159.8	218.6	493.1	72.5	610.1	1284.7

The input temperature was set to the average temperature of all water samples (11.5 °C). Uncertainty levels allow the model some flexibility in achieving parameter concentrations. Since the clusters modeled are averages of many water samples, it was appropriate to allow some uncertainty in the results. Models were tabulated with

2017-002976-0000801

uncertainty levels of +/-2%; secondary models for the same scenarios at greater uncertainty levels were not tabulated.

6.3.2 Modeling Results

No natural evolution models were found for any cluster at uncertainty levels of up to 5%. Four clusters, 3a, 3b-1, 3b-2, and 4b, had mass balance mixing models using produced water as a component with the percentage produced water being greater than 1% (Table 6.10).

Cluster 3b-2, with the most distinct Na-Cl component, can be produced by mixing background water with approximately 10% produced water, plus mineral interactions and cation exchange. Other clusters, 3a, 3b-1, 4a and 4b, require only 1-2% produced water to achieve their observed chemistries. Clusters 4a and 4b were previously interpreted as high TDS background waters, due to their chemistry that is so similar to waters from areas un-impacted by natural gas or petroleum production. If the mixing models are correct, input of small amounts (1-2%) of Williams Fork formation water may be due to natural upward migration from the Williams Fork along structurally controlled pathways. This is consistent with the spatial correlation of cluster 4b with major faults and fractures. The modeling therefore suggests that mixing of up to 2% produced water with natural groundwater may be due to upward migration of formation water in areas of significant structural deformation.

The models presented are not deterministic; they merely evaluate the possibility of given scenarios. Other processes (i.e. redox reactions) may be important in the study area, however, were not included in the model for simplicity, and due to input constraints. In addition, other anthropogenic source inputs may be affecting the water chemistry, especially in clusters 1a-2, 3b-1, 4a, and 4b which show increased nitrate compared to other clusters (see section 5.1).

6.4 Indicators of Anthropogenic Impact

From the tests conducted, certain indicators of impact by natural gas production can be discerned. One set of characteristics denotes impact by methane gas and drilling fluids, and is shown by most of the samples in cluster 2, and a few samples in cluster 3b-

2017-002976-0000802

Table 6.10: Summary of modeling results for mixing background with produced water plus mineral interaction and cation exchange. Mixing amounts shown in percentages. Model uncertainty is 2%. "PW" = produced water, PW-A is normal text, PW-B is italic. Background water is 1a-1. Mineral phases with + = dissolved, - = precipitated. Mass transfer amounts in mol/kg H_2O.

			Phase transfers (mol)				Cation exchanges (mol)		
Cluster	1a-1	PW	Dolomite	Calcite	Gypsum	$CO_2(g)$	Na^+	Ca^{2+}	Mg^{2+}
3a	98.1%	1.9%	-8.0E-04		-1.8E-04	-1.9E-03	1.7E-03	-2.5E-04	-6.1E-04
	98.1%	1.9%	-1.4E-03	1.2E-03	-1.8E-04	-1.9E-03	1.7E-03	-8.6E-04	
	98.1%	1.9%	-5.5E-04	-5.0E-04	-1.8E-04		-1.9E-03	1.7E-03	-8.6E-04
	98.1%	1.9%		-1.6E-03	-1.8E-04	-1.9E-03	1.7E-03	5.5E-04	-1.4E-03
	98.1%	*1.9%*	-3.8E-04		-1.7E-04	-1.1E-03	3.6E-03	-8.0E-04	-1.0E-03
	98.1%	*1.9%*	-1.4E-03	2.0E-03	-1.7E-04	-1.1E-03	3.6E-03	-1.8E-03	
	98.1%	*1.9%*	4.2E-04	-1.6E-03	-1.7E-04	-1.1E-03	3.6E-03		-1.8E-03
	98.1%	*1.9%*		-7.5E-04	-1.7E-04	-1.1E-03	3.6E-03	-4.2E-04	-1.4E-03
3b-1	98.6%	1.4%			3.5E-03	-2.2E-04	1.2E-02	-4.4E-03	-1.3E-03
	98.6%	1.4%	-1.3E-03	2.8E-03	3.5E-03		1.2E-02	-6.0E-03	
	98.6%	1.4%	4.7E-03	-9.1E-03	3.5E-03		1.2E-02		-6.0E-03
	98.6%	1.4%	1.1E-04		3.5E-03		1.2E-02	-4.6E-03	-1.4E-03
	98.6%	1.4%		2.2E-04	3.5E-03		1.2E-02	-4.7E-03	-1.3E-03
	98.6%	*1.4%*	3.7E-04		3.5E-03	4.7E-04	1.3E-02	-4.9E-03	-1.7E-03
	98.6%	*1.4%*	-1.3E-03	3.3E-03	3.5E-03	4.7E-04	1.3E-02	-6.6E-03	
	98.6%	*1.4%*	5.3E-03	-9.8E-03	3.5E-03	4.7E-04	1.3E-02		-6.6E-03
	98.6%	*1.4%*		7.4E-04	3.5E-03	4.7E-04	1.3E-02	-5.3E-03	-1.3E-03
3b-2	90.2%	9.8%	-2.9E-03		8.4E-04	-5.8E-03	-7.7E-03	2.2E-03	1.7E-03
	90.2%	9.8%	-1.2E-03	-3.4E-03	8.4E-04	-5.8E-03	-7.7E-03	3.9E-03	
	90.2%	9.8%	-5.1E-03	4.3E-03	8.4E-04	-5.8E-03	-7.7E-03		3.9E-03
	90.2%	9.8%		-5.9E-03	8.4E-04	-5.8E-03	-7.7E-03	5.1E-03	-1.2E-03
	89.9%	*10.1%*	-7.3E-04		8.7E-04	-1.7E-03	2.3E-03	-7.1E-04	-4.3E-04
	89.9%	*10.1%*	-1.2E-03	8.7E-04	8.7E-04	-1.7E-03	2.3E-03	-1.1E-03	
	89.9%	*10.1%*		-1.5E-03	8.7E-04	-1.7E-03	2.3E-03		-1.2E-03
4b	98.0%	2.0%	-2.9E-04		1.3E-02	-3.2E-04	1.7E-02	-1.0E-02	1.9E-03
	98.0%	2.0%	1.6E-03	-3.7E-03	1.3E-02	-3.2E-04	1.7E-02	-8.3E-03	
	98.0%	2.0%	9.9E-03	-2.0E-02	1.3E-02	-3.2E-04	1.7E-02		-8.3E-03
	98.0%	2.0%		-5.8E-04	1.3E-02	-3.2E-04	1.7E-02	-9.9E-03	1.6E-03
	97.9%	*2.0%*	1.5E-04		1.3E-02	5.0E-04	1.9E-02	-1.1E-02	1.4E-03
	97.9%	*2.0%*	1.6E-03	-2.9E-03	1.3E-02	5.0E-04	1.9E-02	-9.3E-03	
	97.9%	*2.0%*	1.1E-02	-2.2E-02	1.3E-02	5.0E-04	1.9E-02		-9.3E-03
	97.9%	*2.0%*		3.1E-04	1.3E-02	5.0E-04	1.9E-02	-1.1E-02	1.6E-03

2017-002976-0000803

1. These samples all show elevated benzene concentrations, thermogenic methane, and elevated iron and manganese concentrations. This combination of characteristics is unique from other clusters and regional waters. A few samples in cluster 2 show methane derived by fermentation, which indicates shallow, bacterially-mediated generation of methane, which is not indicative of anthropogenic impact by natural gas production.

Impact by produced water is not necessarily shown by high chloride concentration nor amount of mixing with produced water. Na/Cl molar ratios versus sulfate concentration for all clusters, regional waters and produced waters are shown in Figure 6.18. The dashed line in Figure 6.18 divides low and high TDS, background waters (top), from produced waters and clusters likely to be impacted by produced waters (bottom). Clusters 3a and 3b-2 both have Na/Cl molar ratios less than 2, which approach the Na/Cl molar ratio of produced water from the study area (1.0-1.3). Although, in most oilfields the Na/Cl molar ratio of produced water is less than 1, it is more important to consider site-specific compositions of produced water (Richter and Kreitler, 1993; Utvik, 1999).

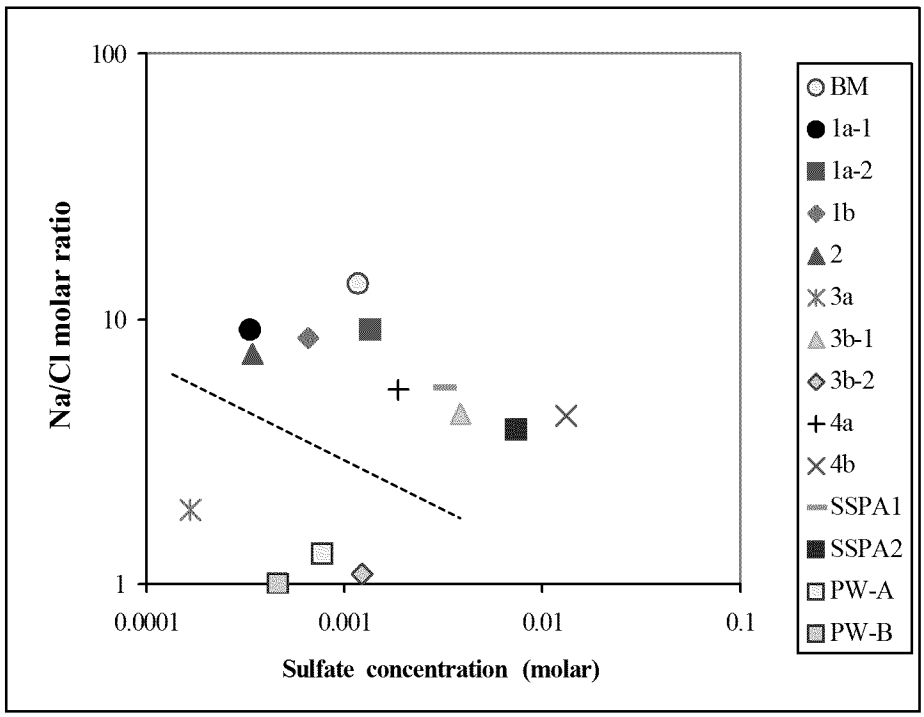

Figure 6.19: Log-log plot of Na/Cl molar ratio versus molar sulfate concentration. "BM" = Battlement Mesa water, average. "SSPA1" and "SSPA2" are cluster means for S.S. Papadopulos and Associates (2007) data. "PW-A" and "PW-B" are produced waters outlined in Table 6.8.

2017-002976-0000804

Clusters 3a and 3b-2 also show reduced sulfate concentrations (see also Figure 5.2). In contrast, the potentially impacted clusters 4a, 4b, and most of cluster 3b-1, have Na/Cl ratios greater than 2, have low concentrations of methane, and show little impact of sulfate reduction. Therefore, these clusters are interpreted to represent the natural evolution of groundwater in the Wasatch Formation mixed with a small, naturally-derived component of formation water from the Williams Fork. Furthermore, impact by produced water may be suggested by Na/Cl molar ratios approaching 1, elevated concentrations of methane derived from thermogenic gas or CO_2-reduction of thermogenic CO_2, and evidence of sulfate reduction processes. Clusters 3b-2 and 3a exhibit this combination of characteristics. Methane in these samples is likely derived from CO_2-reduction of CO_2 sourced from the Williams Fork Formation.

2017-002976-0000805

CHAPTER 7: CONCLUSIONS

Multivariate hierarchical clustering separated water samples into four statistically distinct groups that can be further subdivided into nine statistical clusters that represent water facies. Two groups (4 clusters) are low TDS waters that are typically Ca-Na-HCO_3 type, one group (2 clusters) is moderate to high TDS waters that show increasing sodium, sulfate, bicarbonate or chloride, and one group (3 clusters) is moderate to high TDS waters shows a distinct Na-Cl component. Elevated dissolved methane concentrations are correlated with sodium-chloride signatures.

Spatially, some clusters have a broad distribution. However, cluster 2 low TDS samples are found near or at the West Divide Creek seep and, as expected, show elevated benzene concentrations. In addition, the high TDS water of cluster 4b often occurs near major faults and fractures or near the nose of the Divide Creek anticline, showing the structural control on the spatial distribution of this cluster.

Most clusters are composed primarily of groundwater or surface water samples, but some contain both, which can be used to infer the degree of groundwater-surface water connection. For instance, the group 1 clusters have samples where groundwater and surface water have nearly identical chemistry implying possible hydraulic connection in the study area. In addition, only 5% of cluster 4b is surface water samples, all of which are springs. However, this is consistent with the interpretation of high TDS groundwater influenced by upward migration of deep formation water along structural discontinuities, again implying strong hydraulic connection. In contrast, the moderate to high TDS group 3 is almost entirely composed of groundwater samples implying this water chemistry is confined to Wasatch aquifers that are poorly connected to the surface.

PCA shows the first and third principal components are composed of Na-Cl-F-TDS and redox indicators that effectively separate clusters 2, 3a, and 3b-2 from other clusters. Cluster 2 shows especially elevated iron and manganese and reduced sulfate, while clusters 3a and 3b-2 show a Na-Cl component, elevated methane and reduced sulfate. This suggests that clusters 2, 3a and 3b-2 likely represent anthropogenic impact

2017-002976-0000806

by natural gas productions, whereas groups 1 and 4 represent low and high TDS, background waters, not impacted by natural gas production.

This hypothesis is confirmed by examination of regional water samples from areas that have not had significant petroleum activity and show similar chemical signatures to clusters, 1a-1, 1a-2, 1b, 4a, and 4b. Conversely, clusters 2, 3a, 3b-2 and somewhat 3b-1, are not similar to regional background. Spatially, group 3 may occur more frequently near the Divide Creek anticline, where fracturing is more extensive and the Wasatch Formation is thinned, however, gas wells exhibiting completion and bradenhead problems also occur in this area, and this slight spatial relationship is likely due to the combination of "problem" gas wells and structural deformation. In fact, spatial buffering suggests that clusters 3a, 3b-1, 3b-2, and 4a are more strongly correlated with gas wells than major faults and fractures. However, few water samples have been taken in the central region of the study area where gas wells are especially dense.

Distinguishing parameters of impacted clusters 2, 3a and 3b-2 include significant dissolved methane, benzene, and a strong Na-Cl component. The mean concentration of methane in the study area is positively correlated with increasing drilling of gas wells. Also, the percentage of high methane and chloride values in the study area increases over the period of time of when gas well drilling increased sharply. Methane from cluster 2 samples and some cluster 3b-1 samples is identified as thermogenic based on isotopic values, and is similar to production gas from the Williams Fork Formation. Methane from samples in cluster 3b-2 was apparently formed by CO_2-reduction; isotopic values suggest that the source of CO_2 could be the gas production interval.

Although benzene found in cluster 2 samples from the West Divide Creek seep traveled almost 4000 feet from the source, unless a fracture pathway is available for expedited transport, reactive transport modeling suggests that benzene should degrade to levels below the detection limit within 130-195 feet (40-60m) from the source. However, only 7 water samples were taken within 195 feet of a gas well. The only source of Na-Cl in the study area is the Williams Fork Formation. Inverse mixing models show that cluster 3b-2 requires mixing with 10% produced water. Other cluster chemistries requiring between 1-2% produced water (3a, 3b-1, and 4b) may be due to natural migration along an extensive fracture system or mixing with produced water. However,

2017-002976-0000807

the molar ratio of sodium to chloride and occurrence of sulfate reduction processes can help distinguish that cluster 3a as more likely impacted by produced water, while clusters 3b-1 and 4b appear to be derived from natural leakage of deep formation water. Therefore, elevated benzene concentrations, thermogenic methane as identified from isotopic signatures, and elevated iron and manganese concentrations distinguish waters impacted by methane gas and drilling fluids. Sodium-chloride molar ratios approaching that of produced water, elevated methane sourced from CO_2-reduction, and evidence of sulfate reduction processes may also suggest anthropogenic impact by produced waters in the study area.

7.1 Future Work

Future work following this study should attempt to fill in data gaps, by collecting additional water samples in the central portion of the study area where gas wells are especially dense. Also, data should be collected at regular time intervals from standard sampling sites for use in time-series analysis.

Additional parameters that would be useful in distinguishing anthropogenic impact by natural gas production include: (1) isotopic data for methane, water, and carbon dioxide, and (2) bromide and iodide ion concentrations. Isotope data can help distinguish the source of CH_4 and CO_2, as well as the mechanism of methane formation (Scott et al., 1994). Br/Cl and I/Cl ratios can be useful in distinguishing produced water impact due to their conservative nature (Richter and Kreitler, 1993).

Other anthropogenic sources could also be considered in comparison to the produced water source, such as irrigation return flow and septic system effluent. Although natural gas production is the most widespread potential source in the area, these other anthropogenic sources could contribute salinity to the system. This may be especially important to consider with clusters 1a-2, 3b-1, 4a, and 4b, which shows slightly elevated nitrate levels.

The mechanisms controlling the type and occurrence of methane could be investigated further. Areas which could be clarified include the origin of methane formed from CO_2-reduction processes, mixing processes between biogenic and thermogenic

2017-002976-0000808

methane, and the effects of reactive transport of methane during migration through the Wasatch Formation.

7.2 Recommendations

Recommendations include improvements to water quality monitoring programs at oil and gas fields. This includes establishing a background water quality for the site based on multiple years of data, as well as sampling of produced water signatures specific to that field. Water quality monitoring should cover the entire area, with dispersed spatial coverage and repetitive sampling efforts. Sampling in less developed areas allows for comparison with unaffected samples. Samples should be taken closer to oil and gas wells, in order to notice leaks and impacts early. Subtle impacts of produced water should be regarded as a warning of possible leaks or problem areas, and should be investigated further. Since problem wells appeared to be correlated with the Divide Creek anticline, drilling in areas of intense structural deformation should be conducted with caution.

2017-002976-0000809

REFERENCES CITED

26th Annual Oil Shale Symposium, 2006. Golden, CO.

Andrew, A.S., Whitford, D.J., Berry, M.D., Barclay, S.A. and Giblin, A.M., 2005. Origin of salinity in produced waters from the Palm Valley gas field, Northern Territory, Australia. Applied Geochemistry, 20: 727-747.

Bedient, P.B., Rifai, H.S. and Newell, C.J., 1999. Ground Water Contamination: Transport and Remediation. Prentice-Hall, Upper Saddle River, NJ.

Breit, G.N., 2002. Produced Waters Database. U.S. Geological Survey.

COGCC, 2006. Piceance Basin Reports/Data. Colorado Oil and Gas Conservation Commission.

Colorado Division of Water Resources, 2007. Colorado's Surface Water Conditions. Colorado Department of Natural Resources.

Cordilleran Compliance Services, I., 2007. PRESCO, Inc. 2006 Annual Water Sampling Report, Battlement Mesa Area, Garfield County, Colorado, Arvada.

Crifasi, B., 1999. The Colorado River. In: A. Aikin, Anderman, E., Harmon, E., Paschke, S., Plazak, D., Riemann, M. (Editor), Colorado Ground-Water Atlas. Colorado Ground-Water Association, Lakewood, pp. 33-36.

Czyzewski, G., 1999. The Piceance Creek Basin. In: A. Aikin, Anderman, E., Harmon, E., Paschke, S., Plazak, D., Riemann, M. (Editor), Colorado Ground-Water Atlas. Colorado Ground-Water Association, Lakewood, pp. 63-66.

Davis, S.N., Whittemore, D.O. and Fabryka-Martin, J., 1998. Uses of Chloride/Bromide Ratios in Studies of Potable Water. Ground Water, 36(2): 338-350.

Dodds, M., 2003. Modeling the natural attenuation potential of volatile organic compounds in a landfill leachate plume in Sheridan, Wyoming. MS Thesis, Colorado School of Mines, Golden, 147 pp.

Donnell, J.R., Yeend, W.E. and Smith, M.C., 1989. Geologic Map of the North Mamm Peak Quadrangle, Garfield County, Colorado. USGS.

Dorea, H.S. et al., 2007. Analysis of BTEX, PAHs and metals in the oilfield produced water in the State of Sergipe, Brazil. Microchemical Journal, 85: 234-238.

Dragon, K., 2006. Application of factor analysis to study contamination of a semi-confined aquifer (Wielkopolska Buried Valley aquifer, Poland). Journal of Hydrology, 331(272-279).

2017-002976-0000810

Drever, J.I., 1997. The Geochemistry of Natural Waters: Surface and Groundwater Environments. Prentice Hall, Upper Saddle River, NJ.

EnCana, 2007. Piceance. www.encana.com.

Energy Information Administration, 2007. U.S. Department of Energy, www.eia.doe.gov.

Fontes, J.C. and Matray, J.M., 1993. Geochemistry and origin of formation brines from the Paris Basin, France. 2. Saline solutions associated with oil fields. Chemical Geology, 109(1-4): 177-200.

Garfield County, 2007. Garfield County, Colorado. http://www.garfield-county.com/Index.aspx?page=1.

Gries, R., Dolson, J.C. and Raynolds, R.G.H., 1992. Structural and Stratigraphic Evolution and Hydrocarbon Distribution, Rocky Mountain Foreland. In: R.W.a.L. MacQueen, D.A. (Editor), Foreland basin and fold belts. Association of Petroleum Geologists Memoir, pp. 395-425.

Grout, M.A., Abrams, G.A., Tang, R.L., Hainsworth, T.J. and Verbeek, E.R., 1991. Late Laramide Thrust-Related and Evaporite-Domed Anticlines in the Southern Piceance Basin, Northeastern Colorado Plateau. The American Association of Petroleum Geologists Bulletin, 75(2): 205-218.

Grout, M.A. and Verbeek, E.R., 1991. Fracture History of the Divide Creek and Wolf Creek Anticlines and Its Relation to Laramide Basin Margin Tectonism, Southern Piceance Basin, Northwestern Colorado. Evolution of Sedimentary Basins.

Guler, C. and Thyne, G.D., 2004. Hydrologic and geologic factors controlling surface and groundwater chemistry in Indian Wells-Owens Valley area, southeastern California, USA. Journal of Hydrology, 285(1-4): 177-198.

Guler, C., Thyne, G.D., McCray, J.E. and Turner, A.K., 2002. Evaluation of graphical and multivariate statistical methods for classification of water chemistry data. Hydrogeology Journal, 10: 455-474.

Hannigan, R. and Bickford, N., 2003. Hydrochemical variations in a Spring-Fed River, Spring River, Arkansas. Environmental Geosciences, 10(4): 167-188.

Hatton, T., 1999. White River Basin. In: A. Aikin, Anderman, E., Harmon, E., Paschke, S., Plazak, D., Riemann, M. (Editor), Colorado Ground-Water Atlas. Colorado Ground-Water Association, Lakewood, pp. 41-43.

Helena, B. et al., 2000. Temporal Evolution of Groundwater Composition in an Alluvial Aquifer (Pisuerga River, Spain) by Principal Component Analysis. Water Resources, 34(3): 807-816.

2017-002976-0000811

Hem, J.D., 1985. Study and interpretation of the chemical characteristics of natural water. U.S. Geological Survey Water-Supply Paper 2254.

Hoefs, J., 2004. Stable Isotope Geochemistry. Springer-Verlag, Berlin.

Izbicki, J.A., Christensen, A.H., Newhouse, M.W. and Aiken, G.R., 2005. Inorganic, isotopic, and organic composition of high-chloride water from wells in a coastal southern California aquifer. Applied Geochemistry, 20: 1496-1517.

Johnson, R.C., 1989. Geologic History and Hydrocarbon Potential of Late Cretaceous-Age, Low-Permeability Reservoirs, Piceance Basin, Western Colorado. U.S. Geological Survey Bulletin 1787-E.

Johnson, R.C. and Flores, R.M., 2003. History of the Piceance Basin from Latest Cretaceous Through Early Eocene and the Characterization of Lower Tertiary Sandstone Reservoirs. In: K.M. Peterson, Olson, T.M., and Anderson, D.S. (Editor), Piceance Basin 2003 Guidebook. Rocky Mountain Association of Geologists, Denver, pp. 21-58.

Johnson, R.C. and Rice, D.D., 1990. Occurence and Geochemistry of Natural Gases, Piceance Basin, Northwest Colorado. The American Association of Petroleum Geologists Bulletin, 74(6): 805-829.

Kharaka, Y.K. and Hanor, J.S., 2005. Deep Fluids in the Continents: Sedimentary Basins. In: J.I. Drever (Editor), Surface and Ground Water, Weathering, and Soils. Treatise on Geochemistry. Elseveir-Pergamon, Oxford, pp. 499-540.

Kharaka, Y.K. and Otton, J.K., 2003. Introduction and Summary. In: Y.K. Kharaka and J.K. Otton (Editors), Environmental impacts of petroleum production: initial results from the Osage-Skiatook Petroleum Environmental Research Sites, Osage County, Oklahoma. USGS, Menlo Park, CA, pp. 1-13.

Kharaka, Y.K., Thordsen, J.J., Kakouros, E. and Herkelrath, W.N., 2005. Impacts of petroleum production on ground and surface waters: Results from the Osage-Skiatook Petroleum Environmental Research A site, Osage County, Oklahoma. Environmental Geosciences, 12(2): 127-138.

Langmuir, D., 1997. Aqueous environmental geochemistry. Prentice-Hall, Inc., Upper Saddle River, 600 pp.

Lecomte, K.L., Pasquini, A.I. and Depetris, P.J., 2005. Mineral Weathering in a Semiarid Mountain River: Its assessment through PHREEQC inverse modeling. Aquatic Geochemistry, 11(2): 173-194.

Lee, J., Cheon, J., Lee, K., Lee, S. and Lee, M., 2001. Statistical Evaluation of Geochemical Parameter Distribution in a Ground Water System Contaminated with Petroleum Hydrocarbons. Journal of Environmental Quality, 30: 1548-1563.

2017-002976-0000812

Lewis-Russ, A., 1999. Gunnison River Basin. In: A. Aikin, Anderman, E., Harmon, E., Paschke, S., Plazak, D., Riemann, M. (Editor), Colorado Ground-Water Atlas. Colorado Ground-Water Association, Lakewood, pp. 45-50.

Lonkevich, D., 2007. Gas processing plant slated for Colorado, Denver Post, Denver.

Lorenz, J.C., 2003. Fracture Systems in the Piceance Basin: Overview and Comparison with Fractures in the San Juan and Green River Basins. In: K.M. Peterson, Olson, T.M., and Anderson, D.S. (Editor), Piceance Basin 2003 Guidebook. Rocky Mountain Association of Geologists, Denver, pp. 75-94.

Lorenz, J.C. and Nadon, G.C., 2002. Braided River Deposits in a Muddy Depositional Setting: The Molina Member of the Wasatch Formation (Paleogene), West-Central Colorado, USA. Journal of Sedimentary Research, 72(3): 376-385.

Madole, R.F., 1999. Geologic Map of the Hunter Mesa Quadrangle, Garfield County, Colorado. Colorado Geological Survey.

Mahlknecht, J., Steinich, B. and Navarro de Leon, I., 2004. Groundwater chemistry and mass transfers in the Independence aquifer, central Mexico, by using multivariate statistics and mass-balance models. Environmental Geology, 45(6): 781-795.

McNeil, V.H., Cox, M.E. and Preda, M., 2005. Assessment of chemical water types and their spatial variation using multi-stage cluster analysis, Queensland, Australia. Journal of Hydrology, 310: 181-200.

Miller, E., 2007. Ritter, Salazar raise heat on W. Slope drilling, Rocky Mountain News, Denver.

National Energy Technology Laboratory, 2006. Technologies: Oil and Natural Gas Supply. U.S. Department of Energy, www.netl.doe.gov/technologies/oil-gas/.

Parkhurst, D.L. and Appelo, C.A.J., 1999. User's guide to PHREEQC - A computer program for speciation, reaction-path, 1D-transport, and inverse geochemical calculations. U.S. Geological Survey Water-Resources Investigation Report, Technical Report 99-4259.

Pereira, H.G., Renca, S. and Saraiva, J., 2003. A case study on geochemical anomaly identification through principal components analysis supplementary projection. Applied Geochemistry, 18: 37-44.

Raabe, S., 2007. Exxon Mobil plans Piceance plant, Denver Post, Denver.

Richter, B.C. and Kreitler, C.W., 1993. Geochemical Techniques for Identifying Sources of Ground-Water Salinization. C.K. Smoley, Boca Raton, 258 pp.

2017-002976-0000813

Roy, S., Gaillardet, J. and Allegre, C.J., 1999. Geochemistry of dissolved and suspended loads of the Seine river, France: Anthropogenic impact, carbonate and silicate weathering. Geochimica et Cosmochimica Acta, 63(9): 1277-1292.

S.S. Papadopulos & Associates, I., 2007. Piceance Basin Phase IV Baseline Water Quality Study - Garfield County, Colorado, Boulder.

Sanford, R.F., Pierson, C.T. and Crovelli, R.A., 1993. An Objective Replacement Method for Censored Geochemical Data. Mathematical Geology, 25(1): 59-80.

Schwartz, F.W. and Zhange, H., 2003. Fundamentals of Ground Water. John Wiley & Sons, New York, 583 pp.

Scott, A.R., Kaiser, W.R. and Ayers Jr., W.B., 1994. Thermogenic and Secondary Biogenic Gases, San Juan Basin, Colorado and New Mexico - Implications for Coalbed Gas Producibility. AAPG Bulletin, 78(8): 1186-1209.

Shrestha, S. and Kazama, F., 2007. Assessment of surface water quality using multivariate statistical techniques: A case study of the Fuji river basin, Japan. Environmental Modelling & Software, 22: 464-475.

Shroba, R.R. and Scott, A.R., 2001. Geologic Map of the Silt Quadrangle, Garfield County, Colorado. USGS.

Shroba, R.R. and Scott, R.B., 1997. Geologic Map of the Rifle Quadrangle, Garfield County, Colorado. USGS.

Simeonov, V. et al., 2003. Assessment of the surface water quality in Northern Greece. Water Research, 37: 4119-4124.

Spencer, C.W., 1995. Uinta-Piceance Basin Province (020). In: D.L. Gautier, G.L. Dolton, K.I. Takahashi and K.L. Varnes (Editors), National assessment of United States oil and gas resources-Results, methodology, and supporting data. U.S. Geological Survey Digital Data Series 30.

StatSoft, I., 1997. Electronic statistics textbook. StatSoft, Inc., Tulsa, OK.

Subba Rao, N., Devadas, D.J. and Srinivasa Rao, K.V., 2006. Interpretation of groundwater quality using principal component analysis from Anantapur district, Andhra Pradesh, India. Environmental Geosciences, 13(4): 239-259.

Swan, A.R.H. and Sandilands, M., 1995. Introduction to Geological Data Analysis. Blackwell Science, Inc., Malden.

Thyne, G.D., Guler, C. and Poeter, E., 2004. Sequential Analysis of Hydrochemical Data for Watershed Characterization. Ground Water, 42(5): 711-723.

2017-002976-0000814

Topper, R., Spray, K.L., Bellis, W.H., Hamilton, J.L. and Barkmann, P.E., 2003. Ground Water Atlas of Colorado, Special Publication 53. Colorado Geological Survey.

Tremain, C.M. and Tyler, R., 1995. Cleat, Fracture, and Stress Patterns in the Piceance Basin, Colorado: Controls on Coal Permeability and Coalbed Methane Producibility. In: R. Tyler et al. (Editors), Geologic characterization and coalbed methane occurrence: Williams Fork Formation, Piceance Basin, northwest Colorado. Bureau of Economic Geology, University of Texas, Austin, TX, pp. 192-197.

Uliana, M.M., 2005. Identifying the source of saline groundwater contamination using geochemical data and modeling. Environmental & Engineering Geoscience, 11(2): 107-123.

URS, 2006. Phase I Hydrogeologic Characterization of the Mamm Creek Field Area in Garfield County, Denver.

USGS, 1995. Ground Water Atlas of the United States. U.S. Geological Survey.

USGS, 2000. Estimated Use of Water in the United States County-Level Data for 2000. http://water.usgs.gov/watuse/data/2000/index.html.

Utvik, T.I.R., 1999. Chemical characterization of produced water from four offshoe oil production platforms in the North Sea. Chemosphere, 39(15): 2593-2606.

Van Stempvoort, D., Maathuis, H., Jaworski, E., Mayer, B. and Rich, K., 2005. Oxidation of Fugitive Methane in Ground Water Linked to Bacterial Sulfate Reduction. Ground Water, 43(2): 187-199.

Veil, J.A., Puder, M.G., Elcock, D. and Redwick, J., R.J., 2004. A white paper describing produced water from production of crude oil, natural gas, and coal bed methane, Argonne National Laboratory.

Wayland, K.G. et al., 2003. Identifying Relationships between Baseflow Geochemistry and Land Use with Synoptic Sampling and R-Mode Factor Analysis. Journal of Environmental Quality, 32: 180-190.

Weeks, J.B., Leavesley, G.H., Welder, F.A. and Saulnuier, J., G.J., 1974. Simulated Effects of Oil-Shale Developtment on the Hydrology of Piceance Basin, Colorado. U.S. Geological Survey Professional Paper 908: 84.

Williams Production RMT Company, 2006. An Overview of the Williams Fork Geological Model and Supporting Reservoir Engineering Data for 10-acre Density Development.

WRCC, 2007. Western Regional Climate Center, http://www.wrcc.dri.edu/.

2017-002976-0000815

Yacob, S.K., 2004. Using Multivariate Statistical Analysis to Characterize Effects of Population Growth on Water Quality in a Mountain Watershed. MS Thesis, Colorado School of Mines, Golden, 104 pp.

2017-002976-0000816

APPENDIX A

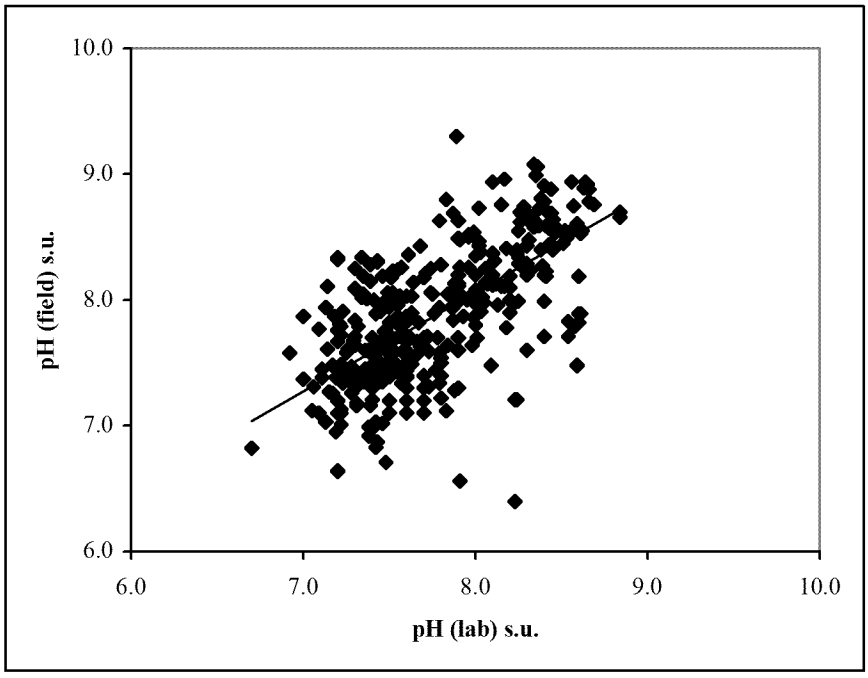

Figure A1: Correlation of field and lab pH measurements. R^2=0.44.

2017-002976-0000817

APPENDIX B

APPENDIX C

APPENDIX D

APPENDIX E

2017-002976-0000818